THE

LONDON, EDINBURGH, AND DUBLIN

PHILOSOPHICAL MAGAZINE

AND

JOURNAL OF SCIENCE.

[SEVENTH SERIES.]

APRIL 1936.

LVIII. *The Effect of Heat Treatment on the Structure of Gold- and Silver-leaf.* *By* G. D. PRESTON, *M.A.*, *and* L. L. BIRCUMSHAW, *M.A.*, *D.Sc.*, *of the National Physical Laboratory**.

[Plate XII.]

Introduction.

THE investigations, the results of which are described below, were originally undertaken to ascertain whether any difference, due to the formation of an oxide film, could be detected in the electron diffraction patterns produced by gold- and silver-leaf by heating in air and in hydrogen. No difference ascribable to the existence of oxides has been observed, but the experiments have shown that the behaviour of the films is dependent on the nature of the atmosphere in which they are heated, a result which seems to be of sufficient interest to be briefly recorded.

The effect of heat on the optical properties of leaves of gold and other metals supported on transparent solid mounts was described by Faraday[1] in the Bakerian Lecture for the year 1857. He observed that gold-leaf mounted on glass loses its characteristic green colour when viewed by transmitted light. After heating

* Communicated by C. H. Desch, D.Sc., Ph.D., F.R.S., F.I.C.

it transmits white light and seems to disappear. He also found that when heated unsupported in oil it shrinks up " even before it loses its green colour, which finally happens." The loss of colour was independent of the nature of the substance in contact with the gold being formed with leaves laid on mica, quartz, silver, and platinum, and when the surrounding medium was air, oil, or carbon dioxide. Chapman and Porter [2] investigated the contraction of strips of gold-leaf heated in air. They found that the shrinkage began at 340° C., and that the leaf became less transparent and finally opaque as shrinkage proceeded. This temperature does not appear to bear any relation to the " annealing temperature," *i. e.*, the temperature at which cold-worked gold must be annealed to produce softening, which has been determined (for massive specimens) by Kirke Rose [3]. He found that pure cold-rolled gold softened when annealed at 150° C., but that small traces of impurity raised this temperature. Phelps [4] found that by melting gold in hydrogen the annealing temperature was raised from below 150° C. to about 300° C. Recently Andrade [5], by direct microscopic observation, has observed the growth of crystallites in sputtered films of gold and of silver. The crystals grow as octahedra with a (111) face parallel to the surface of the film.

We have in the present work confirmed this last result for gold-leaf heated in air, and have repeated Chapman and Porter's experiment. The growth of crystals in the beaten leaf can be seen on the electron diffraction photographs by the appearance of spots on the ring spectrum of gold. We have also examined specimens heated in hydrogen and *in vacuo*, and find that the changes which occur in air are very much slower or do not occur at all. Many of the diffraction photographs show rings which do not belong to the spectrum of gold or silver, and the origin of these rings has been investigated, and is ascribed to contamination of the films by mercury vapour.

Experimental.

The heat-treatment of the specimens was carried out in a transparent silica tube about 3 cm. diameter and 30 cm. long, sealed at one end. A small silica boat attached to the silica sheath of a thermocouple held the

specimen, which lay in an easily visible position against the tip of the couple sheath. The containing tube could be closed and evacuated or filled with hydrogen. The heating was carried out by a gas flame, so that any changes in the appearance of the leaf could be watched. The metal leaf was mounted on pieces of sheet metal (gold for gold-leaf, silver for silver-leaf) 1 cm. wide and 2 cm. long, at one end of which a hole 0·5 cm. diameter had been punched. The leaf was placed over this hole, so that it could be examined by a transmitted beam of electrons. No adhesive was used, the leaf being folded over the edges of the support. The mount was washed in acetone before affixing the leaf, and in some cases the leaf itself was washed in acetone before mounting.

Gold-leaf heated in Air.

The general nature of the results obtained may be described as follows:—The leaf as received was a deep olive-green colour by transmitted light, and yielded electron diffraction photographs showing well-marked orientation, the crystals of gold being arranged with a cube face parallel to the surface of the leaf, as reported by Trillat [6] and others. In the material at our disposal the crystals appear to depart from the mean orientation by about $\pm 20°$, as judged by the length of the arcs into which the (200) ring is broken. A typical photograph of gold-leaf is shown in fig. 1 (Pl. XII.). The first effect of heating in air at about 400° C. is that a number of spots appear on the (220) ring of the diagram. This is accompanied by a marked contraction of the leaf, which becomes tightly stretched on the mount; as the treatment proceeds the leaf becomes more transparent, and finally tears. A specimen heated quickly to 420° C., and maintained at that temperature for two minutes, showed signs of contraction, but no spots appeared on the (220) ring in the electron diffraction photograph. A further five minutes at 450° C. yielded the photograph in fig. 2 (Pl. XII.), the leaf being now tightly stretched on the mount. The (220) ring is now covered with a series of spots, each of which is due to reflexion from a single crystal grain. Photographs of other specimens in this condition were taken with the normal to the surface of the leaf parallel to the incident beam and inclined at about

30° to it. In the inclined position spots appear on the (111) and (200) rings of the photographs. The experiments thus show that the crystal growth which produces the spots on the (220) ring is accompanied by a re-orientation of the grains. The new grains grow in a position which is favourable for reflexion from the (110) planes. Three such planes $(1\bar{1}0)$, $(10\bar{1})$, and $(01\bar{1})$ intersect in a cube diagonal [111], and if we assume that the new crystals have a (111) face parallel to the surface of the sheet the observations are satisfactorily explained. When the electron beam is perpendicular to the surface of the sheet it is travelling along a [111] direction in the new grains. The (100) and (111) planes are inclined at too large an angle to the beam to reflect, so no spots appear on these rings. The beam, however, is now parallel to the line of intersection of three (110) planes, and a small deviation of about 1° will suffice to produce reflexion. That the absence of spots from the (111) and (200) rings is due to orientation is proved by the photographs taken with the sheet inclined to the beam. Spots then appear on these rings, showing that the crystals producing them were unfavourably oriented for reflexion when the beam was perpendicular to the surface. The growth of crystals with this orientation has been observed microscopically by Andrade[5] in sputtered gold films.

Further heat-treatment at 420° C. leads to an intensification of the spots, while the original (200) arcs become less intense and finally disappear. This condition is illustrated in fig. 3 (Pl. XII.), where the (111) and (200) rings are scarcely to be seen when the specimen is perpendicular to the incident beam. Fig. 4 (Pl. XII.) shows the same specimen inclined about 30° to the beam ; the (111) and (200) rings are now seen as groups of spots. During this stage the contraction of the leaf continues. If it is held at its edges by the support it becomes more transparent and finally ruptures ; if free to contract the transparency decreases and the leaf crumples up gradually.

These experiments show that the contraction produced in gold-leaf by heating in air, studied by Chapman and Porter[2], is connected with recrystallization and re-orientation of the metal crystals. It was natural to enquire whether the contraction was wholly accounted for by a change from orientation with a (100) plane

parallel to the surface to orientation of the crystals with a (111) plane parallel to the surface. In the face-centred cubic structure of gold the atoms on the cube faces, one of which is initially parallel to the surface of the sheet, are arranged at the corners of a square network of side $a/\sqrt{2}$, where a is the side of the unit cube. The (111) planes consist of equilateral triangular networks, the side of the triangle being again $a/\sqrt{2}$. In the (100) planes the area associated with each atom is $a^2/2$, in the (111) planes the area per atom is $a^2\sqrt{3}/4$. A contraction would be produced by atomic movements of the type

Fig. 5.

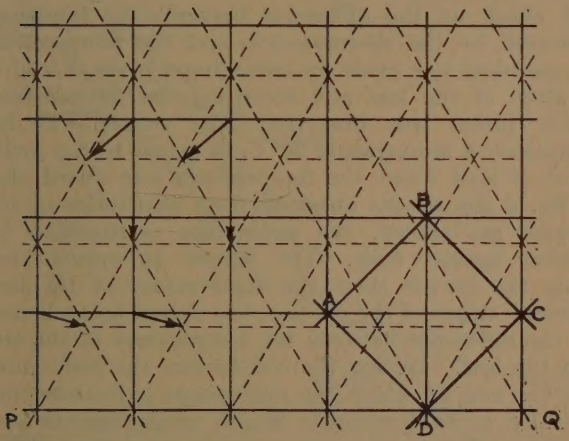

indicated in fig. 5. In this diagram ABCD represents a face of the unit cube of a gold crystal, the centre of the face being occupied by an atom. The diagonals of this face form the network of side $a/\sqrt{2}$, at the intersections of which all the atoms are situated. Taking any row of atoms such as PQ, and supposing it to remain unchanged, it is clear that the transformation to a triangular network of side $a/\sqrt{2}$ can be produced by movements of the atoms in the surface as indicated by the arrows in the diagram. The area per atom is reduced in the ratio $1 : \sqrt{3}/2$, or by about 14 per cent. If no other factors were operative we might therefore expect to observe a linear contraction

of about 7 per cent. Chapman and Porter were primarily interested in the temperature at which the contraction started, and their published diagram only gives the results of observations up to about 8 per cent. change of length. Their experiment was accordingly repeated with a view to ascertaining whether the contraction stopped at this point. For this purpose a small strip of gold-leaf 1·5 cm. long and 0·2 cm. wide was hung on a gold wire supported on a steel rod in a pyrex glass test-tube. The test-tube was wrapped with sheet metal in which vertical slots about 0·4 cm. wide were cut, to enable the leaf to be viewed by means of a travelling microscope. A thermocouple was mounted with the junction close to the middle of the leaf. The test-tube was heated by a gas flame.

A check on the difference between the temperature indicated by the thermocouple and the temperature of the gold-leaf was made by mounting a piece of lead strip in place of the leaf and recording the temperature at which fusion was observed. The couple was found to indicate a temperature 30° C. in excess of the melting-point of lead when the temperature was raised slowly. In fig. 6 the results obtained from two series of observations are shown, the percentage contraction being plotted against time. The figures at various points along the curves show the temperature of the leaf at different stages of the process, the values being corrected for the difference between the temperature of the couple and the leaf. During the contraction the leaf crumples and the end on which the microscope is focussed moves laterally, so that accurate length measurements are not possible. The two curves were obtained from different specimens, one of which was unloaded ; the other was loaded at its lower end by being wrapped round a small piece of capillary pyrex tube. The loading does not appear to affect the nature of the results. In the first specimen contraction started at 370° C., in the second at 350° C., the difference being probably due to the difficulty of measuring the temperature with accuracy. Chapman and Porter found 340° C. for the temperature at which contraction started. The irregularity in the curves at the point at which the film becomes opaque is in one case known to be due to lateral movement of the end of the leaf and in the other is probably ascribable to the same cause. The contraction proceeds uniformly at about

the same rate in both cases up to 22 per cent., and thereafter more slowly until it exceeds 30 per cent., when the experiments were stopped after nearly two hours heating. The amount of the contraction is greatly in excess of that to be expected from a process such as is indicated in fig. 5. A small excess might be accounted for by the crumpling of the leaf, but as the loaded specimen shows as large a contraction as the unloaded it may be assumed that the crumpling is not the cause of the large excess contraction. An electron diffraction photograph of one of these specimens after the treatment showed the rings

Fig. 6.

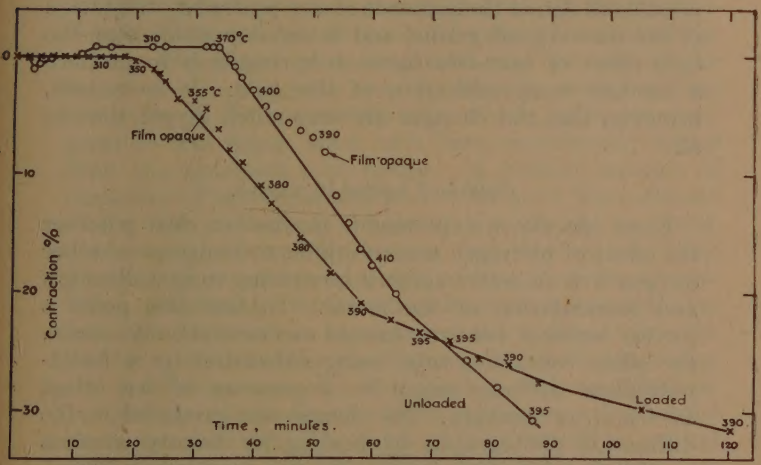

of gold with random distribution of spots on them, both at normal incidence and when inclined. The intensity of the rings is not so strong as in the untreated leaf, possibly on account of the increased thickness of the specimen, which, after a linear contraction of 30 per cent., would be twice its original thickness.

Gold-leaf heated in Hydrogen.

The hydrogen was obtained from an electrolytic generator, and, after passing through a tube containing iron-wire gauze heated to 600° C., was dried by silica gel.

The gas was passed into the silica tube containing the specimen and thermocouple, described above, for one hour or more before heating was started. Very little effect was observed by heating for periods up to twenty minutes at 420° C. The preferred orientation of the beaten leaf appeared to be slightly improved, the arcs into which the rings are broken up becoming a little shorter and sharper. Ten minutes heating at 600° C. produced some faint spots on the rings, but these did not appear first on the (220) rings as in the case of heat-treatment in air. After further heat-treatment at 600° C. for twenty minutes the specimen ruptured and the rings became spotted. It has not been possible to detect the presence of any preferred orientation of the new crystal grains, and it seems possible that the only effect of heat-treatment in hydrogen is to produce a random recrystallization of the gold. It is certain, however, that the changes are very much slower than in air.

Gold-leaf heated in vacuo.

From the above experiments it was not clear whether the effect of hydrogen was to inhibit a change or whether oxygen was an active agent in producing recrystallization and reorientation of the metal. To test this point a further series of heat-treatments was carried out *in vacuo*, the silica containing-tube being exhausted by a butyl-phthallate diffusion-pump to a pressure of less than 10^{-4} mm. of mercury. No change was produced in the diffraction photographs by heating for twenty minutes at 530° C. A further heating for five minutes at 700° C. was also without effect.

This last series of experiments shows that gold-leaf can be heated *in vacuo* to temperatures up to 700° C. without appreciable change. The recrystallization observed when the leaf is heated in the neighbourhood of 400° C. in air must therefore be caused by one of the constituents of the atmosphere. Owing to the difficulty of freeing nitrogen from small traces of oxygen we have not considered it practicable to ascertain whether nitrogen is partly responsible for the changes produced in the leaf, and for the present, bearing this reservation in mind, we may assume that oxygen is the active agent. The effects produced by heating in hydrogen are much

less marked and much slower than in oxygen, even at the higher temperatures. There is no doubt that some crystal growth takes place; the appearance of spots on the rings is direct evidence of this, but it is not certain whether this may not be due to minute traces of oxygen or water vapour in the hydrogen or to the contamination of the film. The hydrogen used is believed to have been of a high degree of purity, but adsorbed gases or water vapour may have been released from the silica tube in which the heat-treatments were carried out. The small effects observed in hydrogen may have been due to some such cause. The arrangement of the apparatus in which the heating was carried out was such that the silica boat containing the specimen was supported on the thermo-couple sheath and did not touch the walls of the containing-tube. When the containing-tube was evacuated the specimen can only have received heat by radiation from the walls of the containing-tube, which, while the temperature was rising, must have been considerably hotter than the specimen and couple. A certain amount of degassing of the apparatus must thus have been effected during the preliminary stages of the heating *in vacuo*, the material released by heating from the surface being pumped off or condensed in the cold parts of the system. When the heating is done with hydrogen in the containing-tube the temperature lag between the walls of the tube and the specimen will be much reduced, as both convection and conduction can play their part in heat transference. In addition the presence of the hydrogen will obstruct the removal of any gases released from the silica, so that the chances of contamination from this source are increased.

The changes which occur on heating gold-leaf in hydrogen are small compared with those observed when the heating is carried out in air. It is these last which seem at the moment to be most interesting, because it is clear, from the absence of any observable effect *in vacuo*, that the gaseous environment of the metal has a controlling effect on the process of recrystallization and reorientation. Although no direct evidence of the existence of any oxide film on the gold has been obtained in this work, it seems possible that the process may be due to the formation of an oxide which immediately decomposes, liberating gold atoms on the surface of the metal

which recrystallize in the new orientation. If a chemical reaction of this type is involved the observations suggest that it is confined to the surface of the metal, because if the oxygen penetrated the metal to any appreciable extent the reaction would proceed throughout the thickness of the leaf and the original cold-worked structure would disappear very quickly. Actually this is not what occurs. The original cold-worked structure disappears gradually, and is still present to a marked extent when the new grains are large enough to produce individual spots on the diffraction photographs (see Pl. XII. fig 2.) at a stage when the contraction has proceeded to about half its final value. This is consistent with the view that the reaction takes place at the surface and that the oxygen does not penetrate the metal to an appreciable depth.

Silver-leaf.

The results obtained from heat-treatment of silver-leaf in air, hydrogen, and *in vacuo* are less conclusive than in the case of gold, and will be only briefly referred to. The leaf as received was rather too thick (10^{-5} cm.) to yield good diffraction photographs, but when thinned by flotation on dilute nitric acid yielded photographs showing the same type of preferred orientation as that exhibited by gold-leaf. The effect of heating the leaf (as received) in air is much more rapid than with gold. After five minutes at 290° C., although no change was visible in the leaf, the electron diffraction photograph showed by the granular appearance of the rings that crystal growth had started. At higher temperatures, in the neighbourhood of 400° C., the leaf quickly becomes transparent and ruptures by contraction. We have not been able to detect with certainty the existence of any preferred orientation in the recrystallized metal, and, as far as our observations go, it is possible that the silver crystals merely grow larger without assuming a new orientation when heated in air. In hydrogen, however, even after heating for ten minutes at 600° C., no spots appeared on any of the rings, and the electron diffraction photographs were not distinguishable from those obtained from the leaf before heat-treatment.

The heat-treatments carried out *in vacuo* yielded variable results. After ten minutes at 500° C. a photo-

graph was obtained the rings of which did not correspond with those of silver. It seems likely therefore that the results were being affected by some source of contamination not under our control. The experiments were therefore abandoned at this point, and attention was directed to an investigation of the origin of the extra rings which appeared in most of the photographs of silver and on a number of those of gold.

Extra Rings.

It was mentioned in the introductory paragraph that a number of the diffraction photographs showed rings which did not belong to the spectrum characteristic of gold or of silver. The most prominent of these "extra" rings were two, the first of small radius corresponding to a spacing of 4·50 Å., and the second just within the (111) ring of the metals with a spacing of 2·57 Å. These two rings frequently occurred on the same photograph. Other extra rings of less intensity are found occasionally, but with the possible exception of a ring of spacing 3·27 Å. their appearance is haphazard, and we are inclined to ascribe them to contamination by grease films. The two rings mentioned above have been observed, however, in the spectrum obtained from gold-foil washed in acetone, and we are convinced that they arise from contamination of the metal by mercury vapour. In the apparatus used by us the diffraction camera is evacuated by a butyl-phthallate diffusion-pump, the discharge-tube where the electron beam is generated being exhausted by a mercury diffusion-pump connected to the same rough vacuum. The apparatus has been in use for some years, and has been constantly filled with air and exhausted. No doubt in course of time mercury must diffuse through the connecting tubes and into the camera.

To test this point specimens of gold- and silver-leaf were contaminated with mercury vapour. A small drop of pure mercury, about 1 mm. in diameter, was placed at the bottom of a test-tube mounted in a nearly horizontal position. The leaf on its mount was introduced into the test-tube, and lay about 1 cm. from the drop, which was then warmed by a small flame until mercury could be seen condensing on the tube in the neighbourhood

of the specimen. The spreading of mercury on the gold-leaf could be seen by the colour changing from golden to silver, and in this case the process was stopped by removing the specimen when the line of demarcation between the two colours was rather less than halfway across the part of the specimen available for examination in the electron camera. The mercury continued to spread over the surface of the leaf, and by the time the specimen was put into the apparatus and the system evacuated (about thirty minutes) the whole area was silver-coloured. The leaf was now grey by transmitted light and had ruptured by contraction. It yielded a photograph having an intense inner ring with the same spacing, 4·50 Å., as that observed in the photographs of gold. The remaining rings were too broad to be measured. The specimen was left in the apparatus over night, and a photograph obtained about fifteen hours after the treatment in mercury vapour gave much sharper rings. The spacings shown in the following table have been calculated from measurement of the photographs :—

Spacings observed from specimens of Gold- and Silver-leaf contaminated by Mercury.

Gold.		Silver.	
	Å.		Å.
vs.....	4·50	vs.....	4·29
m.....	3·27	—	
vs.....	2·57	s.....	2·54
w.....	2·12	mw.	2·00
m.....	1·715	m.....	1·68
m.....	1·50	m.....	1·50
m.....	1·28	m.....	1·28

The two most intense rings correspond exactly with those observed in the photographs of gold-leaf. The treatment of the silver-leaf was carried out in a similar manner. Immediately after treatment four of the most intense rings could be seen on the photograph, and a rather better photograph was obtained by leaving the specimen in the apparatus for fifteen hours. The figures given in the table were obtained after heating the specimen in a steam-oven at 100° C. for two hours. It has not been possible to identify the spectra with the X-ray

data for the gold-mercury and silver-mercury systems. The former has been examined by Stenbeck [7], who has identified five intermediate phases. Only one of these, β, has a structure assigned to it; it is a close-packed hexagonal lattice of side 2·91 Å. and axial ratio 1·65, with a composition close to 25 weight per cent. of mercury. We are indebted to Professor A. Westgren and to Dr. Stenbeck for a letter in which they have communicated the spacings recorded in an X-ray investigation of the phase richest in mercury in the gold-mercury system, and for the information that the spacings in the table do not agree with any they have observed in the X-ray investigation of gold amalgams. The silver-mercury system has been investigated by one of us [8], and the results confirmed by Stenbeck (*loc. cit.*). There are two intermediate phases, one a close-packed hexagonal structure with dimensions approximately equal to those of the similar structure in the gold-mercury system, but with a composition near AgHg, the other a cubic structure of side 10·0 Å. of the γ-brass type, with 52 atoms in the unit and of composition Ag_5Hg_8. Neither of these structures gives a satisfactory account of the spacings recorded from the gold- and silver-leaf contaminated with mercury. It is nevertheless established that the most intense rings of the spectra obtained from the purposely contaminated specimens correspond very closely with the "extra" rings observed in some of the earlier work above described.

Other investigators have found "extra" rings on electron diffraction photographs of gold- and silver-leaf. Trillat [9] has examined the origin of the rings observed in his laboratory, and concludes that they arise from grease films, the presence of which can only be avoided by very careful manipulation. The spacings observed in the present work do not correspond with those most commonly found by Trillat, and as we have observed the extra rings on specimens washed in acetone we think that the most intense of these are not due to grease. The fainter ones, which do not correspond with the spacings observed in the specimens purposely contaminated with mercury, are probably due to contamination by grease. Finch, Quarrell, and Wilman [10] have also observed "extra" rings, and investigated their origin, and they assign them to the solution of gas in the metal.

They give a list of six rings with spacings 4·81, 4·00, 2·79, 1·83, 1·61, and 1·49 Å. The first, third, fourth, and fifth of these are just 7 per cent. larger than the first, third, fifth, and sixth spacings given in the table above. The discrepancy of 7 per cent. in the spacings makes it doubtful, however, if these two series of rings arise from the same cause. Our own values may be in error by ± 2 per cent., and the others are probably more accurate, so that the difference is at least twice any that could be ascribed to experimental error. Finch, Quarrell, and Wilman [10] observe that their series could be accounted for by a close-packed hexagonal structure of side 5·58 Å. and axial ratio 1·28; the rings observed by us could be ascribed to a structure of this type of side 5·20 Å. and axial ratio 1·26. No such structure has been observed in either of the systems, gold-mercury or silver-mercury, and so far as our own observations go we regard the agreement between the tabulated spacings and those calculated for the hexagonal structure as fortuitous. The failure to identify the spacings observed with any known phase of these binary systems is an interesting point that requires further investigation. It suggests the possibility that the phases in equilibrium in thin films may not be the same as those in the massive state.

Summary.

Gold- and silver-leaf heated in air, in hydrogen, and *in vacuo* have been examined by the electron diffraction method.

The contraction which takes place when gold-leaf is heated in air at about 350° C. has been shown to be accompanied by a recrystallization and reorientation of the crystals in the leaf. The effects are either absent or else occur very slowly even at higher temperatures when the treatment is carried out in an atmosphere of hydrogen. At pressures of 10^{-4} cm. mercury or less no recrystallization is observed even at 700° C. It is inferred that the changes observed at low temperatures in annealing gold-leaf in air are caused by the presence of oxygen.

Similar effects are observed with silver-leaf, but the effect in air takes place at lower temperatures and is not easily controlled. The reorientation of the crystals

has not been definitely observed, although crystal growth takes place. Certain "extra" rings which appear in a number of the electron diffraction photographs have been ascribed to contamination of the metal by mercury vapour. The spectra obtained from gold- and silver-leaf treated with mercury vapour do not, however, correspond with those to be expected from any of the known phases of the gold-mercury and silver-mercury systems. It is suggested that the phases present in very thin films may not have the structure observed in the massive state.

Acknowledgment.

This work has been carried out in the Department of Metallurgy and Metallurgical Chemistry of the National Physical Laboratory. Our thanks are due to Dr. C. H. Desch for his interest in and encouragement of the investigation.

References.

(1) Faraday, Phil. Trans. Roy. Soc. p. 145 (1857).
(2) Chapman and Porter, Proc. Roy. Soc. lxxxiii. A, p. 65 (1910).
(3) Kirke Rose, J. Inst. Metals, x. p. 150 (1930).
(4) Phelps, J. Inst. Metals, xii. p. 125 (1914).
(5) Andrade, Trans. Far. Soc. xxxi. p. 1137 (1935).
(6) Trillat and Hirsch, *Comptes Rendus*, cxciii. p. 649 (1931).
(7) Stenbeck, *Zeit. f. anorg. chem.* ccxiv. p. 16 (1933).
(8) Preston, J. Inst. Metals, xlvi. p. 522 (1931).
(9) Trillat, Trans. Far. Soc. xxxi. p. 1129 (1935).
(10) Finch, Quarrell, and Wilman, Proc. Far. Soc.

September 1935.

LIX. *Note on the Slow Motion of Fluid.*

By W. R. Dean, *M.A., Trinity College, Cambridge.**

THE work of this paper is to some extent connected with the problem, solved by G. Hamel †, of the steady two-dimensional radial flow of viscous liquid. In the part of his paper in which he examines flow in the angle included between two rigid plane boundaries, Hamel shows that if the motion is divergent there is a limiting relation between the inclination of the planes and the

* Communicated by the Author.

† *Jahresb. d. deutschen Math. Ver.* xxv. pp. 34–60 (1917).

maximum velocity at unit distance from the common line of the planes : the maximum velocity must not exceed a value that is a function of the angle between the planes ; as the angle increases the limiting value decreases, and tends to zero as the angle tends to π. It follows that only a slow divergent motion is possible in the extreme case when the two boundaries are coplanar.

As the limiting cases of the radial motion are of interest, it appeared desirable to examine some cases of the slow motion of fluid bounded by two semi-infinite plane boundaries, the boundaries being coplanar and having their straight edges parallel and at a finite distance apart. The motion considered is therefore that due to a jet of fluid, a jet of finite width ($2a$ in fig. 1) in contrast with the limiting case of radial motion, which may be described as due to a jet of infinitesimal width. We have therefore a less artificial motion than the radial motion to the extent that the velocity of the fluid is everywhere finite ; the pressure, on the other hand, is not finite at the edges, though the infinity is of a lower order than it is in the radial motion.

In § 2 is given the simple expression for the stream-function if it is supposed that the fluid enters through BC with a constant uniform velocity in a direction perpendicular to the boundaries. This motion is not considered in any detail since it is very similar to the limiting case of radial motion.

In § 3 the case of an inclined jet is considered ; here it is supposed that at entry the fluid velocity, while constant and uniform as before, is in a direction inclined to the normal to the boundaries. The jet now leaves the wall on one side, however small the inclination of the direction of the initial velocity to the normal. The motion in this case corresponds to a radial motion that is partly divergent and partly convergent *. The stream-lines of this motion have been calculated and are shown in fig. 2. The biharmonic functions used in §§ 2, 3 occur in many well-known solutions of problems of plane stress and strain.

In the rest of the paper, §§4–10, a second approximation is found to the stream-function of the motion due to

* See Hamel, *loc. cit.* p. 45.

a normal jet, that is, in effect, a partial allowance is made for the effect of inertia on the motion. This calculation is somewhat heavy, and part of the second approximation cannot be expressed in finite terms, so that it is doubtful if the process of successive approximation could be carried further; it happens, however, that in this particular problem further approximation is unnecessary, for the result of the second approximation is to show that however small the initial velocity the jet breaks away from the boundary, provided, of course, that the motion is divergent. There is consequently no critical velocity, though it seemed possible before calculation that there might be one. The question whether a critical velocity would be found if the fluid were led up to the opening by a channel (so that the velocity was zero at B and C) remains open; it should be possible to decide this by the fairly general method of these paragraphs, though the work would clearly be much heavier.

§ 2. It is assumed that the fluid is bounded by the plane $y=0$, and that through a strip, $|x| \leqslant a$, of the plane fluid is introduced normally with a constant uniform velocity. In terms of a stream-function ψ the component velocities u, v of the fluid can be written

$$u=-\frac{\partial\psi}{\partial y}, \quad v=\frac{\partial\psi}{\partial x};$$

if the inertia terms in the equations of motion are neglected, ψ must satisfy the differential equation

$$\left(\frac{\partial^2}{\partial x^2}+\frac{\partial^2}{\partial y^2}\right)^2\psi\equiv\nabla_1^4\psi=0, \quad . \quad . \quad . \quad . \quad (1)$$

and the boundary conditions

$$\frac{\partial\psi}{\partial x}=0, \quad \frac{\partial\psi}{\partial y}=0, \quad y=0, \quad |x|>a; \quad . \quad . \quad (2)$$

$$\frac{\partial\psi}{\partial x}=\text{const.}, \quad \frac{\partial\psi}{\partial y}=0, \quad y=0, \quad |x|<a. \quad . \quad (3)$$

An expression for the stream-function is

$$\psi=(x-a)\theta_1-(x+a)\theta_2+\pi a, \quad . \quad . \quad . \quad . \quad (4)$$

where, as shown in fig. 1,

$$\theta_1=\tan^{-1}\left(\frac{y}{x-a}\right), \quad \theta_2=\tan^{-1}\left(\frac{y}{x+a}\right);$$

the constant πa is added so that the stream-function may be an odd function of x. Since θ_1 and θ_2 are harmonic, $x\theta_1$ and $x\theta_2$ are biharmonic, hence ψ satisfies equation (1). It is clear that ψ is constant on AB and CD, assuming the values $-\pi a$ and πa, respectively, while at points of BC, $\psi=\pi x$; hence $\partial\psi/\partial x$ has the correct value at all points of the plane. Lastly

$$\frac{\partial\psi}{\partial y}=\frac{(x-a)^2}{(x-a)^2+y^2}-\frac{(x+a)^2}{(x+a)^2+y^2},$$

and vanishes at all points (except B and C) of AD. It is clear that at entry the jet is normal ; its velocity is π.

For the present purpose the important question is whether the jet breaks away from the wall and so causes

Fig. 1.

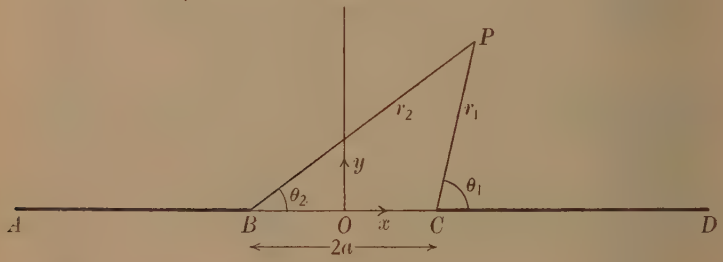

a flow and return of the external fluid. In this example it is evident that the jet does not break away, and it has not been thought necessary to draw the stream-lines. It is sufficient to consider the approximate value of the stream-function at great distance from O ; the value is

$$a(\sin 2\theta+\pi-2\theta), \quad . \quad . \quad . \quad . \quad . \quad (5)$$

where $x=r\cos\theta$, $y=r\sin\theta$, and decreases steadily as θ increases from 0 to π. A comparison of this result with the following example of an oblique jet is enough to show that there is no break-away in the present case.

The expression (5) is the stream-function of the slow fluid motion due to a jet of infinitesimal width, the limiting case of the radial divergent motions considered by Hamel.

§ 3. The stream-function for the motion due to an oblique jet is nearly as simple as that of the previous example.

If we suppose that fluid is introduced through the strip at a constant uniform velocity in a direction (the same at all points of the strip) inclined to the normal to the wall, we require a function that satisfies, as before, equations (1) and (2), and is such that

$$\frac{\partial\psi}{\partial x}=\text{const.}, \quad \frac{\partial\psi}{\partial y}=\text{const.}, \quad y=0, \quad |x|<a. \quad . \quad (6)$$

These conditions are satisfied by

$$\psi=(x+\kappa y-a)\theta_1-(x+\kappa y+a)\theta_2+\pi a, \quad . \quad . \quad (7)$$

where κ is constant. The function is biharmonic, has the constant values $-\pi a$ and πa on AB and CD, respectively, while at points of BC, $\psi=\pi x$. Lastly,

$$\frac{\partial\psi}{\partial y}=\frac{(x-a)^2}{(x-a)^2+y^2}-\frac{(x+a)^2}{(x+a)^2+y^2}+\kappa(\theta_1-\theta_2)$$
$$+\kappa y\left[\frac{x-a}{(x-a)^2+y^2}-\frac{x+a}{(x+a)^2+y^2}\right],$$

so that at points of AD (other than B and C)

$$\frac{\partial\psi}{\partial y}=\kappa(\theta_1-\theta_2);$$

the normal derivative is therefore zero at points of AB and CD, and has the constant value $\kappa\pi$ at points of BC. The angle that the jet initially makes with the normal to the plane is $\tan^{-1}\kappa$.

The value of ψ at a great distance from the origin shows the general type of the motion. At such points

$$\theta_1-\theta_2=\frac{2a}{r}\sin\theta,$$

approximately, hence ψ tends to the finite value

$$a[\sin 2\theta+\pi-2\theta+\kappa(1-\cos 2\theta)]. \quad . \quad . \quad . \quad (8)$$

We can suppose without loss of generality that κ is positive; then, as θ increases from 0 to π, the expression (8) at first increases and then decreases whatever the value of κ. This expression is the stream-function for another slow motion between two walls inclined at an angle π, the motion being radial, but partly convergent and partly divergent. It seems evident that in the motion represented by (7) the jet breaks away from the wall on one side

of the opening, and that there is a flow and return of the external fluid between the jet and the wall.

The stream-lines of the motion given by (7) are drawn in fig. 2. As the limiting expression for ψ shows that the motion is not essentially affected by the value of κ, a single value, unity, has been taken. Along the curves ψ/a, reckoned in degrees, takes the constant values marked. The coordinates of points of the contours were obtained

Fig. 2.

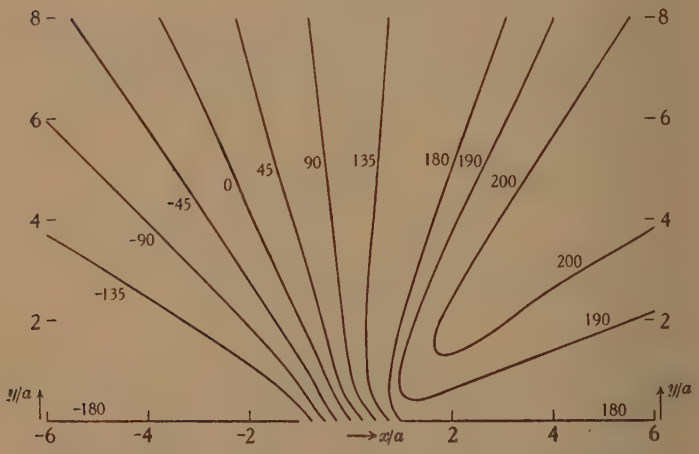

by linear interpolation and are shown in the following tables.

Values of x/a.

	$y/a=1$	$y/a=2$	$y/a=4$	$y/a=8$
$\psi/a=-135$ ...	−1·81	−3·30	−6·46	—
$\psi/a=-90$ ...	−1·22	−2·12	−4·06	—
$\psi/a=-45$ ...	−0·87	−1·48	−2·80	−5·54
$\psi/a=0$ ...	−0·57	−1·00	−1·90	−3·76
$\psi/a=45$ ...	−0·29	−0·58	−1·13	−2·25
$\psi/a=90$ ...	0	−0·14	−0·39	−0·81
$\psi/a=135$ ...	0·33	0·31	0·44	0·78
$\psi/a=180$ ...	0·80	1·00	1·64	3·11

An additional point on the contour $\psi/a=-90$ is

$x/a=-6·00$, $y/a=5·96$.

The coordinates of some points of two contours which correspond to the values 190 and 200 of ψ/a and which lie in the part of the fluid external to the jet are shown below. Each of these contours intersects twice any line parallel to the wall, and two values of x/a are therefore given where this is necessary for the figure.

$\psi/a = 190.$

y/a	0·41	0·51	1·00	2·00	4·00	8·00
x/a	1·40	1·00	0·99	1·27	2·11	4·01
			2·91	5·64		

$\psi/a = 200.$

y/a	1·32	2·00	3·82	4·00	8·00
x/a	2·00	1·77	6·00	2·92	5·53
		3·13			

This motion and that of § 2 are, of course, artificial; actually it would be necessary to lead the fluid up to the strip BC by a channel with parallel walls, the channel being in the direction of the normal to AB in one case and inclined in the other. The results suggest that the fluid would break away if the channel were inclined but not if it were normal to the boundary. There is, however, a difference between the two cases, for it seems clear that in an actual motion where the velocity would be zero at B and C and would increase inwards from these points, the tendency to break away would be less than in a motion with no variation in velocity across the strip. In the case of the normal channel we can conclude (in the limiting case of slow motion) that there will be no break away; if the channel is inclined the question remains open.

§ 4. The simplicity of the expression for the stream-function in the motion considered in § 2 due to a normal jet suggested the possibility of finding a second approximation, and so of making a partial allowance for the effect of inertia on the motion. For this we must start from

the exact equation satisfied by the stream-function in a steady motion, namely,

$$\nu\nabla_1{}^4\psi=\left(\frac{\partial\psi}{\partial x}\frac{\partial}{\partial y}-\frac{\partial\psi}{\partial y}\frac{\partial}{\partial x}\right)\nabla_1{}^2\psi, \quad . \quad . \quad . \quad (9)$$

where ν is the kinematic coefficient of viscosity. If we write ψ_1 for the first approximation to the stream-function, we have from § 2

$$\psi_1=(x-a)\theta_1-(x+a)\theta_2+\pi a\,; \quad . \quad . \quad . \quad (10)$$

this function is multiplied later by an arbitrary constant. Proceeding to the second approximation we write

$$\psi=\psi_1+\psi_2,$$

and find, since $\nabla_1{}^4\psi_1=0$, the equation

$$\nu\nabla_1{}^4\psi_2=\left(\frac{\partial\psi_1}{\partial x}\frac{\partial}{\partial y}-\frac{\partial\psi_1}{\partial y}\frac{\partial}{\partial x}\right)\nabla_1{}^2\psi_1 \quad . \quad . \quad (11)$$

for ψ_2. The boundary conditions for ψ_2 are

$$\frac{\partial\psi_2}{\partial x}=\frac{\partial\psi_2}{\partial y}=0, \quad y=0. \quad . \quad . \quad . \quad . \quad (12)$$

It is easily seen that

$$\nabla_1{}^2\psi_1=-2\left(\frac{\sin\theta_1}{r_1}-\frac{\sin\theta_2}{r_2}\right),$$

r_1, r_2 being shown in fig. 1, whence

$$\frac{\partial}{\partial x}\nabla_1{}^2\psi_1=2\left(\frac{\sin 2\theta_1}{r_1{}^2}-\frac{\sin 2\theta_2}{r_2{}^2}\right),$$

$$\frac{\partial}{\partial y}\nabla_1{}^2\psi_1=-2\left(\frac{\cos 2\theta_1}{r_1{}^2}-\frac{\cos 2\theta_2}{r_2{}^2}\right).$$

Substituting in equation (11) we have, after some reduction,

$$\begin{aligned}\nu\nabla_1{}^4\psi_2=&-2\left(\frac{\theta_1\cos 2\theta_1}{r_1{}^2}+\frac{\theta_2\cos 2\theta_2}{r_2{}^2}\right)\\&+2\left(\frac{\theta_1\cos 2\theta_2}{r_2{}^2}+\frac{\theta_2\cos 2\theta_1}{r_1{}^2}\right)\\&+\left(\frac{1}{r_1{}^2}-\frac{1}{r_2{}^2}\right)\sin 2(\theta_1-\theta_2). \quad (13)\end{aligned}$$

§5. The particular integrals of (13) arising from the terms involving a single suffix can be found directly, for we can write

$$\nabla_1^2 = \frac{\partial^2}{\partial r_1^2} + \frac{1}{r_1}\frac{\partial}{\partial r_1} + \frac{1}{r_1^2}\frac{\partial^2}{\partial \theta_1^2} = \frac{\partial^2}{\partial r_2^2} + \frac{1}{r_2}\frac{\partial}{\partial r_2} + \frac{1}{r_2^2}\frac{\partial^2}{\partial \theta_2^2}.$$

It can be shown that a solution of

$$\nabla_1^4 \phi_1 = \frac{\theta_1 \cos 2\theta_1}{r_1^2}$$

is

$$\phi_1 = -\frac{r_1^2}{64}(5\theta_1 \cos 2\theta_1 + 2\theta_1^2 \sin 2\theta_1).$$

For the evaluation of the other particular integrals complex variables can be conveniently used. We have first to find a solution of the equation

$$\nabla_1^4 \phi_2 = \frac{\theta_1 \cos 2\theta_2}{r_2^2} + \frac{\theta_2 \cos 2\theta_1}{r_1^2}.$$

Let

$$z = x + iy, \quad z' = x - iy,$$

and we have the equation

$$64i \frac{\partial^4 \phi_2}{\partial z^2 \partial z'^2} = \left[\frac{1}{(z+a)^2} + \frac{1}{(z'+a)^2}\right] \log \frac{z-a}{z'-a} + \left[\frac{1}{(z-a)^2} + \frac{1}{(z'-a)^2}\right] \log \frac{z+a}{z'+a},$$

of which a solution is

$$\begin{aligned} 128i\phi_2 = {} & z^2\left[\log(z'+a)\log(z'-a) - \frac{z'-a}{a}\log(z'-a) + \frac{z'+a}{a}\log(z'+a)\right] \\ & - z'^2\left[\log(z+a)\log(z-a) - \frac{z-a}{a}\log(z-a) + \frac{z+a}{a}\log(z+a)\right] \\ & + \log(z-a)[(z'+a)^2 \log(z'+a) - \tfrac{3}{2}(z'+a)^2] \\ & + \log(z+a)[(z'-a)^2 \log(z'-a) - \tfrac{3}{2}(z'-a)^2] \\ & - \log(z'-a)[(z+a)^2 \log(z+a) - \tfrac{3}{2}(z+a)^2] \\ & - \log(z'+a)[(z-a)^2 \log(z-a) - \tfrac{3}{2}(z-a)^2]; \end{aligned}$$

the value to be assigned to $\log(z'-a)$, for instance, is $\log r_1 - i\theta_1$. It will be observed that the expression for ϕ_2 is the sum of three terms of the form

$$(u+iv)(u'-iv') - (u-iv)(u'+iv'),$$

$u+iv$ and $u'+iv'$ denoting functions of z, and hence of three terms of the form

$$2i(u'v-uv').$$

Any biharmonic, and hence any harmonic, function can be added to the particular integral that has been found, and therefore, since $uv'+u'v$ is harmonic, we can replace the last form by either $4iu'v$ or $-4iuv'$. The integral can thus be expressed in the real form

$$\begin{aligned}32\phi_2=[x^2-y^2]\Big[&-\theta_1\log r_2-\theta_2\log r_1+\frac{1}{a}\{(x-a)\theta_1\\&-(x+a)\theta_2+y(\log r_1-\log r_2)\}\Big]\\&+\theta_1[\{(x+a)^2-y^2\}\{\log r_2-\tfrac{3}{2}\}-2(x+a)y\theta_2]\\&+\theta_2[\{(x-a)^2-y^2\}\{\log r_1-\tfrac{3}{2}\}-2(x-a)y\theta_1].\end{aligned}$$

Lastly, we require a solution of

$$\nabla_1{}^4\phi_3=\left(\frac{1}{r_1{}^2}-\frac{1}{r_2{}^2}\right)\sin 2(\theta_1-\theta_2)\,;$$

in terms of z, z' this is

$$4i\,\frac{\partial^4\phi_3}{\partial z^2\partial z'^2}=\frac{a^2(z^2-z'^2)(zz'-a^2)}{(z^2-a^2)^2(z'^2-a^2)^2},$$

or

$$\begin{aligned}4i\,\frac{\partial^4\phi_3}{\partial z^2\partial z'^2}=\frac{a}{4}\Big[&\frac{1}{(z+a)(z'-a)^2}+\frac{1}{(z+a)^2(z'-a)}\\&-\frac{1}{(z-a)(z'+a)^2}-\frac{1}{(z-a)^2(z'+a)}\Big],\end{aligned}$$

and a solution is

$$\begin{aligned}16i\phi_3=a&\log(z-a)[(z'+a)\log(z'+a)-(z'+a)]\\&-a\log(z'-a)[(z+a)\log(z+a)-(z+a)]\\&+a\log(z'+a)[(z-a)\log(z-a)-(z-a)]\\&-a\log(z+a)[(z'-a)\log(z'-a)-(z'-a)].\end{aligned}$$

Terms of the form $zf(z')$ or $z'f(z)$ can be ignored, for these will give biharmonic terms in ϕ_3; the last equation therefore reduces to

$$\begin{aligned}16i\phi_3=a(z+z')[&\log(z-a)\log(z'+a)\\&-\log(z+a)\log(z'-a)],\end{aligned}$$

whence

$$4\phi_3=ax[\theta_1\log r_2-\theta_2\log r_1].$$

§ 6. Combining the results of the last paragraph we have a particular integral of (13)

$$16v\psi_2 = r_1^2[\tfrac{5}{2}\theta_1 \cos 2\theta_1 + \theta_1^2 \sin 2\theta_1] + r_2^2[\tfrac{5}{2}\theta_2 \cos 2\theta_2 + \theta_2^2 \sin 2\theta_2] + [x^2 - y^2]\Big[-\theta_1 \log r_2 - \theta_2 \log r_1 + \frac{1}{a}\{(x-a)\theta_1 - (x+a)\theta_2 + y(\log r_1 - \log r_2)\}\Big] + \theta_1[\{(x+a)^2 - y^2\}\{\log r_2 - \tfrac{3}{2}\} - 2(x+a)y\theta_2] + \theta_2[\{(x-a)^2 - y^2\}\{\log r_1 - \tfrac{3}{2}\} - 2(x-a)y\theta_1] + 4ax[\theta_1 \log r_2 - \theta_2 \log r_1];$$

ignoring some biharmonic functions and simplifying we have

$$16v\psi_2 = \frac{x^2 - y^2}{a}[x(\theta_1 - \theta_2) + y(\log r_1 - \log r_2)] + 2xy[\theta_1 - \theta_2]^2 - 2ay[\theta_1^2 - \theta_2^2] + 6ax[\theta_1 \log r_2 - \theta_2 \log r_1].$$

Since $[x^2+y^2][x(\theta_1-\theta_2)+y(\log r_1 - \log r_2)]$ is biharmonic, an alternative form is

$$8v\psi_2 = -\frac{y^2}{a}[x(\theta_1 - \theta_2) + y(\log r_1 - \log r_2)] + xy[\theta_1 - \theta_2]^2 - ay[\theta_1^2 - \theta_2^2] + 3ax[\theta_1 \log r_2 - \theta_2 \log r_1]. \quad . \quad (14)$$

§ 7. The problem is now to add to ψ_2 a biharmonic function so as to satisfy the boundary conditions (12). So far as the first three terms

$$-\frac{y^2}{a}[x(\theta_1 - \theta_2) + y(\log r_1 - \log r_2)] + xy[\theta_1 - \theta_2]^2 - ay[\theta_1^2 - \theta_2^2]$$

of (14) are concerned this is straightforward, for the sum of the terms vanishes at the boundary, while the differential coefficient of the sum with regard to y is

$$x(\theta_1 - \theta_2)^2 - a(\theta_1^2 - \theta_2^2)$$

when $y=0$, and accordingly vanishes at all points of AD except between B and C. To satisfy the boundary condition we must add a biharmonic function zero at all points of AD and with a normal derivative equal to

$$\pi^2(a-x)$$

at points of BC and zero elsewhere on AD. A convenient form for the function is yv, where v is harmonic, for on

AD this vanishes and its normal derivative is equal to v; the determination of v is therefore simple. Let us take provisionally for the required biharmonic function

$$\pi y[(a-x)(\theta_1-\theta_2)-y(\log r_1-\log r_2)];$$

this determination and others below are not unique, and it will be necessary to consider the choice of the functions more closely later.

The fourth term, which is, apart from a constant factor,

$$x(\theta_1 \log r_2-\theta_2 \log r_1), \quad . \quad . \quad . \quad . \quad (15)$$

presents more difficulty, partly because it is not zero on the boundary. By adding a biharmonic function we can replace (15) by

$$(\theta_1-\theta_2)[(x+a) \log r_2+(x-a) \log r_1-2x \log 2a]; \quad (16)$$

the latter form is more convenient, for it is an odd function of x, while its boundary value is everywhere finite and is actually zero except between B and C. When $y=0$ the normal derivative of (16) is

$$\frac{2a}{x^2-a^2}\left[(x+a) \log \frac{r_2}{2a}+(x-a) \log \frac{r_1}{2a}\right], \quad . \quad (17)$$

and this value can be annulled as above by the addition of a biharmonic function of the form yv, the boundary value of v being equal and opposite to (17). Adding this second biharmonic function we now have

$$\begin{aligned}(\theta_1-\theta_2)[(x+a) \log r_2+(x-a) \log r_1-2x \log 2a] \\ -2ay\left[\frac{1}{r_1^2}\left\{(x-a) \log \frac{r_2}{2a}+y\theta_2\right\}\right. \\ \left.+\frac{1}{r_2^2}\left\{(x+a) \log \frac{r_1}{2a}+y\theta_1\right\}\right], \quad . \quad . \quad (18)\end{aligned}$$

in place of (15).

We have finally to add to (18) a biharmonic function that, when $y=0$, has a zero normal derivative and a value equal and opposite to (16). If v is harmonic, $v-y\frac{\partial v}{\partial y}$ is biharmonic and has a zero normal derivative when $y=0$; this function will therefore satisfy both conditions if the boundary value of v is equal and opposite to (16). On AD expression (16) vanishes when $|x| \geqslant a$, while for all other values of x the second factor can be

expanded as a power series in x; the boundary value of v must therefore be equal and opposite to

$$2a(\theta_1-\theta_2)\sum_{n=1}^{\infty}\left[\frac{1}{2n(2n+1)}\left(\frac{x}{a}-\frac{x^{2n+1}}{a^{2n+1}}\right)\right].$$

The imaginary part of the function

$$\frac{z^{2n+1}}{a^{2n+1}}[\log(z-a)-\log(z+a)]+\frac{2z^{2n}}{a^{2n}}+\frac{2z^{2n-2}}{3a^{2n-2}}+\ldots+\frac{2z^2}{(2n-1)a^2}$$

is harmonic, is finite when $|z|$ is large, and has the boundary value

$$\frac{x^{2n+1}}{a^{2n+1}}(\theta_1-\theta_2)$$

when $y=0$. The problem is therefore formally completed by taking for v a series of these functions.

§ 8. Collecting the previous results we have finally

$$\begin{aligned}8\nu\psi_2=&-\frac{y^2}{a}[x(\theta_1-\theta_2)+y(\log r_1-\log r_2)]+xy[\theta_1-\theta_2]^2\\&-ay[\theta_1{}^2-\theta_2{}^2]+\pi y[(a-x)(\theta_1-\theta_2)-y(\log r_1-\log r_2)]\\&+3a[\theta_1-\theta_2][(x+a)\log r_2+(x-a)\log r_1-2x\log 2a]\\&-6a^2y\left[\frac{1}{r_1{}^2}\left\{(x-a)\log\frac{r_2}{2a}+y\theta_2\right\}\right.\\&\left.+\frac{1}{r_2{}^2}\left\{(x+a)\log\frac{r_1}{2a}+y\theta_1\right\}\right]+6a^2\left[\mathrm{V}-y\frac{\partial \mathrm{V}}{\partial y}\right],\end{aligned}$$

. . . (19)

where V is the imaginary part of $\mathrm{F}(z)$ which is given by

$$\mathrm{F}(z)=\sum_{n=1}^{\infty}\frac{1}{2n(2n+1)}\left[\left\{\frac{z^{2n+1}}{a^{2n+1}}-\frac{z}{a}\right\}\{\log(z-a)-\log(z+a)\}+\frac{2z^{2n}}{a^{2n}}+\frac{2z^{2n-2}}{3a^{2n-2}}+\ldots+\frac{2z^2}{(2n-1)a^2}\right]. \quad (20)$$

It can be shown that $\mathrm{F}(z)$, defined as the sum of the series, is analytic at all points of the upper half-plane except B and C.

The function ψ_2 is not, however, uniquely determined by equations (11) and (12), and it is not difficult to see that expression (19) requires modification, for in order that the fluid motion may be symmetrical about Oy, the

stream-function must be an odd function of x, while the term

$$-6a^2y\left[\frac{1}{{r_1}^2}\left\{(x-a)\log\frac{r_2}{2a}+y\theta_2\right\}\right.$$
$$\left.+\frac{1}{{r_2}^2}\left\{(x+a)\log\frac{r_1}{2a}+y\theta_1\right\}\right]$$

of (19) is not odd. This term becomes an odd function if $\theta_1-\pi$ is substituted for θ_1, the effect of which is to add

$$6\pi a^2y^2/{r_2}^2$$

to (19). Now $y^2/{r_2}^2$ or $\sin^2\theta_2$ is (as the product of y and a harmonic function) a biharmonic function ; it is finite at great distance from O and vanishes together with its normal derivative on the boundary. Consequently after this alteration ψ_2 will still satisfy equations (11) and (12). The stream-function is now, as it should be, an odd function of x, but the choice is still not free from ambiguity, for, so far as the differential equation and boundary conditions are concerned, a function of the form

$$\mathrm{A}\sin^2\theta_1+\mathrm{B}\sin^2\theta_2,$$

where A and B are any constants, can be added, while there are further functions, as for instance

$$\frac{y\sin 2\theta_1}{{r_1}^2},$$

which tend to infinity as B or C is approached, and functions which tend to infinity at great distance from O. What determines the choice of additional functions is the condition that they must remove, so far as this is possible, singularities from ψ_2 and its derivatives. All that can be done in this case by the addition of functions of the above kind is to make the velocity derived from ψ_2 finite, and we proceed now to show that this is effected by the substitution of $\theta_1-\pi$ for θ_1 in the sixth term of (19).

§ 9. It will be sufficient to consider the values of ψ_2 in the neighbourhood of the point B, for the values near C will be numerically the same ; B is selected because the values near this point show the need for modifying the sixth term of (19). Since our purpose is merely to show that the velocity is finite near B, we can ignore all terms except those which individually would lead to an infinity

in the gradient of ψ_2. Thus all terms which involve only the suffix 1 can be left out, and also such terms as

$$xy\theta_2, \quad y^2 \log r_2,$$

which can be written in terms of r_2, θ_2 in the forms

$$(-a+r_2 \cos\theta_2) r_2\theta_2 \sin\theta_2, \quad r_2^2 \log r_2 \sin^2\theta_2,$$

and clearly have finite gradients near B. The first four terms and part of the fifth term of (19) can be ignored, so that we have only to consider, writing $\theta_1-\pi$ for θ_1 in the sixth term, the gradient of

$$3a(x+a)\theta_1 \log r_2 - 3a\theta_2[(x+a)\log r_2 + (x-a)\log r_1 - 2x \log 2a] - 6a^2 y\left[\frac{1}{r_1^2}\left\{(x-a)\log\frac{r_2}{2a} + y\theta_2\right\} + \frac{1}{r_2^2}\left\{(x+a)\log\frac{r_1}{2a} + y(\theta_1-\pi)\right\}\right] + 6a^2\left[\mathrm{V} - y\frac{\partial \mathrm{V}}{\partial y}\right].$$

Since near B

$$\log\frac{r_1}{2a} = -\frac{r_2\cos\theta_2}{2a}, \quad \theta_1-\pi = -\frac{r_2\sin\theta_2}{2a},$$

to the first power of r_2/a, the expression can be reduced further to

$$3ay \log r_2 + 3a(\theta_1-\theta_2)(x+a)\log r_2 + 6a^2\left[\mathrm{V} - y\frac{\partial \mathrm{V}}{\partial y}\right],$$

or

$$3ar_2 \log r_2[\sin\theta_2 + (\theta_1-\theta_2)\cos\theta_2] + 6a^2\left[\mathrm{V} - y\frac{\partial \mathrm{V}}{\partial y}\right]. \quad (21)$$

It remains now to consider the important part of the gradient of the last term.

When $|z|>a$, we have from equation (20),

$$\mathrm{F}(z) = \sum_{n=1}^{\infty} \frac{2}{2n+1}\left[\frac{1}{2n+1} + \frac{a^2}{3(2n+3)z^2} + \frac{a^4}{5(2n+5)z^4} + \dots\right],$$

or

$$\tfrac{1}{2}\mathrm{F}(z) = \sum_{m=0}^{\infty} \frac{a^{2m}}{(2m+1)z^{2m}}\left[\frac{1}{3(2m+3)} + \frac{1}{5(2m+5)} + \dots\right]$$

$$= \frac{\pi^2}{8} - 1 + \sum_{m=1}^{\infty} \frac{a^{2m}}{2m(2m+1)z^{2m}}\left[\frac{1}{3} + \frac{1}{5} + \dots + \frac{1}{2m+1}\right].$$

It follows that

$$\tfrac{1}{2}\mathrm{F}''(z) = \sum_{m=1}^{\infty} \frac{a^{2m}}{z^{2m+2}}\left[\frac{1}{3} + \frac{1}{5} + \dots + \frac{1}{2m+1}\right],$$

whence

$$\frac{1}{2}\left[1-\frac{a^2}{z^2}\right]F''(z)=\sum_{m=1}^{\infty}\frac{a^{2m}}{(2m+1)z^{2m+2}}$$

$$=-\frac{1}{2az}\left[\frac{2a}{z}+\log(z-a)-\log(z+a)\right],$$

so that finally

$$F''(z)=-\frac{2}{z^2-a^2}-\frac{z}{a(z^2-a^2)}[\log(z-a)-\log(z+a)].$$

This equality must hold for all values of z with which we are concerned; the direct proof of it is longer when $z_1<a$. Neither $F'(z)$ nor $F(z)$ can be expressed in finite terms, but we can readily find simple expressions for the parts of these functions that can lead to an infinity of the gradient of ψ_2. It can be shown that near $z=-a$ the relevant part of $F'(z)$ is

$$\frac{\log(z+a)}{4a}[4+\log(z+a)-2\log(z-a)],$$

and of $F(z)$

$$\frac{(z+a)\log(z+a)}{4a}[2+\log(z+a)-2\log(z-a)].$$

The expression actually required is

$$I[F(z)]-yR[F'(z)],$$

and the relevant part of this is

$$\frac{1}{2a}[-r_2\log r_2\sin\theta_2$$

$$+r_2\cos\theta_2\{-(\theta_1-\theta_2)\log r_2+\theta_2(1-\log r_1)\}].$$

The last term in the bracket can be ignored, and we find for the required term in

$$V-y\frac{\partial V}{\partial y},$$

$$-\frac{r_2\log r_2}{2a}[\sin\theta_2+(\theta_1-\theta_2)\cos\theta_2];$$

introducing this into expression (21), we see that the gradient of ψ_2 is finite in the neighbourhood of B. The expression found for ψ_2 is therefore correct.

§10. To determine the general character of the motion it suffices in this case to consider the values of the stream-function at a great distance from O. It is easily seen that when r is large we have approximately

$$6\nu\psi_2 = a^2 \sin^2\theta\left[\sin 2\theta + 12\left(\frac{\pi}{2} - \theta\right)\right]$$

from equation (19) after the alteration explained. This expression must be multiplied by U^2 if we take for the first approximation to the stream-function

$$U[(x-a)\theta_1 - (x+a)\theta_2 + \pi a].$$

so that the initial velocity of the jet is πU, U being, of course, a constant ; if this is done we have

$$\frac{\psi}{Ua} = \sin 2\theta + 2\left(\frac{\pi}{2} - \theta\right) + \frac{Ua}{6\nu}\sin^2\theta\left[\sin 2\theta + 12\left(\frac{\pi}{2} - \theta\right)\right], \quad . \quad . \quad . \quad (22)$$

for the sum of the first and second approximations at a great distance from O. It follows that

$$\frac{1}{Ua}\frac{d\psi}{d\theta} = \sin^2\theta\left[-4 + \frac{a}{3\nu}\left\{2\cos 2\theta - 5 + 12\cot\theta\left(\frac{\pi}{2} - \theta\right)\right\}\right].$$

If U is positive, so that the jet is divergent, as θ increases from 0 to $\frac{\pi}{2}$, $\frac{d\psi}{d\theta}$ is at first positive then negative and is zero once and only once, whatever the magnitude of Ua/ν; ψ therefore at first increases and then decreases. A divergent jet therefore breaks away from the boundary however small its velocity. We do not therefore find a critical velocity for the break-away, though at first sight it seemed possible that there would be one.

If the jet is convergent it is clear on other grounds that the motion is everywhere convergent and the case is of less interest. This is confirmed by expression (22) so far as it applies, for ψ can be shown to be monotonic (as θ increases from 0 to $\pi/2$) if U is negative, provided that the magnitude of Ua/ν is small enough ; ψ is not monotonic if Ua/ν is numerically greater than 12/7, but the second approximation would then be of the same order of magnitude as the first and expression (22) would not give an adequate approximation.

Equation (22) gives the type of stream-function that is found in the case of a jet of infinitesimal width, for an expression of exactly the same form is reached by taking expression (5) for the first approximation and calculating the second approximation as in the last paragraphs. We therefore find that the particular distribution of

initial velocity that is considered here is without influence on the flow at infinity, so far as the first two approximations are concerned. This no doubt holds for all subsequent approximations, in which case to find the motion at infinity for any initial velocity all that has to be done is to select the appropriate solution of the radial motion. This result cannot be wholly independent of the initial distribution of velocity, for the example of § 3 shows the importance of direction. It would, of course, be desirable to examine a distribution with a zero velocity at B and C, but the detailed calculation on the above lines of the second approximation would require somewhat heavy analysis, though there is no reason to suppose that the method used is not applicable to this case. The flow at infinity in the case of a more complicated distribution of velocity could, however, probably be found without trouble, for there is an alternative, suitable for this purpose, to the method of these paragraphs. The second approximation requires a solution of

$$\nabla_1^4 \psi = f(x, y)$$

where $f(x, y)$ is a given function, subject to the conditions

$$\frac{\partial \psi}{\partial x} = \frac{\partial \psi}{\partial y} = 0, \quad y = 0,$$

and it is known from a problem in the theory of elasticity * that a solution is given by

$$\psi = \frac{1}{8\pi} \int\int \left[-\mathrm{R}^2 \log \frac{\mathrm{R}'}{\mathrm{R}} + \tfrac{1}{2}(\mathrm{R}'^2 - \mathrm{R}^2) \right] f(x', y') dx' dy',$$

where

$$\mathrm{R}^2 = (x-x')^2 + (y-y')^2, \quad \mathrm{R}'^2 = (x-x')^2 + (y+y')^2,$$

the integral being taken over the upper half-plane. For the above calculation of the second approximation this method was not found convenient and was rejected, but it should find quite simply the limiting form of the expression for the stream-function. On the other hand, what is ultimately of interest is rather the local flow near B and C than that at a great distance, for the most important case, if such a one exists, would be one in which the break-away of the jet was confined to a limited region, and the general character of a motion of this kind could not be inferred from the flow at infinity.

* A. E. H. Love, ' Mathematical Theory of Elasticity ' (3rd Edition), § 314 (*b*).

LX. *The Transverse Vibration of a Square Plate clamped at Four Edges.* *By* S. Tomotika, *D.Sc.* *

Introduction.

§1. THE problem of transverse vibration of a rectangular or square plate clamped at all four edges is one of the most important and interesting characteristic-value problems ("Eigenwertprobleme") in elastokinetics †. However, the complete analytical solution of the problem has not yet been made not, as is pointed out by A. E. H. Love ‡ and also by R. Courant §. Some time ago K. Sezawa || discussed the subject, assuming a simple form of displacement which satisfies the differential equation of transverse vibration but does not satisfy the edge conditions except at the corners and the mid-points of the sides. His result for the fundamental mode of vibration of a square plate is expressed as $\rho ha^4p^2/D\pi^4 = 14{\cdot}4$, where p is the frequency of vibration in 2π seconds, ρ the density of the material of the plate, a the length of the side of the square, h the thickness of the plate, which is assumed to be uniform. D is the flexural rigidity, and is given by the formula $D = \frac{1}{12}Eh^3\,(1-\sigma^2)^{-1}$, where E and σ are Young's modulus and Poisson's ratio of the material of the plate respectively.

On the other hand, if we apply the well-known Rayleigh's principle to the case of a square plate, assuming the transverse displacement w of the plate in the form

$$w = w_0 \cos^2(\pi x/a)\cos^2(\pi y/a)\cos(pt+\epsilon),$$

which satisfies the boundary conditions at the edges $x = \pm a/2$, $y = \pm a/2$, but not the differential equation of vibration, the axes of x and y being supposed to be taken parallel to the edges, we can easily obtain the result that $\rho ha^4p^2/D\pi^4 = 14{\cdot}22$ for the fundamental mode

* Communicated by Prof. G. I. Taylor, F.R.S.

† R. Courant-D. Hilbert, 'Methoden der mathematischen Physik,' vol. i. 2nd ed. pp. 263–264 (1931).

‡ A. E. H. Love, 'The Mathematical Theory of Elasticity,' 4th ed. p. 496 (1927).

§ R. Courant-D. Hilbert, *loc. cit.* p. 264.

|| K. Sezawa, "On the Lateral Vibration of a Rectangular Plate clamped at Four Edges," Report Aeron. Res. Inst. Tokyo Imp. Univ. no. 70 (1931).

of vibration. Further, a better approximate value can be obtained by assuming the displacement in the form

$$w = w_0 \cos^2(\pi x/a) \cos^2(\pi y/a) \times \{1 + \lambda \cos(\pi x/a) \cos(\pi y/a)\} \cos(pt + \epsilon),$$

and choosing λ such that the value of p will become a minimum, and the result is $\rho h a^4 p^2/D\pi^4 = 13{\cdot}37$ for the fundamental mode of vibration. Since, as is well known, even the " Rayleigh " values thus calculated are greater than the true value, it is seen that Sezawa's value is too high.

Recently Prof. G. I. Taylor * has discussed the statical problem of the buckling under edge thrusts of a rectangular plate which is clamped at its four edges. He has obtained a formal solution of the problem by finding the forms of displacement which satisfy both the clamped edge condition and the differential equation of neutral equilibrium, and the magnitudes of the thrusts which are necessary in order to maintain these displacements have been expressed as values which cause an infinite determinant to vanish. By performing various numerical calculations he has determined for the case of a square plate subjected to equal thrusts perpendicular to all its edges the lowest critical edge thrust under which the neutral equilibrium is stable.

A similar analysis can be applied to the problem of transverse vibration of a rectangular or square plate clamped at four edges, and the object of the present paper is to show the result of such an application.

In the present paper a formal solution for the transverse vibration of a square plate is given when all four edges are clamped. The forms of displacement which satisfy both the clamped edge condition and the differential equation of transverse vibration are found, and the frequencies of vibration are expressed as values which cause an infinite determinant to vanish. The numerical work necessary for completing the solution is carried out for the case of the fundamental mode of vibration of the square plate, and the frequency of the said mode is determined.

* G. I. Taylor, " The Buckling Load for a Rectangular Plate with Four Clamped Edges," *Zeits. f. angw. Math. Mech.* xiii. pp. 147–152 (1933).

Formal Solution of the Problem.

§ 2. Let the coordinate axes (x, y) be taken in the middle plane of a square plate of uniform small thickness in such a way that the origin coincides with the centre of the plate and the axes are parallel to the sides, and let the length of the side of the square and the thickness of the plate be denoted by a and h respectively.

We denote the density, Young's modulus, and Poisson's ratio of the material of the plate, which is assumed to be uniform and isotropic, by ρ, E, and σ respectively.

Then, if w be the transverse displacement of a point on the middle plane, the differential equation for the transverse vibration of the plate is given by *

$$\mathrm{D}\left(\frac{\partial^4 w}{\partial x^4}+2\frac{\partial^4 w}{\partial x^2\partial y^2}+\frac{\partial^4 w}{\partial y^4}\right)+\rho h\frac{\partial^2 w}{\partial t^2}=0, \quad . \quad . \quad (1)$$

where D denotes the flexural rigidity, given in terms of h, E, σ by the formula

$$\mathrm{D}=\frac{1}{12}\frac{\mathrm{E}h^3}{1-\sigma^2}.$$

When the four edges of the square plate are clamped, the boundary conditions at the edges are

$$\left.\begin{aligned} w=0, \quad \frac{\partial w}{\partial x}=0, \quad \text{at} \quad x=\pm\frac{a}{2};\\ w=0, \quad \frac{\partial w}{\partial y}=0, \quad \text{at} \quad y=\pm\frac{a}{2}. \end{aligned}\right\} \quad . \quad . \quad . \quad (2)$$

Writing $x=a\xi/\pi$, $y=a\eta/\pi$, the square whose sides are $x=\pm a/2$, $y=\pm a/2$ is transformed into a square whose sides are $\xi=\pm\pi/2$, $\eta=\pm\pi/2$, and equation (1) becomes

$$\frac{\partial^4 w}{\partial\xi^4}+2\frac{\partial^4 w}{\partial\xi^2\partial\eta^2}+\frac{\partial^4 w}{\partial\eta^4}+\frac{\rho h a^4}{\mathrm{D}\pi^4}\frac{\partial^2 w}{\partial t^2}=0, \quad . \quad . \quad (3)$$

while the boundary conditions become as follows :—

$$\left.\begin{aligned} w=0, \quad \frac{\partial w}{\partial\xi}=0, \quad \text{at} \quad \xi=\pm\frac{\pi}{2};\\ w=0, \quad \frac{\partial w}{\partial\eta}=0, \quad \text{at} \quad \eta=\pm\frac{\pi}{2}. \end{aligned}\right\} \quad . \quad . \quad . \quad (4)$$

* See, *e. g.*, A. E. H. Love, 'The Mathematical Theory of Elasticity,' 4th ed. p. 496 (1927).

When the plate vibrates in a normal mode, the displacement w is of the form

$$w = \mathrm{W}\cos(pt+\epsilon), \quad . \quad . \quad . \quad . \quad . \quad . \quad (5)$$

where W is a function of x, y, or transforming x, y into ξ, η, it is a function of ξ, η, and p is the frequency of vibration in 2π seconds. $\cos(pt+\epsilon)$ is the normal coordinate, and W is the normal function. If we put (5) in (3) we get the partial differential equation for W, namely,

$$\frac{\partial^4 \mathrm{W}}{\partial\xi^4} + 2\frac{\partial^4 \mathrm{W}}{\partial\xi^2\partial\eta^2} + \frac{\partial^4 \mathrm{W}}{\partial\eta^4} - k^2\mathrm{W} = 0, \quad . \quad . \quad . \quad (6)$$

with

$$k^2 \equiv \frac{\rho h a^4 p^2}{\mathrm{D}\pi^4}, \quad . \quad . \quad . \quad . \quad . \quad . \quad . \quad (7)$$

which is a non-dimensional quantity, *i. e.*, a pure number.

The boundary conditions to be satisfied by the normal function W at the edges of the plate are easily seen to be $\mathrm{W} = 0$, $\partial\mathrm{W}/\partial\xi = 0$ at $\xi = \pm\pi/2$ and $\mathrm{W} = 0$, $\partial\mathrm{W}/\partial\eta = 0$ at $\eta = \pm\pi/2$.

Thus, our problem is to find a solution of (6) other than $\mathrm{W} = 0$ which satisfies the condition $\mathrm{W} = 0$ at $\xi = \pm\pi/2$ and $\eta = \pm\pi/2$ and also the conditions $\partial\mathrm{W}/\partial\xi = 0$ at $\xi = \pm\pi/2$ and $\partial\mathrm{W}/\partial\eta = 0$ at $\eta = \pm\pi/2$.

§ 3. The method of solving the problem adopted in the present paper is quite similar to that adopted by Prof. G. I. Taylor * in his treatment of the statical problem of the buckling of a rectangular plate—that is to say, the method adopted is first to find solutions of the differential equation (6), which satisfy the condition $\mathrm{W} = 0$ at the edges, and then it is shown that an infinite number of these can be combined together in such a way that the remaining clamped edge conditions $\partial\mathrm{W}/\partial\xi = 0$, $\partial\mathrm{W}/\partial\eta = 0$ are also satisfied provided a certain relationship exists between the size of the plate and the frequency of vibration.

In the following work we shall only consider such normal modes of vibration in which displacements are symmetrical with respect to both axes ξ, η, so that ξ and η occur in W only as even functions.

* G. I. Taylor, *loc. cit.*

The function $e^{\lambda\eta}\cos n\xi$ satisfies the condition $W=0$ at $\xi=\pm\pi/2$ provided n is an odd integer, and it also satisfies equation (6) provided

$$\lambda^4-2n^2\lambda^2+n^4-k^2=0,$$

or
$$(\lambda^2-n^2)^2=k^2. \quad . \quad . \quad . \quad . \quad . \quad . \quad (8)$$

The roots of this equation are

$$\left.\begin{aligned} \lambda&=\pm\sqrt{k+n^2}, \quad \pm i\sqrt{k-n^2}, \quad \text{when } n<\sqrt{k}\,; \\ \lambda&=\pm\sqrt{n^2+k}, \quad \pm\sqrt{n^2-k}, \quad \text{when } n>\sqrt{k}. \end{aligned}\right\} \quad (9)$$

Thus, when $n<\sqrt{k}$ particular solutions of (6) are

$$e^{\pm\sqrt{k+n^2}\eta}\cos n\xi,\ e^{\pm i\sqrt{k-n^2}\eta}\cos n\xi,$$

and by a suitable combination of these four terms an even function W is obtained which satisfies $W=0$ at $\eta=\pm\pi/2$. We have

$$W=(\cosh\tfrac{1}{2}\pi\sqrt{k+n^2}\cos\sqrt{k-n^2}\eta$$
$$-\cos\tfrac{1}{2}\pi\sqrt{k-n^2}\cosh\sqrt{k+n^2}\eta)\cos n\xi. \quad (10\,a)$$

Similarly, when $n>\sqrt{k}$ we have

$$W=(\cosh\tfrac{1}{2}\pi\sqrt{n^2+k}\cosh\sqrt{n^2-k}\eta$$
$$-\cosh\tfrac{1}{2}\pi\sqrt{n^2-k}\cosh\sqrt{n^2+k}\eta)\cos n\xi, \quad (10\,b)$$

which satisfies the condition $W=0$ at $\eta=\pm\pi/2$.

Since functions of the forms (10 *a*) and (10 *b*) satisfy both the differential equation (6) and the boundary condition $W=0$ at $\xi=\pm\pi/2$, $\eta=\pm\pi/2$ provided n is any odd integer; a linear combination of such functions also satisfies the equation (6) and the boundary condition $W=0$.

If W is a function satisfying (6), then when W and $dW/d\nu$ are given at all points of a closed boundary, W is in general determined at all points within it, $dW/d\nu$ denoting the rate of change in W along a normal ν to the boundary. Therefore in order that a series of functions of forms (10 *a*) and (10 *b*) may be capable of representing all possible values of W inside the square consistent with $W=0$ at its edges, it must be capable of representing arbitrary symmetrical distributions of $\partial W/\partial\eta$ along $\eta=\pm\pi/2$ and of $\partial W/\partial\xi$ along $\xi=\pm\pi/2$.

Now we construct the series

$$\begin{aligned} W = {} & \sum_{n<\sqrt{k}}{}_0 A_n(\cosh \tfrac{1}{2}\pi\sqrt{k+n^2} \cos \sqrt{k-n^2}\eta \\ & \quad -\cos \tfrac{1}{2}\pi\sqrt{k-n^2} \cosh \sqrt{k+n^2}\eta) \cos n\xi \\ & + \sum_{n>\sqrt{k}}{}_0 A_n(\cosh \tfrac{1}{2}\pi\sqrt{n^2+k} \cosh \sqrt{n^2-k}\eta \\ & \quad -\cosh \tfrac{1}{2}\pi\sqrt{n^2-k} \cosh \sqrt{n^2+k}\eta) \cos n\xi, \\ & \qquad\qquad\qquad\qquad\qquad\qquad . \quad . \quad . \quad (11) \end{aligned}$$

where Σ_0 indicates that only the positive odd integral values of n are to be included in the summation.

Then. this series satisfies the differential equation (6) and the condition $W = 0$ at the edges of the plate, and it is capable of representing any assigned symmetrical distribution of $\partial W/\partial\eta$ along $\eta = \pm\pi/2$, because any even function of ξ which vanishes at $\xi = \pm\pi/2$ can be expanded between the limits $\pm\pi/2$ in a cosine series of odd multiples of ξ.

Similarly, since the differential equation (6) is symmetrical with respect to ξ and η, the series

$$\begin{aligned} W = {} & \sum_{n<\sqrt{k}}{}_0 B_n(\cosh \tfrac{1}{2}\pi\sqrt{k+n^2} \cos \sqrt{k-n^2}\xi \\ & \quad -\cos \tfrac{1}{2}\pi\sqrt{k-n^2} \cosh \sqrt{k+n^2}\xi) \cos n\eta \\ & + \sum_{n>\sqrt{k}}{}_0 B_n(\cosh \tfrac{1}{2}\pi\sqrt{n^2+k} \cosh \sqrt{n^2-k}\xi \\ & \quad -\cosh \tfrac{1}{2}\pi\sqrt{n^2-k} \cosh \sqrt{n^2+k}\xi) \cos n\eta, \\ & \qquad\qquad\qquad\qquad\qquad\qquad . \quad . \quad . \quad (12) \end{aligned}$$

where Σ_0 has the same meaning as before, satisfies the said differential equation (6) as well as the boundary condition $W = 0$ at all edges of the plate. Also this series can represent any assigned symmetrical distribution of $\partial W/\partial\xi$ along the edges $\xi = \pm\pi/2$.

Next, combining (11) and (12), we consider the double series

$$\begin{aligned} W = {} & \sum_{n<\sqrt{k}}{}_0 [A_n(\cosh \tfrac{1}{2}\pi\sqrt{k+n^2} \cos \sqrt{k-n^2}\eta \\ & \quad -\cos \tfrac{1}{2}\pi\sqrt{k-n^2} \cosh \sqrt{k+n^2}\eta) \cos n\xi \\ & \quad +B_n(\cosh \tfrac{1}{2}\pi\sqrt{k+n^2} \cos \sqrt{k-n^2}\xi \\ & \quad -\cos \tfrac{1}{2}\pi\sqrt{k-n^2} \cosh \sqrt{k+n^2}\xi) \cos n\eta] \end{aligned}$$

$$+\sum_{n>\sqrt{k}}{}_0\,[\mathrm{A}_n(\cosh\tfrac{1}{2}\pi\sqrt{n^2+k}\,\cosh\sqrt{n^2-k}\eta - \cosh\tfrac{1}{2}\pi\sqrt{n^2-k}\,\cosh\sqrt{n^2+k}\eta)\cos n\xi + \mathrm{B}_n(\cosh\tfrac{1}{2}\pi\sqrt{n^2+k}\,\cosh\sqrt{n^2-k}\xi - \cosh\tfrac{1}{2}\pi\sqrt{n^2-k}\,\cosh\sqrt{n^2+k}\xi)\cos n\eta], \quad . \ . \ . \quad (13)$$

which evidently satisfies (6) and the condition $\mathrm{W}=0$ at the edges.

When an assigned distribution of the inclination of the plate at the edges is symmetrical with respect to the axes ξ and η, $(\partial\mathrm{W}/\partial\xi)_{\xi=-\pi/2} = -(\partial\mathrm{W}/\partial\xi)_{\xi=\pi/2}$ and $(\partial\mathrm{W}/\partial\eta)_{\eta=-\pi/2} = -(\partial\mathrm{W}/\partial\eta)_{\eta=\pi/2}$, and in the present case the expression for $(\partial\mathrm{W}/\partial\xi)_{\xi=\pi/2}$, for instance, takes, by (13), the form

$$(\partial\mathrm{W}/\partial\xi)_{\xi=\pi/2} = \sum_{n<\sqrt{k}}{}_0\,[(-1)^{\frac{n+1}{2}} n\mathrm{A}_n(\cosh\tfrac{1}{2}\beta_n\pi\cos\alpha_n\eta - \cos\tfrac{1}{2}\alpha_n\pi\cosh\beta_n\eta) - \mathrm{B}_n(\alpha_n\cosh\tfrac{1}{2}\beta_n\pi\sin\tfrac{1}{2}\alpha_n\pi + \beta_n\cos\tfrac{1}{2}\alpha_n\pi\sinh\tfrac{1}{2}\beta_n\pi)\cos n\eta] + \sum_{n>\sqrt{k}}{}_0\,[(-1)^{\frac{n+1}{2}} n\mathrm{A}_n(\cosh\tfrac{1}{2}\beta_n\pi\cosh\alpha_n^*\eta - \cosh\tfrac{1}{2}\alpha_n^*\pi\cosh\beta_n\eta) + \mathrm{B}_n(\alpha_n^*\cosh\tfrac{1}{2}\beta_n\pi\sinh\tfrac{1}{2}\alpha_n^*\pi - \beta_n\cosh\tfrac{1}{2}\alpha_n^*\pi\sinh\tfrac{1}{2}\beta_n\pi)\cos n\eta], \quad . \ . \ . \quad (14)$$

where we put for brevity

$$\left.\begin{aligned} &\alpha_n = \sqrt{k-n^2}, \quad [n<\sqrt{k}]\,; \quad \beta_n = \sqrt{k+n^2}\,; \\ &\alpha_n^* = \sqrt{n^2-k}, \quad [n>\sqrt{k}]. \end{aligned}\right\} \quad (15)$$

If all the A_n's were known, the series containing the A_n's in (14) would be a known function of η, $\mathrm{F}(\eta)$ say, which could be expanded in a cosine series of odd multiples of η between the limits $\eta = \pm\pi/2$. The given arbitrary symmetrical distribution of $(\partial\mathrm{W}/\partial\xi)_{\xi=\pi/2}$ could also be expressed in such a series, and consequently the values of B_n could be determined, by equating coefficients of $\cos n\eta$. In like manner, if the B_n's were known the values of A_n could be determined, so that $\partial\mathrm{W}/\partial\eta$ could have any arbitrary symmetrical distribution along $\eta = \pm\pi/2$.

Therefore the double series (13) appears to be capable of representing a function for which $\partial\mathrm{W}/\partial\xi$ along $\xi = \pm\pi/2$,

and $\partial W/\partial\eta$ along $\eta = \pm\pi/2$ have any assigned symmetrical distributions. The determination of the actual values of the A_n's and B_n's in any given case would necessitate the solution of an infinite series of linear equations.

If $\partial W/\partial\xi = 0$ along $\xi = \pm\pi/2$ and $\partial W/\partial\eta = 0$ along $\eta = \pm\pi/2$, the solution of this series of equations would in general yield the result that all the A_n's and all the B_n's are zero; but if a certain special relationship exists between the dimensions of the plate and the frequency p of vibration, namely, if the relation obtained by eliminating all the A_n's and B_n's from the system of linear equations exists, we can obtain a displacement in the normal mode of vibration, and with the aid of the said relationship the frequency of vibration can be determined as a function of the dimensions of the plate, the elastic constants and density of the material of the plate.

§ 4. In the analysis which follows we shall confine ourselves to the most important case of the fundamental mode of vibration of the square plate. It is easily seen that we may put $A_n = B_n$ in this case, and the appropriate form for the normal function W is

$$\begin{aligned} W = {} & \sum_{n<\sqrt{k}} A_n[(\cosh \tfrac{1}{2}\pi\sqrt{k+n^2} \cos \sqrt{k-n^2}\eta \\ & \quad -\cos \tfrac{1}{2}\pi\sqrt{k-n^2} \cosh \sqrt{k+n^2}\eta) \cos n\xi \\ & +(\cosh \tfrac{1}{2}\pi\sqrt{k+n^2} \cos \sqrt{k-n^2}\xi \\ & \quad -\cos \tfrac{1}{2}\pi\sqrt{k-n^2} \cosh \sqrt{k+n^2}\xi) \cos n\eta] \\ & + \sum_{n>\sqrt{k}} A_n[(\cosh \tfrac{1}{2}\pi\sqrt{n^2+k} \cosh \sqrt{n^2-k}\eta \\ & \quad -\cosh \tfrac{1}{2}\pi\sqrt{n^2-k} \cosh \sqrt{n^2+k}\eta) \cos n\xi \\ & +(\cosh \tfrac{1}{2}\pi\sqrt{n^2+k} \cosh \sqrt{n^2-k}\xi \\ & \quad -\cosh \tfrac{1}{2}\pi\sqrt{n^2-k} \cosh \sqrt{n^2+k}\xi) \cos n\eta], \end{aligned} \qquad \ldots (16)$$

and the boundary conditions $(\partial W/\partial\xi)_{\xi=\pm\pi/2} = 0$ give, with the notations (15),

$$\begin{aligned} & \sum_{n<\sqrt{\ }} A_n[(-1)^{\frac{n-1}{2}} n(\cosh \tfrac{1}{2}\beta_n\pi \cos \alpha_n\eta - \cos \tfrac{1}{2}\alpha_n\pi \cosh \beta_n\eta) \\ & \quad +(\alpha_n \cosh \tfrac{1}{2}\beta_n\pi \sin \tfrac{1}{2}\alpha_n\pi + \beta_n \cos \tfrac{1}{2}\alpha_n\pi \sinh \tfrac{1}{2}\beta_n\pi) \cos n\eta] \end{aligned}$$

$$+\sum_{n>\sqrt{k}}{}_0 A_n[(-1)^{\frac{n-1}{2}} n(\cosh \tfrac{1}{2}\beta_n\pi \cosh \alpha_n^*\eta - \cosh \tfrac{1}{2}\alpha_n^*\pi \cosh \beta_n\eta)$$
$$+(-\alpha_n^* \cosh \tfrac{1}{2}\beta_n\pi \sinh \tfrac{1}{2}\alpha_n^*\pi$$
$$+\beta_n \cosh \tfrac{1}{2}\alpha_n^*\pi \sinh \tfrac{1}{2}\beta_n\pi) \cos n\eta] = 0,$$
. . . (17)

which must be fulfilled for all values of η between $\pm\pi/2$.

To carry out the operation indicated at the end of the preceding paragraph it is convenient to expand each term of the series in (17) in a cosine series of even multiples of η, and the coefficient of $\cos s\eta$ in the series so obtained is then equated to zero for each even value of s in order that the above condition (17), *i. e.*, the condition $\partial W/\partial\xi = 0$ at the edges $\xi = \pm\pi/2$, may be satisfied for all values of η between $\pm\pi/2$.

The necessary cosine series valid between $\eta = \pm\pi/2$ are

$$\cosh \alpha\eta = \frac{4\alpha}{\pi} \sinh \frac{1}{2}\alpha\pi\left(\frac{1}{2\alpha^2} - \frac{\cos 2\eta}{\alpha^2+2^2} + \frac{\cos 4\eta}{\alpha^2+4^2} - \ldots\right),$$
. . . (18)

$$\cos \alpha\eta = \frac{4\alpha}{\pi} \sin \frac{1}{2}\alpha\pi\left(\frac{1}{2\alpha^2} - \frac{\cos 2\eta}{\alpha^2-2^2} + \frac{\cos 4\eta}{\alpha^2-4^2} - \ldots\right). \quad (19)$$

Inserting expansions of this type for $\cos n\eta$, $\cos \alpha_n\eta$, $\cosh \alpha_n^*\eta$, $\cosh \beta_n\eta$ in the left-hand side of (17), it is found that the condition $\partial W/\partial\xi = 0$ at $\xi = \pm\pi/2$ is satisfied if for every even value of s

$$\sum_n{}_0 (-1)^{\frac{n-1}{2}} n a_{ns} A_n = 0, \quad . \quad . \quad . \quad . \quad (20)$$

where a_{ns} takes different forms according as n is less or greater than $\sqrt{k}$, namely :—

(i) When $n < \sqrt{k}$,

$$a_{ns} = \frac{\alpha_n \cosh \tfrac{1}{2}\beta_n\pi \sin \tfrac{1}{2}\alpha_n\pi}{\alpha_n^2 - s^2} - \frac{\beta_n \cos \tfrac{1}{2}\alpha_n\pi \sinh \tfrac{1}{2}\beta_n\pi}{\beta_n^2 + s^2}$$
$$+ \frac{\alpha_n \cosh \tfrac{1}{2}\beta_n\pi \sin \tfrac{1}{2}\alpha_n\pi + \beta_n \cos \tfrac{1}{2}\alpha_n\pi \sinh \tfrac{1}{2}\beta_n\pi}{n^2 - s^2}; \quad (21\,a)$$

(ii) When $n > \sqrt{k}$,

$$a_{ns} = \frac{\alpha_n^* \cosh \tfrac{1}{2}\beta_n\pi \sinh \tfrac{1}{2}\alpha_n^*\pi}{\alpha_n^{*2} + s^2} - \frac{\beta_n \cosh \tfrac{1}{2}\alpha_n^*\pi \sinh \tfrac{1}{2}\beta_n\pi}{\beta_n^2 + s^2}$$
$$+ \frac{-\alpha_n^* \cosh \tfrac{1}{2}\beta_n\pi \sinh \tfrac{1}{2}\alpha_n^*\pi + \beta_n \cosh \tfrac{1}{2}\alpha_n^*\pi \sinh \tfrac{1}{2}\beta_n\pi}{n^2 - s^2}.$$
. . . (21 *b*)

It is easily found that the remaining boundary conditions $\partial W/\partial\eta = 0$ at $\eta = \pm\pi/2$ leads to the same series of equations as (20).

Eliminating the A_n's between the equations (20) we obtain the infinite determinantal equation :

$$\Delta = \begin{vmatrix} a_{10} & a_{30} & a_{50} & \cdot & \cdot & \cdot & \cdot \\ a_{12} & a_{32} & a_{52} & \cdot & \cdot & \cdot & \cdot \\ a_{14} & a_{34} & a_{54} & \cdot & \cdot & \cdot & \cdot \\ \cdot & \cdot & \cdot & \cdot & \cdot & \cdot & \cdot \\ \cdot & \cdot & \cdot & \cdot & \cdot & \cdot & \cdot \end{vmatrix} = 0. \quad . \quad . \quad (22)$$

As mentioned already in the introduction an approximate value of $k^2 = \rho h a^4 p^2/D\pi^4$ for the fundamental mode of vibration is obtained by Rayleigh's principle as 13·37 assuming the normal function W in the form

$$W = w_0 \cos^2\xi \cos^2\eta(1+\lambda\cos\xi\cos\eta).$$

It is, however, evident that the "Rayleigh" value so calculated is in general greater than the true value. Therefore the true value of $\sqrt{k}$ is less than $(13{\cdot}37)^{\frac{1}{2}} = 1{\cdot}912$ approximately. Thus we see that

$$n < \sqrt{k} \quad \text{when} \quad n = 1;$$
$$n > \sqrt{k} \quad \text{when} \quad n \geqq 3.$$

Hence, of the coefficients a_{ns} in (20) only the a_{1s}'s take the form (21 *a*) and all the remaining coefficients take the form (21 *b*).

Using for α_n, α_n^*, β_n their respective original forms given in (15), we put

$$c_{1s} = \sqrt{k-1}\tan\tfrac{1}{2}\pi\sqrt{k-1}\left\{\frac{1}{k-1-s^2} + \frac{1}{1-s^2}\right\}$$
$$-\sqrt{k+1}\tanh\tfrac{1}{2}\pi\sqrt{k+1}\left\{\frac{1}{k+1+s^2} - \frac{1}{1-s^2}\right\}, \quad . \quad . \quad . \quad (23\,a)$$

$$c_{ns} = \sqrt{n^2-k}\tanh\tfrac{1}{2}\pi\sqrt{n^2-k}\left\{\frac{1}{n^2-k+s^2} - \frac{1}{n^2-s^2}\right\}$$
$$-\sqrt{n^2+k}\tanh\tfrac{1}{2}\pi\sqrt{n^2+k}\left\{\frac{1}{n^2+k+s^2} - \frac{1}{n^2-s^2}\right\}.$$
$$[n \geqq 3]. \quad . \quad . \quad (23\,b)$$

Then we have

$$\left.\begin{aligned} a_{1s} &= \cos \tfrac{1}{2}\pi\sqrt{k-1}\,\cosh \tfrac{1}{2}\pi\sqrt{k+1}\,c_{1s}, \\ a_{ns} &= \cosh \tfrac{1}{2}\pi\sqrt{n^2-k}\,\cosh \tfrac{1}{2}\pi\sqrt{n^2+k}\,c_{ns}, \quad [n \geqq 3] \end{aligned}\right\}$$

and the determinantal equation (22) becomes

$$\Delta = \begin{vmatrix} c_{10} & c_{30} & c_{50} & \cdot & \cdot & \cdot & \cdot \\ c_{12} & c_{32} & c_{52} & \cdot & \cdot & \cdot & \cdot \\ c_{14} & c_{34} & c_{54} & \cdot & \cdot & \cdot & \cdot \\ \cdot & \cdot & \cdot & \cdot & \cdot & \cdot & \cdot \\ \cdot & \cdot & \cdot & \cdot & \cdot & \cdot & \cdot \end{vmatrix} = 0. \quad . \quad . \quad (24)$$

When a, h are fixed the only variable remaining in the determinant Δ is the frequency p, so that the smallest root of $\Delta = 0$ will give the frequency of the fundamental mode of vibration with which we are mainly concerned in the present paper.

The solution expressed by (24) is, however, merely formal. To find out whether it can be used to determine the actual value of the frequency of the fundamental mode of vibration we must examine its convergence. For this purpose we may form, as in Prof. G. I. Taylor's treatment of the statical problem, a series of finite determinants $\Delta_1, \Delta_2, \Delta_3, \ldots . \Delta_N$ by taking 1, 2, 3, ... N rows and columns starting at the left-hand top corner of Δ, so that $\Delta_1 = c_{10}$, $\Delta_2 = \begin{vmatrix} c_{10} & c_{30} \\ c_{12} & c_{32} \end{vmatrix}$, etc. If it is found that the smallest root of $\Delta_N = 0$ converges to a definite limit as N increases this root gives the required frequency of the fundamental mode of vibration of the square plate under consideration.

Search for Roots of $\Delta = 0$.

§ 5. The writer has calculated the smallest roots k of $\Delta_1 = 0$, $\Delta_2 = 0$, $\Delta_3 = 0$, $\Delta_4 = 0$, and $\Delta_5 = 0$ with a view to finding out whether they converge to a definite limit, each determinant containing a single pure number $k = \sqrt{\rho h a^4 p^2/D\pi^4}$ as a variable. It is clear that the smallest root of equation (24) is not greater than $\sqrt{13 \cdot 37} = 3 \cdot 6565$ nearly, since this "Rayleigh" value is greater than the true value of k. Further, it seems, however, probable that the true value of k would be near to the above "Rayleigh"

value, namely 3·6565. Accordingly the twenty-five values of c_{rs} were calculated for $n = 1, 3, 5, 7, 9$, and $s = 0, 2, 4, 6, 8$, for each of several values of k ranging from 3·53 to 3·66 *. The full determinant up to five rows and columns is set out in detail in Table I. for the case $k = 3·64$, in order to show the general character of the determinant,

TABLE I.

Construction of Δ_5 for $k = 3·64$.

$n=$	1	3	5	7	9	s
	−0·18793	−0·28821	−0·05871	−0·02127	−0·01090	0
	−0·19596	−0·28200	−0·05304	−0·01991	−0·00957	2
Δ_5	−0·02364	−0·19351	−0·08492	−0·01983	−0·00902	4
	−0·05098	−0·06324	−0·06858	−0·04097	−0·01032	6
	−0·03047	−0·03566	−0·02234	−0·03531	+0·02412	8

TABLE II.

k	Δ_1	$10\Delta_2$	$10^2\Delta_3$	$10^2\Delta_4$	$10^2\Delta_5$
3·53	−0·00868	—	—	—	—
3·54	+0·00974	−0·6612	−0·7910	−4·693	−1·666
3·60	−0·1181	−0·2842	−0·3486	−2·102	−0·7588
3·63	+0·1709	−0·09588	−0·1218	−0·7397	−0·2692
3·64	+0·1879	−0·03481	−0·04742	−0·2883	−0·1051
3·645	+0·1966	−0·00360	−0·00926	−0·0555	−0·0201
3·65	+0·2052	+0·02773	+0·02915	+0·1795	+0·0659
3·66	+0·2222	+0·08974	+0·1055	+0·6485	+0·2382
Root k =	3·5347	3·6456	3·6462	3·6462	3·6462

The values of $\Delta_1, \Delta_2, \Delta_3, \Delta_4$, and Δ_5 were then calculated by taking 1, 2, 3, 4, and 5 rows and columns of Δ. Their values are given in Table II., where the values of the Δ's for $k = 3·645$ were calculated by the usual bisection formula $\frac{q+r}{2} + \frac{q+r-(p+s)}{16}$.

* For the determination of the smallest root of $\Delta_1 = 0$ further values of c_{31}, which is equal to Δ_1, were calculated for $k = 3·50$, 3·51, 3·52, 3·55, which, however, are not reproduced here.

We see from this table that the root of $\Delta_1 = 0$ lies between $k = 3{\cdot}53$ and $k = 3{\cdot}54$, but the roots of $\Delta_2 = 0$, $\Delta_3 = 0$, $\Delta_4 = 0$, and $\Delta_5 = 0$ all lie between $k = 3{\cdot}645$ and $k = 3{\cdot}65$.

Using Lagrange's quadratic interpolation formula applied to the three values of Δ_1 at $k = 3{\cdot}53$, $3{\cdot}535$, and $3{\cdot}54$, the second of which was calculated by the bisection formula, the root of $\Delta_1 = 0$ was first determined. It was found to be $k = 3{\cdot}5347$.

Next, the roots of $\Delta_2 = 0$, $\Delta_3 = 0$, $\Delta_4 = 0$, and $\Delta_5 = 0$ have been determined in two slightly different ways, namely, in the first place the roots have been determined by Lagrange's cubic interpolation formula applied to the values of the Δ's at $k = 3{\cdot}63$, $3{\cdot}64$, $3{\cdot}65$, and $3{\cdot}66$, and, in the second place, use has been made of Lagrange's quadratic interpolation formula applied to the values of the Δ's at $k = 3{\cdot}64$, $3{\cdot}645$, and $3{\cdot}65$. In each case the two values of the root determined by these two methods coincide with each other. The roots thus determined are shown at the foot of Table II.*

It is seen that the convergence is extremely rapid: the root of $\Delta_1 = 0$ is $k = 3{\cdot}5347$, that of $\Delta_2 = 0$ is $k = 3{\cdot}6456$, while those of $\Delta_3 = 0$, $\Delta_4 = 0$, and $\Delta_5 = 0$ are all equal to $3{\cdot}6462$, to the fourth decimal place. We may therefore take $k = 3{\cdot}6462$ as the final result of our calculations. Consequently the frequency p in 2π seconds of the fundamental mode of vibration of a square plate clamped at its four edges is given by

$$k^2 = \frac{\rho h a^4 p^2}{\mathrm{D}\pi^4} = 13{\cdot}2948. \quad . \quad . \quad . \quad . \quad (25)$$

since $k^2 = (3{\cdot}6462)^2 = 13{\cdot}2948$.

Lastly, we shall compare our result with those obtained by approximate methods. By his approximate method K. Sezawa obtained, for the fundamental mode of vibration, the result that $\rho h a^4 p^2\, \mathrm{D}\pi^4 = 14{\cdot}4$. The Rayleigh principle gives, on the other hand, the value $\rho h a^4 p^2\, \mathrm{D}\pi^4 = 14{\cdot}22$ if we assume the normal function W in the form $\mathrm{W} = w_0 \cos^2 \xi \cos^2 \eta$, which satisfies the boundary conditions at the clamped edges of the plate but not the

* The values of Δ_3 and Δ_4 at $k = 3{\cdot}646$ were also calculated, obtaining the results that $10\Delta_3 = +0{\cdot}00033$ and $10^2\Delta_4 = -0{\cdot}00076$. Thus we see that the root of $\Delta_2 = 0$ lies between $k = 3{\cdot}645$ and $k = 3{\cdot}646$, and that of $\Delta_3 = 0$ is a little greater than $k = 3{\cdot}646$, the results being in agreement with those shown in Table II.

differential equation for W. Further, a much improved value is obtained by using the same principle, assuming W in the form

$$W = w_0 \cos^2 \xi \cos^2 \eta (1 + \lambda \cos \xi \cos \eta)$$

and choosing λ such that the value of p will become a minimum. The result is $\rho h a^4 p^2 / D\pi^4 = 13{\cdot}37$. It is remarkable that the latter value is very near to the true value 13·2948 and the error is less than 0·6 per cent.

§ 6. After finishing the above calculations the present writer became aware of Dr. A. Weinstein's interesting paper * on a minimal problem in the theory of elasticity, in which he has re-discussed a statical problem previously treated by Prof. G. I. Taylor †, namely, the problem of the stability of a square plate with four clamped edges subjected to equal thrusts perpendicular to all its edges.

Dr. Weinstein has considered a minimal problem of finding the least value μ_m of the expression

$$\iint (\Delta v)^2 d\xi d\eta / \iint (\text{grad}\, v)^2 d\xi d\eta,$$

where $\Delta = \partial^2/\partial\xi^2 + \partial^2/\partial\eta^2$ and the integrals are taken over the square $|\xi| \leqq \pi/2$, $|\eta| \leqq \pi/2$, for all functions $v(\xi, \eta)$ which vanish on the boundary of the square and which, moreover, satisfy the following m boundary conditions :—

$$G_{2i-1} = \int \frac{\partial v}{\partial n} g_{2i-1} ds = 0, \quad (i = 1, 2, \ldots . m),$$

in which ds and dn are respectively the line elements along and perpendicular to the boundary, and g_{2i-1} is taken to be equal to $c_i \cos(2i-1)\xi$ for $\eta = \pm\pi/2$, $-\pi/2 \leqq \xi \leqq \pi/2$, and to $c_i \cos(2i-1)\eta$ for $\xi = \pm\pi/2$, $-\pi/2 \leqq \eta \leqq \pi/2$, c_i being a certain constant, and to this problem he has applied the following general principle :—

If in a minimal problem some of the conditions are made less stringent the minimum value in the modified problem cannot be greater than that in the original problem.

* The paper will be published shortly. Dr. Weinstein has kindly given to the present writer a copy of the manuscript of his paper before publication, for which the writer wishes to express his cordial thanks.

† *Loc. cit.*

Thus, he has obtained a non-decreasing sequence of lower limits for the true minimum value of the thrust under which the equilibrium of the square plate is stable, and combining them with the "Rayleigh" values, which give evidently a sequence of upper limits, he has obtained inequalities for the true value of the thrust.

A similar method can be applied to the problem of transverse vibration of a square plate with four clamped edges which has been treated in the present paper by a different method. The present writer has carried out the necessary calculations *, and has obtained the result that, for the fundamental mode of vibration,

$$(3{\cdot}6461)^2 = 13{\cdot}2940 \lessapprox \frac{\rho h a^4 p^2}{D\pi^4}.$$

Thus, taking the "Rayleigh" value 13·37 into account, we get inequalities

$$13{\cdot}2940 \lessapprox \frac{\rho h a^4 p^2}{D\pi^4} < 13{\cdot}37.$$

We see that this result is in perfect agreement with the result obtained in the present paper.

Summary.

§ 7. The transverse vibration of a square plate of uniform small thickness clamped at its four edges is discussed, confining ourselves to such normal modes of vibration in which displacements are symmetrical with respect to the axes ξ and η taken parallel to the edges of the square.

By finding the forms of displacement which satisfy both the clamped-edge condition and the differential equation for the transverse vibration of the plate a formal solution of the problem is obtained, and the frequencies of the normal modes of vibration are expressed as values which cause an infinite determinant to vanish.

The numerical work necessary for completing the solution is carried out for the case of the fundamental mode of vibration, and the frequency p of vibration in the fundamental mode is found to be given by $\rho h a^4 p^2/D\pi^4 = 13{\cdot}2948$, where a, h are the length of the side

* Details of the calculations will be published in Report Aeron. Res. Inst. Tokyo Imp. Univ.

and the thickness of the plate respectively, ρ the density of the material of the plate, and D is the flexural rigidity, expressed in terms of h, E, σ by $D = \frac{1}{12}Eh^3(1-\sigma^2)^{-1}$, E and σ being Young's modulus and Poisson's ratio respectively of the material of the plate.

In conclusion, the writer wishes to express his cordial thanks to Prof. G. I. Taylor for his kind inspection of the present paper.

Cambridge.
February 1935.

LXI. *Numerical Solution of an Integral Equation.*

By V. R. Coles, *B.Sc.**

THE following article is intended to indicate methods of obtaining easy numerical solutions of an integral equation of a certain type. The equation occurs in work concerned with electronic movements [1], and also in the passage of electrons through matter [2], where solutions of the unknown function $F(v)$ are to be computed from tabulated values of known functions $f(v)$ and (Gv).

The equation is

$$G(v) = \int_v^{v+u_0-a} f(v-\phi+u_0)F(\phi)d\phi \quad . \quad . \quad . \quad (1)$$

where $$f(a) = f(u_0) = 0.$$

The method to be adopted is outlined formally as follows. The kernel of the integral equation is supposed to be capable of resolution into

$$f(v) = f_1(v) + f_2(v) + \ldots + f_n(v).$$

If we assume a solution $F(v)$ for the equation (1) and calculate

$$G_r(v) = \int_v^{v+u_0-a} f_r(v-\phi+u_0)F(\phi)d\phi, \quad r = 1, 2, \ldots n,$$

we have

$$G(v) = G_1(v) + G_2(v) + \ldots + G_n(v).$$

* Communicated by Prof. E. H. Neville.

We assume at the outset that $G(v)$ and $f(v)$ are finite and continuous, and possess finite derivatives of all necessary orders, and we see with Volterra [3] that the equation has a unique continuous solution. This only holds if we assume $F(v)=0$ for $0 \leqslant v \leqslant (u_0-a)$. Otherwise the equation does not possess a unique solution. Also we suppose $G(v)=0$ when $v \leqslant b$ $(<a)$. Then

$$\int_v^{v+u_0-a} f(v-\phi+u_0)F(\phi)d\phi = 0, \quad v \leqslant b.$$

This equation has, by the same considerations as above, only one continuous solution $F(\phi)$, which must be zero for

$$\phi \leqslant b+u_0-a.$$

We assume for the first case that

$$f(v) = Ae^{\alpha v}+Be^{\beta v},$$

a method of representation due to Prony [4], involving four disposable constants, which in general traces the curve to a very close approximation. Then

$$G_1(v) = \int_v^{v+u_0-a} Ae^{\alpha(v-\phi+u_0)}F(\phi)d\phi,$$

$$\frac{dG_1}{dv} = \alpha G_1(v)+Ae^{\alpha a}F(v+u_0-a)-Ae^{\alpha u_0}F(v). \quad . \quad (2)$$

Similarly,

$$\frac{dG_2}{dv} = \beta G_2(v)+Be^{\beta a}F(v+u_0-a)-Be^{\alpha u_0}F(v) \quad . \quad (3)$$

Adding

$$\frac{dG}{dv} = \alpha G_1(v)+\beta G_2(v),$$

since $f(a)=f(u_0)=0.$

Also $G = G_1+G_2,$

so that $G_1 = \left(\beta G-\frac{dG}{dv}\right)\Big/(\beta-\alpha).$

Substituting in (2) we then get a difference equation for the determination of $F(v)$. This equation is fairly easily soluble, since we have $F(\phi)=0$ for $0 \leqslant \phi \leqslant b+u_0-a$, whence we can obtain $F(v)$ over intervals of (u_0-a). A more accurate solution, of course, involves the actual analytical solution of the difference equation. We have

assumed tacitly that all derivatives of $G(v)$ exist, and are finite. That is to say, we have assumed $G(v)$ to be a "respectable" function, which is assured at the outset in all physical cases requiring numerical solutions. The obvious extension to the full Prony series of n exponential terms

$$f(v) = Ae^{\alpha v} + Be^{\beta v} + \ldots + Le^{\lambda v}$$

raises another problem, namely, that of solving a difference-differential equation, and the corresponding solution is complicated.

Suppose as a second representation for $f(v)$ we take

$$f(v) = a_0 + a_1 \cos m_1(v-a) + b_1 \sin m_1(v-a),$$

where $$m_1 = 2\pi/(u_0 - a).$$

Then writing

$$G_0(v) = \int_v^{v+u_0-a} a_0 F(\phi) d\phi,$$

we have

$$\frac{dG_0}{dv} = a_0[F(v+u_0-a) - F(v)];$$

and writing

$$G_1(v) = \int_v^{v+u_0-a} [a_1 \cos m_1(v-\phi+u_0-a) + b_1 \sin m_1(v-\phi+u_0-a)]F(\phi)\,d\phi,$$

we have

$$\frac{dG_1}{dv} = \int_v^{v+u_0-a} [m_1 b_1 \cos m_1(v-\phi+u_0-a) - m_1 a_1 \sin m_1(v-\phi+u_0-a)]F(\phi)d\phi, + a_1[F(v+u_0-a) - F(v)].$$

Differentiating the last equation again,

$$\frac{d^2G_1}{dv^2} + m_1^2 G_1 = m_1 b_1 L(v) + a_1 L'(v), \quad . \quad . \quad . \quad (4)$$

where $$L(v) = F(v+u_0-a) - F(v).$$

Also $$\frac{d^2G_0}{dv^2} = a_0 L'(v).$$

Adding to (4), and remembering that $a_0+a_1=0$, since $f(u_0)=f(a)=0$, and that $G_0+G_1=G$, we have

$$\frac{d^2G}{dv^2}+m_1^2G_1=m_1b_1L(v). \quad . \quad . \quad . \quad . \quad (5)$$

Eliminating G_1 from (4) and (5) we obtain a differential equation of the second order for $L(v)$. This in turn gives a difference equation $\Delta_{u_0-a}F(v)=L(v)$, which can be solved. The complementary function of the differential equation can be neglected, unless the function G happens to be composed of the same exponential factors as the complementary function, because, on solving the difference equation, we are left with the same exponential factors for $F(v)$, and these obviously do not satisfy the initial integral equation. If the function G happens to be composed of exponential factors, say

$$G(v)=K_1e^{k_1v}+K_2e^{k_2v}+\ldots+K_ne^{k_nv},$$

the solution is given as

$$A_1e^{k_1v}+A_2e^{k_2v}+\ldots+A_ne^{k_nv},$$

where the A_r's can be determined at once by direct substitution in the initial integral equation, and equating exponential coefficients.

This second representation leads to a simple generalization for more terms in the trigonometrical series; for example, if

$$f(v)=a_0+a_1\cos m_1(v-a)+b_1\sin m_1(v-a)$$
$$+a_2\cos 2m_1(v-a)+b_2\sin 2m_1(v-a),$$

then
$$G(v)=G_1(v)+G_2(v)+G_3(v),$$

where

$$G_2(v)=\int_v^{v+u_0-a}[a_2\cos 2m_1(v-\phi+u_0-a)$$
$$+b_2\sin 2m_1(v-\phi+u_0-a)]F(\phi)d\phi.$$

The extension to the representation of $f(v)$ as a Fourier expansion involves the solution of a differential equation of infinite order, and is under consideration. For any ordinary physical representation five terms of the Fourier expansion give an extremely close approximation to the curve $f(v)$.

The kernel in the integral equation used by White and Millington [2] is found to be capable of representation by the function

$$f(v) = Ae^{kv} \sin m_1 (v-a) \quad . \quad . \quad . \quad . \quad (6)$$

where $m_1 = \pi/(u_0 - a)$. This, of course, gives us four disposable constants, but the curve is not so generally useful in statistical work as, for instance, Pearson's representation

$$f(v) = A(v-a)^{\lambda a}(u_0 - v)^{\mu a},$$

if only because the former function yields only one point of inflexion between a and u_0, whilst Pearson's function, with the same number of disposable constants, gives two. The difference equation corresponding to the representation (6) is

$$m_1 Ae^{kv} F(v + u_0 - a) - m_1 Ae^{kv_0} F(v)$$
$$= G''(v) - 2kG'(v) + (k^2 + m_1^2)G(v),$$

which can be solved by the method indicated above. The extension from (6) to

$$f(v) = e^{kv}[A \sin m_1(v-a) + B \sin 3m_1(v-a)],$$

gives a differential equation for $\phi(v)$ where

$$\phi(v) = e^{ka} F(v + u_0 - a) + e^{ku_0} F(v).$$

It is clear that the representations for $f(v)$ cited above could be equally well applied to an equation of the type

$$G(v) = \int_0^{v+u_0-a} f(v - \phi + u_0) F(\phi) d\phi.$$

The various representations have, however, been chosen because of the comparative simplicity of the solutions, assuming both limits of the integral equation to be variable.

References.

(1) Hertz, *Math. Annalen*, vol. lxv. p. 1 (1908).
(2) White and Millington, Roy. Soc. Proc. A, vol. cxx. p. 701 (1928).
(3) Volterra, *Alt. Accad. Torino*, vol. xxxi. p. 231 (1896).
(4) Prony, *J. Ec. Poly.* Cat. 2, p. 29 (an. 4).

LXII. *Stresses in a Notched Plate under Tension.* By F. G. Maunsell, *Ph.D., University College, Southampton* *.

THE purpose of this paper is to determine the stresses in a semi-infinite plate, notched by a single semicircular notch, under a uniform tension T. The problem belongs to a very general class to which a good deal of attention has been given. The simplest of the class is that of determining the stresses in the neighbourhood of a circular hole in a relatively large plate. It is well known that when a tension T, uniform at a great distance from the hole, is applied to such a plate the stress at the edge of the hole is as high as 3T at two points. Even higher concentrations of stress may appear when there are additional free boundaries near the hole †.

The presence of such additional boundaries adds much to the difficulty of the problem, and only a few cases have been treated by exact methods ‡. No problem of the present type, in which the boundary consists of two intersecting parts, appears to have been solved. A rough approximate method for the present problem (originally due to Leon), in which the boundary conditions are very inadequately satisfied, is given by Coker and Filon §. From this they have obtained the value 2T for the maximum stress. This value I shall show to be much too low. Apart from this the only results hitherto obtained have been by experimental methods.

Let the middle surface of the plate occupy the upper half of the $x-y$ plane, with the exception of the interior of a semicircle whose centre is at the origin. The radius of this semicircle may be taken as unity without loss of generality. I introduce polar coordinates, as in fig. 1.

Let the plate be in a condition of generalized plane stress ||. The stresses, when averaged across the thickness, are then derivable from a single stress function χ, satisfying

$$\nabla^4\chi=0. \quad . \quad . \quad . \quad . \quad . \quad . \quad . \quad (1)$$

* Communicated by Prof. R. C. J. Howland, M.A., D.Sc.

† Coker and Filon, 'Photoelasticity,' Chap. 6 (London, 1931).

‡ *E. g.*, Knight, Quart. Journ. Math. v. pp. 255–268 (1934); Howland, Proc. Roy. Soc. A, cxlviii. pp. 471–491 (1935); see also the additional references given in these papers.

§ *Loc. cit.* p. 559.

|| Filon, Phil. Trans. A, cci. p. 67 (1903); Love, 'Theory of Elasticity,' 4th ed. p. 138 (Cambridge, 1927).

In the absence of the notch a uniform tension in the direction of the x-axis would be given by

$$X=\tfrac{1}{2}Ty^2. \quad . \quad . \quad . \quad . \quad . \quad . \quad . \quad (2)$$

The method of satisfying the conditions when the notch is present is to construct a series of functions satisfying (1) and giving no stresses on the straight boundary or at infinity. These are added to X, and the boundary conditions at the rim of the notch are then satisfied. The functions are derived by differentiation from two fundamental functions having singularities at the origin*.

For the first fundamental function I take

$$\chi_0=r\theta\cos\theta, \quad . \quad . \quad . \quad . \quad . \quad . \quad . \quad (3)$$

Fig. 1.

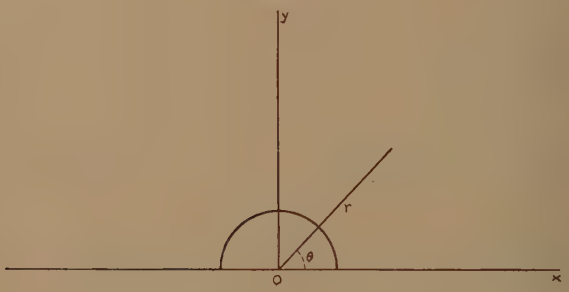

which, in an unnotched plate, would represent an isolated normal force at the origin †. Since the stress components in polars are given by

$$\left.\begin{aligned} \widehat{rr}&=\frac{1}{r^2}\frac{\partial^2\chi}{\partial\theta^2}+\frac{1}{r}\frac{\partial\chi}{\partial\theta},\\ \widehat{\theta\theta}&=\frac{\partial^2\chi}{\partial r^2},\\ \widehat{r\theta}&=\widehat{\theta r}=-\frac{\partial}{\partial r}\left(\frac{1}{r}\frac{\partial\chi}{\partial\theta}\right), \end{aligned}\right\} \quad . \quad . \quad . \quad (4)$$

* *Cf.* the papers by Howland and Knight mentioned above.
† Love, 'Elasticity,' p. 211.

χ_0 gives stresses

$$\widehat{rr} = -\frac{2\sin\theta}{r}, \quad \widehat{\theta\theta} = \widehat{r\theta} = 0. \quad . \quad . \quad . \quad (5)$$

It therefore gives no tractions on the straight edge and no stresses at infinity.

Differentiation with respect to x will also give functions with the required properties, but the odd derivatives must be excluded, since they are not even in x and cannot enter into the symmetrical system required. χ_0 itself must also be excluded because it represents an unbalanced force which would have to be balanced at infinity.

The series of functions is therefore

$$\chi_2 = \frac{\partial^2 \chi_0}{\partial x^2}, \quad \chi_4 = \frac{\partial^4 \chi_0}{\partial x^4}, \quad \cdots$$

and it is easily found that

$$\chi_{2m} = \frac{1}{r^{2m-1}}\{(2m-1)\sin(2m+1)\theta - (2m+1)\sin(2m-1)\theta\}, \ (m \geqslant 1), \quad (6)$$

where the factor $\frac{1}{2}(2m-2)\,!$ has been dropped for simplicity.

For the second fundamental function I take

$$\chi' = r\theta\sin\theta, \quad . \quad . \quad . \quad . \quad . \quad . \quad (7)$$

which would represent an isolated tangential force at the origin. Here only the odd derivatives are required, giving the series

$$\chi_0' = \frac{\partial \chi'}{\partial x} \qquad \chi_2' = \frac{\partial^3 \chi'}{\partial x^3}, \quad \cdots$$

where

$$\chi'_{2m} = \frac{1}{r^{2m}}\{\cos 2m\theta - \cos(2m+2)\theta\}. \quad (m \geqslant 0). \quad . \quad . \quad (8)$$

Here the factor $\frac{1}{2}(2m)\,!$ has been dropped.

Since X in polars becomes $\frac{1}{4}\mathrm{T}r^2(1-\cos 2\theta)$, the stress-function is taken as

$$\chi = \mathrm{T}\left\{\frac{1}{4}r^2(1-\cos 2\theta) + \sum_{m=1}^{\infty} \mathrm{A}_m\chi_{2m} + \sum_{m=0}^{\infty} \mathrm{B}_m\chi'_{2m}\right\}, \quad (9)$$

and the problem reduces to determining the A's and B's so that $\widehat{rr}$ and $\widehat{r\theta}$ are zero when r is unity.

Since χ_{2m} contains sines of odd multiples of θ, and the same is true for $\widehat{rr}$ of χ_{2m}, while $\widehat{r\theta}$ contains cosines of odd

multiples of θ, it is necessary to expand these sines and cosines in Fourier series of cosines or sines respectively, of multiples of 2θ valid from $\theta=0$ to $\theta=\pi$. The required expansions are

$$\sin(2m+1)\theta = \frac{2}{\pi}\left\{\frac{1}{2m+1} + \sum_{n=1}^{\infty} \frac{2(2m+1)}{(2m+1)^2-4n^2}\cos 2n\theta\right\}, \quad . \quad . \quad . \quad . \quad (10)$$

$$\cos(2m+1)\theta = \frac{2}{\pi}\sum_{n=1}^{\infty} \frac{-4n}{(2m+1)^2-4n^2}\sin 2n\theta. \quad . \quad (11)$$

The value of $\widehat{rr}$ for χ_{2m} is found to be

$$\begin{aligned}
&\left(\frac{1}{r^2}\frac{\partial^2}{\partial\theta^2}+\frac{1}{r}\frac{\partial}{\partial r}\right)\chi_{2m} \\
&= \frac{2m(2m-1)}{r^{2m+1}}\{(2m+1)\sin(2m-1)\theta \\
&\qquad -(2m+3)\sin(2m+1)\theta\}, \\
&= \frac{16(2m+1)2m(2m-1)}{\pi r^{2m+1}}\left\{\frac{2m-1}{2(4m^2-1)^2}\right. \\
&\qquad \left. + \sum_{n=1}^{\infty}\frac{2m-1+4n^2}{((2m-1)^2-4n^2)((2m+1)^2-4n^2)}\cos 2n\theta\right\}, \\
&= \frac{16(2m+1)2m(2m-1)}{(16m^2-1)\pi r^{2m+1}}\sum_{n=0}^{\infty}(4n^2+2m-1)^m\alpha_n\cos 2n\theta.
\end{aligned} \quad . \quad . \quad . \quad . \quad (12)$$

where

$$\left.\begin{aligned}
{}^m\alpha_0 &= \frac{16m^2-1}{2(4m^2-1)^2}, \\
{}^m\alpha_n &= \frac{16m^2-1}{((2m+1)^2-4n^2)((2m-1)^2-4n^2)}. \quad (n>0)
\end{aligned}\right\} \quad . \quad (13)$$

The value of $\widehat{r\theta}$ for χ_{2m} is found to be

$$\left.\begin{aligned}
&-\frac{\partial}{\partial r}\left(\frac{1}{r}\frac{\partial}{\partial\theta}\right)\chi_{2m} \\
&\quad = \frac{(2m+1)2m(2m-1)}{r^{2m+1}}\{\cos(2m+1)\theta \\
&\qquad -\cos(2m-1)\theta\}, \\
&\quad = \frac{16(2m+1)2m(2m-1)}{(16m^2-1)\pi r^{2m+1}}\sum_{n=1}^{\infty}4nm\,{}^m\alpha_n\sin 2n\theta.
\end{aligned}\right\} \quad . \quad (14)$$

To avoid factors put

$$A'_m = \frac{16(2m+1)2m(2m-1)}{(16m^2-1)\pi} A_m. \quad . \quad . \quad . \quad (15)$$

The stresses derived from χ'_{2m} are as follows :—

$$\widehat{rr} = \frac{1}{r^{2m+2}}\{-2m(2m+1)\cos 2m\theta + 2(m+2)(2m+1)\cos(2m+2)\theta\}, \quad (16)$$

$$\widehat{r\theta} = \frac{1}{r^{2m+2}}\{-2m(2m+1)\sin 2m\theta + (2m+1)(2m+2)\sin(2m+2)\theta\}. \quad (17)$$

Finally, we have the following expressions for the stresses derived from χ :—

$$\widehat{rr} = T\Big\{\tfrac{1}{2}(1+\cos 2\theta) + \sum_{m=1}^{\infty} \frac{A'_m}{r^{2m+1}}\Big[\sum_{n=0}^{\infty}(4n^2+2m-1)\,{}^m\alpha_n \cos 2n\theta\Big] + \sum_{m=0}^{\infty} \frac{2(2m+1)B_m}{r^{2m+2}}[-m\cos 2m\theta + (m+2)\cos(2m+2)\theta]\Big\}, \quad (18)$$

$$\widehat{r\theta} = T\Big\{-\tfrac{1}{2}\sin 2\theta + \sum_{m=0}^{\infty} \frac{A'_m}{r^{2m+1}}\Big[\sum_{n=0}^{\infty} 4nm\,{}^m\alpha_n \sin 2n\theta\Big] + \sum_{m=0}^{\infty} \frac{2(2m+1)B_m}{r^{2m+2}}[-m\sin 2m\theta + (m+2)\sin(2m+2)\theta]\Big\}. \quad (19)$$

Equating the constant term and the coefficients of $\sin 2m\theta$, $\cos 2m\theta$ to zero in (18) and (19), we get

$$\tfrac{1}{2} + \sum_{m=1}^{\infty}(2m-1)\,{}^m\alpha_0 A'_m = 0, \quad . \quad . \quad . \quad . \quad . \quad . \quad . \quad (20)$$

$$\tfrac{1}{2} + \sum_{m=1}^{\infty}(2m+3)\,{}^m\alpha_1 A'_m + 4B_0 - 6B_1 = 0, \quad . \quad . \quad . \quad (21)$$

$$\sum_{m=1}^{\infty}(4n^2+2m-1)\,{}^m\alpha_n A'_m + 2(2n-1)(n+1)B_{n-1} - 2n(2n+1)B_n = 0, \quad (n>1) \quad . \quad . \quad (22)$$

$$-\tfrac{1}{2} + \sum_{m=1}^{\infty} 4m\,{}^m\alpha_1 A'_m + 2B_0 - 6B_1 = 0, \quad . \quad . \quad . \quad . \quad (23)$$

$$\sum_{m=1}^{\infty} 4mn^m\alpha_n A'_m + 2n(2n-1)B_{n-1} - 2n(2n+1)B_n = 0. \quad (n>1). \quad . \quad (24)$$

It is easy to solve for B_0 and B_1 in (21) and (23) and for B_{n-1} and B_n in the nth equations of (22) and (24), and so replace equations (21) to (24) by the following:

$$1 - \sum_{m=1}^{\infty} (2m-3)^m\alpha_1 A'_m + 2B_0 = 0, \quad . \quad . \quad . \quad (25)$$

$$\tfrac{1}{2} - \sum_{m=1}^{\infty} (2m-1)^m\alpha_1 A'_m + 2B_1 = 0, \quad . \quad . \quad . \quad (26)$$

$$\sum_{m=1}^{\infty} (2n-2m+1)^m\alpha_n A'_m + 2B_{n-1} = 0, \quad (n>1). \quad (27)$$

$$\sum_{m=1}^{\infty} (2n-2m-1)^m\alpha_n A'_m + 2B_n = 0. \quad (n>1). \quad (28)$$

The B's can now be eliminated, and the following equations obtained ((29) is of course (20) repeated):

$$\tfrac{1}{2} + \sum_{m=1}^{\infty} (2m-1)^m\alpha_0 A'_m = 0, \quad . \quad . \quad . \quad (29)$$

$$\tfrac{1}{2} - \sum_{m=1}^{\infty} \{(2m-1)^m\alpha_1 + (5-2m)^m\alpha_2\} A'_m = 0, \quad . \quad (30)$$

$$\sum_{m=1}^{\infty} \{(2n-2m-1)^m\alpha_n - (2n-2m+3)^m\alpha_{n+1}\} A'_m = 0. \quad (n>1)$$

$$. \quad . \quad . \quad . \quad (31)$$

It has unfortunately been impossible to find any rapidly converging iterative process for the solution of these equations, and it was necessary to have recourse to the crude and laborious process of taking the first n_0 equations and neglecting the A'_n's for n greater than n_0 and solving the n_0 simple equations in n_0 quantities. This was performed finally for fifteen equations, and the values of the first ten A_n''s used in the subsequent calculations. There is, of course, no proof of convergence, but the fact that these values make $\widehat{rr}$ and $\widehat{r\theta}$ vanish on the unit circle to the required degree of approximation shows that the resulting stresses cannot be much in error.

The values of A_n', A_n, B_n thus found are shown in Table I.

Of these the first five are probably correct to five places of decimals and the remainder to two significant figures.

On working out the values of $\widehat{rr}$ and $\widehat{r\theta}$ on the semicircle the greatest value found was ·04 T ($\widehat{rr}$ for $\theta=0$).

TABLE I.—Coefficients in series for χ.

n.	A_n'.	A_n.	B_n.
0.....	....	....	−·7924661
1.....	−·6751566	−·3314167	+·2173722
2.....	+·1370553	+·0282563	−·0087936
3.....	+·0143472	+·0019183	−·0033040
4.....	+·0031720	+·0003151	−·0014912
5.....	+·0008648	+·0000684	−·0007557
6.....	+·0002291	+·0000151	−·0004135
7.....	+·0000299	+·0000017	−·0002373
8.....	−·0000335	−·0000016	−·0001385
9.....	−·0000507	−·0000022	−·0000767
10.....	−·0000518	−·0000020	−·0000209

Since the coefficient of sin $2l\theta$ in the expression for $\widehat{rr}$ when $r=1$ is ·02 approximately, the agreement must be regarded as sufficiently satisfactory. The stresses found for the remainder of the plate are probably correct within ·05 T.

TABLE II.—$\widehat{\theta\theta}$ for $r=1$.

θ.	$\widehat{\theta\theta}$.	θ.	$\widehat{\theta\theta}$.
5°	−·03	50°	+1·57
10°	−·05	60°	+2·07
15°	+·008	70°	+2·62
20°	+·08	80°	+2·96
30°	+·45	90°	+3·05
40°	+·95		

The values of

$\widehat{\theta\theta}$ on the edge of the semicircular notch (Table II.),

$\widehat{rr}$ on the straight edge (Table III.),

$\widehat{rr}$ and $\widehat{\theta\theta}$ along the line of symmetry, Oy (Table IV.),

have been calculated, and are here given (T is taken as unity).

TABLE III.—$\widehat{rr}$ for $\theta = 0$.

r.	$\widehat{rr}$.	r.	$\widehat{rr}$.
1·1	−·02	3	+·68
1·25	−·03	4	+·81
1·5	+·09	5	+·88
1·75	+·23	10	+·97
2	+·37	100	+·9997

The results of Tables I.–IV. are shown graphically in fig. 2.

Fig. 2.

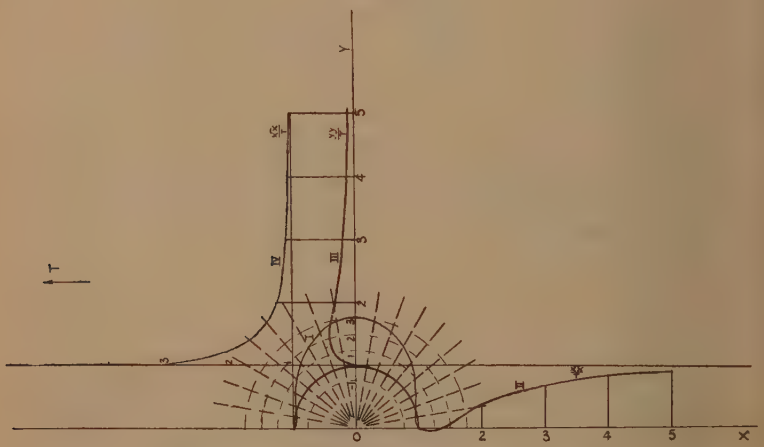

Stresses in the neighbourhood of the notch.

I, Stresses at the rim of the notch; tensions are measured radially outwards from the notch, pressures radially inwards (Table II.).
II, Tension on the straight edge (Table III.).
III, Radial stress on the line of symmetry (Table IV.).
IV, Tension across the line of symmetry (Table IV.).

The most striking feature of the results is that the maximum concentration of stress is very nearly 3T, and it is strongly suggested that 3 T is the accurate value. It is to be noted that this differs from the value 2 T obtained by Leon by an admittedly imperfect method.

TABLE IV.—$\widehat{rr}$ and $\widehat{\theta\theta}$ for $\theta = \pi/2$.

r.	$\widehat{rr}$.	$\widehat{\theta\theta}$.
1·1	+·23	+2·51
1·25	+·37	+2·00
1·5	+·41	+1·57
1·75	+·39	+1·36
2	+·34	+1·24
3	+·20	+1·08
4	+·13	+1·03
5	+·09	+1·02
10	+·03	+1·002
100	+·0003	+1·000

It is also considerably greater than the value 2·5 T deduced by Coker and Filon from Capper's experiments *.

The distribution of stresses shows a general likeness to that around a circular hole in an infinite plate under tension. The principal difference seems to be in the value of $\widehat{\theta\theta}$ near the corners of the notch. This might have been expected, as the nature of the problem makes $\widehat{\theta\theta}$ vanish when θ is zero.

In conclusion, I have to thank Professor R. C. J. Howland for the great interest he has taken in this problem and the valuable encouragement and suggestions he has given.

LXIII. *The Absorption of Monochromatic Light in Iodine Vapour.* By J. HARDING, *B.A., Trinity College, Dublin* (*FitzGerald Research Scholar*) †.

1. *Introduction.*

IN a communication [1] on the absorption of light in vapours, Ditchburn and Braddick show that the absorption of cæsium vapour is greatly reduced by the addition of helium at about 3 cm. pressure. This effect

* 'Photoelasticity,' p. 560.

† Communicated by Prof. R. W. Ditchburn, Ph.D.

is attributed to collisions between the absorbing cæsium atoms and the helium atoms. Mrozowski [2] has shown that the continuous molecular absorption in mercury does not increase in proportion to the number of molecules. It appears possible that this effect is due to interaction between mercury atoms and mercury molecules similar to that between helium and cæsium atoms in the above experiment. The present experiment was designed to seek for a similar effect in iodine vapour. This substance is especially suitable because it has a well developed band spectrum and continuous spectrum (due to photo-dissociation of the molecule) in easily accessible regions of the spectrum. The mercury line λ 5461 is in the band region, and λ 4358 is conveniently placed in the continuous absorption region. Experiments on the variation of absorption with vapour pressure were carried out, with the necessary filters, both with iodine *in vacuo* and with iodine in the presence of 1·8 cm. of helium.

2. *Experimental.*

Light from a mercury arc was collimated, and after passing through a filter and the absorption vessel fell on a Weston photronic cell. The absorption vessel, made from pyrex glass, was supported in a cylindrical furnace, and its temperature was kept at about 115° C. during each experiment. The vapour pressure of the iodine was determined by the temperature of the end of a side-tube which projected into a small furnace; this temperature was recorded by accurately calibrated mercury thermometers reading to 0·1° C. The corresponding vapour pressures were obtained from the International Critical Tables.

At the low intensity of light used the voltage output of the Weston cell is proportional to intensity, provided that the temperature of the cell is kept constant. A sensitive galvanometer was used to determine the voltage, and a null method was adopted in order to eliminate errors due to zero drift. The balancing voltage was applied to the galvanometer by applying a variable voltage across a suitably arranged double potentiometer circuit, and when a balance was obtained this voltage, which is proportional to the light intensity, was measured with an accurate voltmeter.

3. *Results.*

Log (I_0/I), which is proportional to the absorption coefficient, was plotted against P, where I_0=intensity of light for a vapour pressure of iodine corresponding to room-temperature, and I =intensity at pressure P.

Fig. 1.

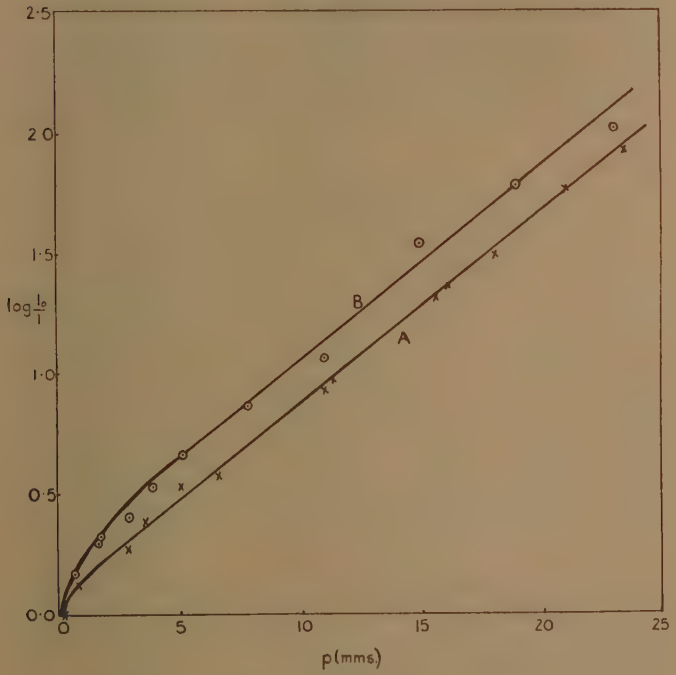

The following results were obtained :—

(*a*) λ 5461.

Curve A (fig. 1) shows the variation of absorption with vapour pressure in iodine *in vacuo*. With the exception of the lower end of the curve, which will be discussed later, the curve is linear, showing that, within the limits of error, the absorption was proportional to the vapour pressure.

Curve B (fig. 1) shows the effect of 1·8 cm. of helium on the absorption. It will be seen that the effect of the

helium is to increase the initial rise in the curve, and that for high pressures of iodine the curve for absorption of iodine with helium runs parallel to that for iodine alone.

The curves are probably correct to ± 1 per cent. at the lower end, but the probable error increases with absorption, and at the upper end the error may be ± 5 per

Fig. 2.

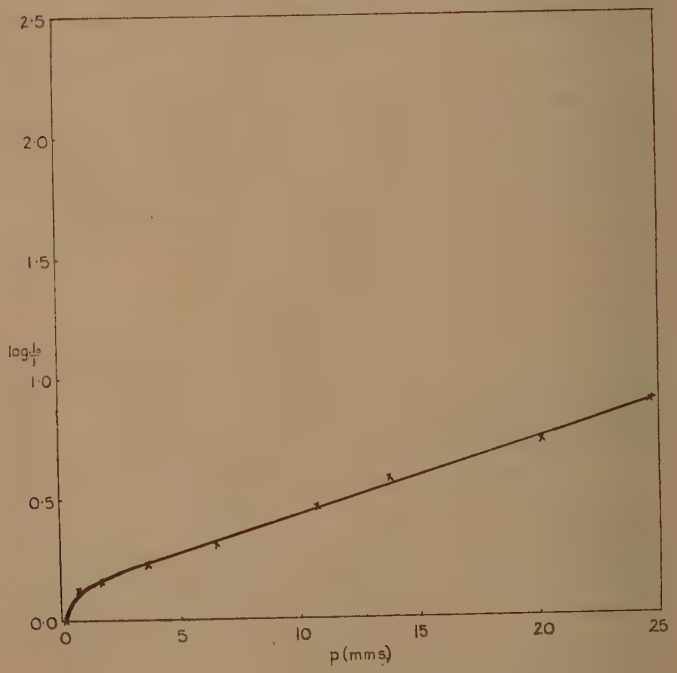

cent. However, over most of its range the curve is probably correct within half this value.

(*b*) λ 4358.

The absorption curve is shown in fig. 2.

Apart from the fact that the absorption is lower it is very similar to the curve for λ 4358. The intensity of the blue line was less than that of the green, consequently the curve is probably less accurate. There is

no evidence that the helium had any effect on the absorption.

(c) There is a possibility that part of the absorption was due to an adsorbed film of iodine on the ends of the absorption vessel, the film being in equilibrium with vapour, as was found by Golub and Kondratjew [3] in the case of NO_2. Following their method, experiments were carried out using an absorption vessel containing a number of pieces of plane glass perpendicular to the beam of light. As a result of these experiments it was concluded that no detectable amount of absorption was due to such adsorbed films.

4. *Discussion.*

The absorption of both lines is a linear function of the vapour pressure. The proportion of iodine atoms at the temperature considered is very small, therefore the vapour pressure is proportional to molecular concentration; consequently the absorption of both lines is proportional to molecular concentration. Thus there is no effect comparable with that which Mrozowski found [2] in the continuous molecular spectra of mercury, cadmium, and zinc. The absorption in the continuous region (λ 4358) is unaffected by the presence of helium. Thus there is no effect in this region comparable with that found by Braddick and Ditchburn for cæsium with helium. The molecular absorption coefficient for λ 4358 is $1{\cdot}5 \times 10^{-19}$ cm.$^{-1}$.

It is not possible to give a detailed explanation of the shape of the absorption curves near the origin. The small departure from linearity is almost certainly due to the fact that the incident light is not homogeneous. In the case of the blue line λ 4358 the initial increase in absorption is probably due to a small proportion of a more easily absorbed radiation passing the filter (*e. g.*, λ 5461). The processes involved in the absorption of the green line are considerably more complicated, and it is intended to discuss these in greater detail in a later paper.

5. *Summary.*

1. The absorption of the Hg lines λ 5461 and λ 4358 in iodine vapour is measured up to a vapour pressure of about 2·5 cm.

2. The absorption in both cases is directly proportional to the pressure.

3. The absorption of λ 5461 is increased in the presence of helium, but that of λ 4358 is not.

4. No appreciable part of the absorption is due to adsorbed films on the windows.

I wish to express my thanks to Prof. Ditchburn for his interest and advice throughout this work.

References.

(1) Proc. Roy. Soc. A, cl. p. 487 (1935).
(2) *Zeits. f. Phys.* xci. p. 600 (1934).
(3) *Phys. Z. Sowjetunion*, i. p. 619 (1932).

LXIV. *The Atomic Scattering Factors of Aluminium Nickel, and Copper for* CuKα *Radiation and their Relation to the Theory of X-ray Dispersion.* *By* G. W. Brindley, *M.Sc., Ph.D., Mackinnon Student of the Royal Society, Physics Laboratories, University of Leeds* *.

1. *Introduction.*

In a recent paper [1] in this Journal results were given of an investigation of the X-ray scattering factors of nickel, copper, and zinc atoms for CuKα radiation obtained by using these metals in the form of very fine powders. The intensities of the X-ray reflexions were measured photographically, and were placed on an absolute scale by comparing them with reflexions from finely powdered KCl. Intensities of reflexions from large crystals of KCl had previously been measured [2] absolutely with the ionization spectrometer, and these results were used to standardize the reflexions from nickel, copper, and zinc. There appeared to be no serious objection to this procedure at the time of publication, but subsequent work with other metals has made it necessary to reconsider the matter.

The scattering factors for large crystals of KCl measured by James and the writer [2], when corrected for thermal vibration, showed on the whole satisfactory agreement

* Communicated by Prof. R. Whiddington, F.R.S.

with purely theoretical values of the scattering factors obtained from the wave-functions of K^+ and Cl^- derived by Hartree's method of self-consistent fields. The agreement was closest for values of $(\sin\theta)/\lambda$ greater than about 0·7, but for $(\sin\theta)/\lambda$ between 0·2 and 0·6 there was a difference between the observed and calculated values which amounted at the most to about 10 per cent. Since the KCl reflexions which were used to standardize the nickel, copper, and zinc results lie in this range of $(\sin\theta)/\lambda$, it is important to know whether this difference arises from approximations in the theoretical work or from errors in the experimental work, or from both these causes.

To test these possibilities, reflexions from KCl powder have been compared with reflexions from powdered aluminium using the method previously described [1], [3], and by assuming the absolute values obtained by James, Brindley, and Wood [4] for single crystals of aluminium the absolute intensities of the KCl reflexions were derived, and hence the scattering factors. These new values for KCl were found to agree much better with the theoretical scattering factors, especially in the region between $(\sin\theta)/\lambda=0{\cdot}2$ and 0·6, than the earlier values. It is not intended to discuss these measurements for KCl in detail here; they indicate, however, the desirability of reconsidering the scattering factors of nickel, copper, and zinc which had previously been measured with respect to KCl.

Apart from certain points of an experimental character relating to the preparation of aluminium powder, which will be discussed in the next section, aluminium is more suitable than KCl as a substance for standardizing the intensities of X-ray reflexions. In the absolute determination of the scattering factor of aluminium by James, Brindley, and Wood [4], a very close agreement was found between the experimental and theoretical scattering factors, and there was no disagreement for small values of $(\sin\theta)/\lambda$ of the kind found with KCl. In the recent experiments on nickel, copper, and zinc, KCl was taken as the standardizing substance in preference to aluminium because KCl can be prepared chemically in a very finely divided form very suitable for experiments of this type, whereas aluminium can only be powdered by mechanical means. But it is believed, as a result of further experi-

ments, that satisfactory aluminium powder can be obtained, and this has now been used to standardize the measurements for nickel, copper, and zinc.

The revised scattering factors for these metals are now about 10 per cent. higher than those previously given; the increase, in fact, is practically equal to the extent that the measurements of James and Brindley [2] for KCl were lower than the theoretical values in the region near $(\sin\theta)/\lambda = 0{\cdot}4$.

Owing to the fact that CuKα radiation has a wave-length near the K-absorption edges of Ni, Cu, and Zn, the scattering factors for this radiation are considerably less than the theoretically calculated values, which are valid only for sufficiently short waves. This effect is closely connected with the theory of X-ray dispersion. Theoretical calculations of the magnitude of the difference between the scattering factors for very short waves and for any particular radiation have been made independently by Williams [5] and by Hönl [6]. It will be shown that the revised scattering factors of nickel and copper for CuKα radiation lead to values of about the magnitude predicted by theory for this dispersion effect.

The present paper will be concerned only with nickel and copper; additional points of interest have arisen in connection with zinc which will be described in a second paper.

2. *The Preparation of Aluminium Powder.*

The preparation of suitable aluminium powder needs careful consideration. Extremely fine powder, such as is used for making aluminium paint, has been found unsuitable [7]; it is produced by a stamp mill process, in which the metal is beaten out into flake-like particles, which show a pronounced preferential orientation of certain atomic planes. Aluminium powder produced by spraying molten metal is very fine, but the particles are too coarsely crystalline. Fine powder can be obtained by filing, and such powder is unlikely to show preferential orientation, but the possibility must be considered that the filing, may cause appreciable lattice distortion. In a previous investigation [8] filing was found to reduce the intensities of reflexion of nickel and copper, but subsequent work on zinc and cadmium

has shown that with these metals filing has no appreciable effect. In these experiments the filed metals were compared with powders produced chemically, but this is not possible with aluminium.

A simple and frequently used test for lattice distortion is to examine whether the $K\alpha_1\alpha_2$ doublet is resolved for high order reflexions; with filed nickel and copper this doublet was not resolved, but filed aluminium gave perfect resolution. This result is in agreement with the view generally held that cold-working of aluminium will not produce a broadening of the X-ray reflexions, whereas with most metals and alloys such a broadening is observed. In the experiments on nickel and copper, filing was found to reduce the intensities of the high order reflexions very much more than of the lower order reflexions; this does not happen with aluminium, as will be shown in the next section. Finally, the intensities from filed aluminium were compared with reflexions from a specimen of very pure aluminium powder supplied by Kahlbaum *; the mode of preparation of the latter is not known. Within the limits of experimental error there was found to be complete agreement between the intensities from the two powders.

These results suggest that filed aluminium powder is not appreciably distorted, and may, therefore, be used in connexion with the measurement of X-ray intensities. The reason why aluminium, zinc, and cadmium are not appreciably distorted by filing, while nickel and copper show considerable distortion, is probably that the temperature at the point where the filing occurs is raised sufficiently to anneal, Al, Zn, and Cd, but not Ni and Cu, which have much higher recrystallization temperatures.

3. *Experimental Results for Aluminium and Comparison with Theory.*

A short account will be given of the intensity measurements of reflexions from filed aluminium powder. The source of the powder was a cast ingot, presented by the British Aluminium Co., of purity approximately 99·8 per cent.; the impurities were stated to be approximately 0·11 per cent. of Si and 0·09 per cent. of Fe. The metal

* I am indebted to Dr. Brentano for a sample of this aluminium powder.

was fully annealed prior to filing, which was carried out with a fine jeweller's file. The finest particles were separated by a sieve having a 350 mesh to the inch. Relative intensity measurements were made in the manner previously described [1], [3] and relative scattering factors were calculated from the equation

$$I_r = (\text{constant})\, p f_T^2 \phi(\theta) A, \quad . \quad . \quad . \quad . \quad (1)$$

where f_T is the effective scattering factor at temperature T, I_r is the reflected intensity, p the multiplicity factor, $\phi(\theta)$ is written for $(1+\cos^2 2\theta)/\sin\theta \sin 2\theta$, and A is an absorption factor depending on the setting of the powder with respect to the incident X-ray beam. For each

Table I.

Experimental Results for Filed Aluminium Powder.

1. Spectra.	2. $(\sin\theta)/\lambda$.	3. I_r/A.	4. p.	5. $\phi(\theta)$.	6. f_T (relative).
111 ...	0·214	362	8	7·841	2·40
200 ...	0·247	166	6	5·608	2·22
220 ...	0·350	*100·0*	12	2·406	1·86
311 ...	0·410	107·4	24	1·683	1·63
222 ...	0·429	31·2	8	1·555	1·58
331 ...	0·539	48·4	24	1·487	1·16
420 ...	0·553	47·8	24	1·581	1·12
422 ...	0·606	53·7	24	2·467	0·95

reflexion several such settings are used, *i. e.*, several values of A; in tabulating the results, values are given of I_r/A relative to $(I_r/A)=100$ for the (220) reflexion.

In Table I. column 1 gives the indices of the reflexions, column 2 the values of $(\sin\theta)/\lambda$, column 3 the experimental values of I_r/A, columns 4 and 5 give p and $\phi(\theta)$, and column 6 gives the relative values of f_T obtained by means of equation (1).

The relative values of f_T in Table I., column 6, have been compared with theoretical values in the following way:—James, Brindley, and Wood [4] calculated the scattering factors of the ions Al^+, Al^{+2} and Al^{+3} from their wave-functions derived by Hartree's method of self-consistent fields; except at values of $(\sin\theta)/\lambda < 0{\cdot}1$, the three scattering factors are practically identical,

and as the first reflexion from aluminium, the (111), occurs at $(\sin\theta)/\lambda=0{\cdot}214$, we shall not be concerned with these differences at small values of $(\sin\theta)/\lambda$.

With CuKα radiation the effect of dispersion on the scattering factor is small but not quite negligible; calculation by Hönl's method [6] shows that dispersion has the effect of raising the scattering factor by 0·18, so that if f_0 denotes the scattering factor for very short waves, $\lambda\to 0$, and if Δf is the dispersion correction, then the scattering factor for CuKα radiation is given by

$$f_{\mathrm{CuK}\alpha}=f_0-\Delta f, \quad . \quad . \quad . \quad . \quad . \quad . \quad (2)$$

TABLE II.

Theoretical and Experimental Scattering Factors for Aluminium.

1. Spectra (h, k, l).	2. $f_0 e^{-M}$ $(\lambda\to 0)$.	3. $-\Delta f e^{-M}$.	4. $f_\perp=(f_0-\Delta f)e^{-M}$ (CuKα).	5. f_T (expt.) (CuKα).
111	8·46	0·17	8·63	8·70
200	7·96	0·17	8·13	8·03
220	6·58	0·16	6·74	*6·74*
311	5·75	0·16	5·91	5·91
222	5·53	0·16	5·69	5·73
331	4·06	0·14	4·20	4·21
420	3·90	0·14	4·04	4·06
422	3·22	0·14	3·46	3·45

where $-\Delta f=+0{\cdot}18$ for CuKα radiation reflected from aluminium. At any temperature T the effective scattering factor, f_T, will be of the form

$$f_T=(f_0-\Delta f)e^{-M}, \quad . \quad . \quad . \quad . \quad . \quad (3)$$

where M for aluminium at 290 Abs. is given by [9]

$$M=0{\cdot}01182\,(h^2+k^2+l^2), \quad . \quad . \quad . \quad . \quad (4)$$

where h, k, and l are the indices of the reflexion.

Table II. contains the data which will be required; column 1 gives the indices of the reflexions, column 2 gives $f_0 e^{-M}$ taken from the third column of Table VI. of the paper by James, Brindley, and Wood [4] (where necessary, values have been obtained by graphical interpolation), column 3 gives the dispersion correction $-\Delta f.e^{-M}$ calculated from the equations given above, column 4 gives the resultant scattering factor of

aluminium at room temperature for CuKα radiation, and column 5 gives the experimental values of f_T relative to the (220) reflexion, for which the calculated value has been assumed. Within the limits of experimental error, columns 4 and 5 are in complete agreement;

Fig. 1.

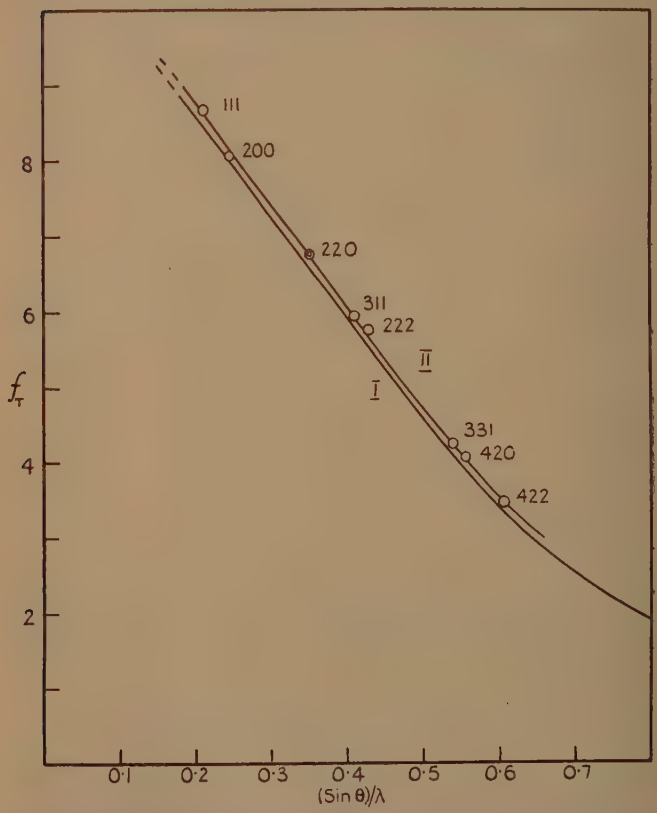

Atomic scattering factors for aluminium: curve I is the theoretical curve for short waves: curve II is for CuKα radiation; the circles are the experimental values relative to the (220) reflexion.

this is strong evidence that any lattice distortion in filed aluminium powder has an inappreciable effect on the intensities of X-ray reflexions.

The results are shown graphically in fig. 1; curve I

is the calculated scattering factor, $f_0 e^{-M}$, valid for sufficiently short waves; curve II is the corresponding curve for CuKα radiation; the circles show the experimental results; a double circle is used for the (220) reflexion to emphasize that the values are relative to this reflexion.

4. *Revised Values for the Scattering Factors of Nickel and Copper.*

The relative scattering factors of nickel and copper for CuKα radiation previously given have been re-standardized in terms of reflexions from aluminium using the experimental values given in column 5 of Table II. for the scattering factors of aluminium.

The conversion factors necessary to translate the relative f_T values of the previous paper into absolute values are, respectively :—

$$\left.\begin{aligned} \text{For nickel,}\quad & \frac{f_T(\text{absolute})}{f_T(\text{relative})} = \underline{4{\cdot}93.} \\ \text{For copper,}\quad & \frac{f_T(\text{absolute})}{f_T(\text{relative})} = \underline{5{\cdot}87.} \end{aligned}\right\}$$

The revised values for nickel and copper are set out in Table III.; column 1 gives the indices of the reflexions, column 2 $(\sin\theta)/\lambda$, column 3 the relative values of f_T for CuKα radiation taken from the previous paper, column 4 the re-standardized values of f_T for CuKα radiation, column 5 the temperature factor e^M as calculated in the previous paper, column 6 the scattering factors for the atoms at rest obtained by the equation $f_T = f \,.\, e^{-M}$, column 7 the theoretical values of f_0 valid for short waves, and column 8 the dispersion correction $\Delta f = f_0 - f$.

The average values of Δf are found to be 3·5 for nickel and 2·6 for copper. According to the theory worked out by Hönl [6], Δf should be 3·53 for nickel and 2·55 for copper, while according to Williams's method [6] of calculation, Δf for copper should be 2·3.

The observed and theoretical values of Δf are in very close agreement; in fact, in view of the various possible sources of experimental error, this close agreement must be regarded as to some extent fortuitous. It should also be pointed out that the "observed" values of Δf do not rest entirely on experimental data, because the f_0

values are derived theoretically, and small but appreciable errors may arise from approximations involved in the theoretical calculations.

TABLE III.

Atomic Scattering Factors of Nickel and Copper.

(a) *Nickel.*

1. Spectra.	2. $(\sin\theta)/\lambda$.	3. f_T (rel.) CuKα.	4. f_T (abs.) CuKα.	5. e^M.	6. f CuKα	7. f_0 $\lambda\to 0$.	8. $\Delta f=$ (7)$-$(6).
111..	0·246	3·33	$16{\cdot}4_3$	1·025	$16{\cdot}8_3$	19·9	$3{\cdot}0_7$
200..	0·284	2·92	$14{\cdot}4_0$	1·034	$14{\cdot}8_5$	18·5	$3{\cdot}6_2$
220..	0·402	2·18	$10{\cdot}7_5$	1·068	$11{\cdot}4_2$	14·7	$3{\cdot}2_1$
311..	0·471	1·77	$8{\cdot}7_2$	1·095	$9{\cdot}5_6$	12·9	$3{\cdot}3_3$
331..	0·619	1·05	$5{\cdot}1_8$	1·170	$6{\cdot}0_6$	10·4	$4{\cdot}3_4$
							$3{\cdot}5_1$

(b) *Copper.*

111..	0·241	3·13	$18{\cdot}3_7$	1·031	$18{\cdot}9_4$	$21{\cdot}4_0$	$2{\cdot}4_6$
200..	0·278	2·82	$16{\cdot}5_5$	1·042	$17{\cdot}2_4$	$20{\cdot}0_0$	$2{\cdot}7_6$
220..	0·393	2·12	$12{\cdot}4_3$	1·086	$13{\cdot}5_2$	$16{\cdot}0_5$	$2{\cdot}5_2$
311..	0·461	1·75	$10{\cdot}2_7$	1·121	$11{\cdot}5_2$	$13{\cdot}9_2$	$2{\cdot}4_0$
222..	0·481	1·62	$9{\cdot}5_1$	1·132	$10{\cdot}7_6$	$13{\cdot}4_6$	$2{\cdot}7_0$
331..	0·605	1·18	$6{\cdot}9_2$	1·218	$8{\cdot}4_4$	$11{\cdot}0_6$	$2{\cdot}6_2$
420..	0·621	1·11	$6{\cdot}5_1$	1·230	$8{\cdot}0_0$	$10{\cdot}8_1$	$2{\cdot}8_1$
							$2{\cdot}6_1$

(c) *Theoretical values of Δf.*

For nickel and CuK radiation, $\Delta f=3{\cdot}5_3$ (Hönl).
„ copper „ „ $\Delta f=2{\cdot}5_5$ „
„ copper „ „ $\Delta f=2{\cdot}3$ (Williams).

In the case of copper, f_0 was calculated by James and Brindley [10] from Hartree's calculation of the electron distribution in Cu^+. As Hartree and others have pointed out [11], approximations are involved in these calculations and, in particular, electron exchange is neglected. Fock and Petrashen [12] have shown in the case of Na and Hartree [11] has shown in the case of Be that allowance for electron exchange makes an appreciable change in the electron distribution ; a similar result may therefore be expected for Cu^+.

In the case of nickel, the electron distribution has not yet been calculated by Hartree's method, and an estimated f_0 curve has therefore been obtained as follows :—For copper the scattering factor calculated from Hartree's data lies approximately mid-way between the curves derived by the more approximate methods of Thomas [13] and of Pauling and Sherman [14]. This is illustrated in fig. 2 (*a*), where the continuous curve, H, is derived from Hartree's data for Cu^+ and the broken curves, T and P.S., are the Thomas and Pauling-Sherman

Fig. 2.

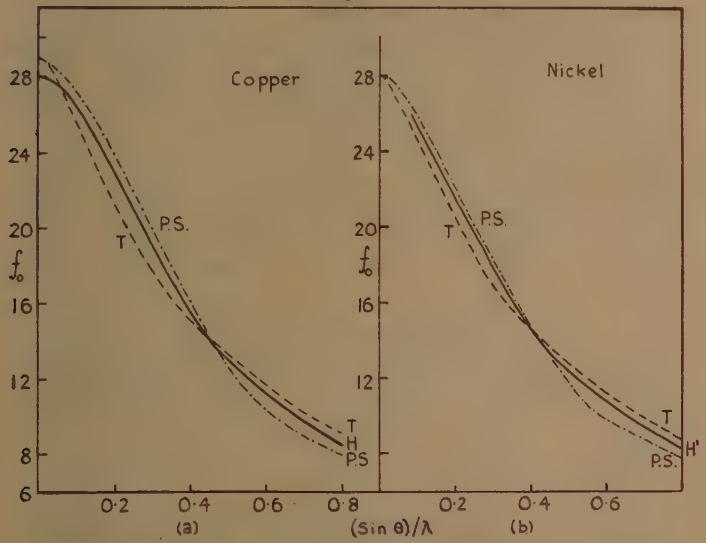

Theoretical scattering factors for copper and nickel : H is calculated from Hartree's data for Cu^+ ; H′ is the estimated curve for nickel ; T and P.S. are respectively Thomas and Pauling-Sherman curves.

curves respectively for neutral copper. Since nickel is the adjacent element to copper in the periodic classification (the atomic numbers are Ni=28 and Cu=29), it may be assumed that the Hartree curve for nickel will bear practically the same relation to the Thomas and Pauling-Sherman curves as in the case of copper. In this way a Hartree curve for nickel has been estimated, and is shown by the full line, H′, in fig. 2 (*b*).

The experimental results are compared with the theoretical scattering factors in fig. 3 (*a*) and (*b*). The upper curves in these figures show the theoretical values of f_0 which are valid for short waves. The second curve in each figure shows $(f_0 - \Delta f)$; the Δf values are those calculated by Hönl's method. The third curve in each figure shows $f_T = (f_0 - \Delta f)\, e^{-M}$; these are the effective scattering factors for CuKα radiation at room temperature.

Fig. 3.

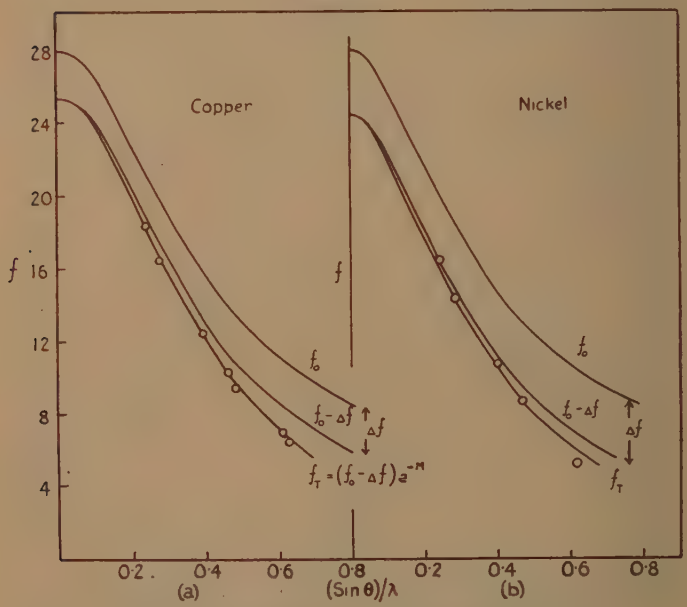

Comparison of experimental and theoretical results for copper and nickel.

The experimental values are shown by circles. The agreement between experiment and theory is good for both metals, but especially so for copper. The figures show clearly the magnitude of Δf in relation to f_0 and f_T.

5. *Discussion.*

Previous measurements of the scattering factor of copper for CuKα radiation by Armstrong [15], Wyckoff [16],

and Rusterholz [17] are lower than those given above, and in consequence, when compared with theoretical f_0 values, they give larger values of Δf. Armstrong and Wyckoff standardized their measurements in terms of the (220) reflexion of rock-salt, and Rusterholz used reflexions from aluminium ; no corrections were applied for the effect of dispersion on the reflexions from these substances, but this omission does not explain the whole of the difference between the results of these experiments and the present results. Although the dispersion corrections for NaCl and Al are small for CuKα radiation, they have an appreciable effect on the small difference Δf.

Only one previous measurement appears to have been made of the scattering factor of nickel for CuKα radiation, namely, by Wyckoff [16]. It was previously observed that Wyckoff's values were higher than those found by the writer and F. W. Spiers, but when comparison is made with the redetermined values in Table III., there is a fairly close agreement between Wyckoff's values and the present ones at large values of $(\sin\theta)/\lambda$, but the agreement is not so good at smaller values of $(\sin\theta)/\lambda$.

6. *Acknowledgments.*

Finally, I wish to thank Prof. Whiddington for his interest in this work, and also the Government Grant Committee of the Royal Society for a grant with which part of the necessary apparatus was purchased.

7. *Summary.*

The atomic scattering factors of nickel and copper for CuKα radiation, which were published a short time ago, have been re-standardized in terms of reflexions from aluminium powder ; the previous *relative* measurements are retained. Reasons are given in section 1 for this re-standardization and for preferring aluminium to KCl as a substance for standardizing the intensities of X-ray reflexions from powders. In section 2 a number of points are discussed relating to the preparation of suitable aluminium powder.

Measurements of the intensities of X-ray reflexions from aluminium are described in section 3, and when comparing these results with theoretical values allowance

is made for the effect of dispersion on the scattering factors for CuKα radiation.

Section 4 gives the re-standardized values for nickel and copper, and comparison is made with theoretical values of the scattering factors valid for short waves. The average values of the difference $\Delta f = f_0 - f_{\mathrm{CuK}\alpha}$ are found to be 3·5 for Ni and 2·6 for Cu. These results are in close agreement with values calculated theoretically by Williams and by Hönl.

References.

(1) G. W. Brindley and F. W. Spiers, Phil. Mag. xx. p. 865 (1935).
(2) R. W. James and G. W. Brindley, Proc. Roy. Soc. A, cxxi. p. 154 (1928).
(3) G. W. Brindley and F. W. Spiers, Proc. Phys. Soc. xlvi. p. 841 (1934).
(4) R. W. James, G. W. Brindley, and R. G. Wood, Proc. Roy. Soc. A, cxxv. p. 401 (1929).
(5) E. J. Williams, Proc. Roy. Soc. A, cxliii. p. 358 (1934).
(6) H. Hönl, *Ann. der Phys.* xviii. p. 625 (1933).
(7) G. W. Brindley and F. W. Spiers, see ref. (3), p. 846.
(8) G. W. Brindley and F. W. Spiers, Phil. Mag. xx. p. 882 (1935).
(9) See ref. (4), p. 408.
(10) R. W. James and G. W. Brindley, Phil. Mag. xii. p. 81 (1931); *Zeit. f. Krist.* lxxviii. p. 470 (1931).
(11) See D. R. Hartree and W. Hartree, Proc. Roy. Soc. A, cl. p. 9 (1935).
(12) V. Fock and M. Petrashen, *Phys. Zeit. Sowjet.* vi. p. 368 (1934).
(13) See R. W. James and G. W. Brindley, *Zeit. f. Krist.* lxxviii. p. 470 (1931).
(14) L. Pauling and J. Sherman, *Zeit. f. Krist.* lxxxi. p. 1 (1932).
(15) A. H. Armstrong, Phys. Rev. xxxiv. p. 931 (1929).
(16) R. W. G. Wyckoff, Phys. Rev. xxxvi. p. 1116 (1930).
(17) A. A. Rusterholz, *Zeit. f. Phys.* lxv. p. 226 (1930); lxxxii. p. 538 (1933).

LXV. *An X-ray Investigation of Atomic Vibrations in Zinc.* *By* G. W. Brindley, *M.Sc., Ph.D., Mackinnon Student of the Royal Society, Physics Laboratories, University of Leeds* *.

1. *Introduction.*

MEASUREMENTS have been made of the intensity of X-ray reflexions from metallic zinc and cadmium with a view to obtaining information about the nature of the thermal vibrations of the atoms. Interest in this

* Communicated by Prof. R. Whiddington, F.R.S.

problem developed as a result of certain observations made by the writer and F. W. Spiers [1] in connexion with the measurement of the atomic scattering factors of nickel, copper, and zinc for X-rays; it was found in the case of zinc that, although most of the measured reflexions gave values for the atomic scattering factor which lay on or near a smooth curve when plotted against $(\sin\theta)/\lambda$ in the usual way, certain reflexions gave values which were well off the curve. These results were consistently obtained for specimens of zinc prepared in different ways, and similar results have since been obtained with cadmium. The first investigation was confined to the strongest reflexions which could be measured most accurately; other reflexions have since been measured which have increased the number of these apparent discrepancies.

In a recent note to 'Nature' [2] a brief description of these results has been given, and it has been pointed out that they can be correlated with the anisotropic nature of the lattice vibrations in these metals. A theoretical paper by Zener [3] has at the same time appeared in which he derives expressions for the effect of lattice vibration on the intensities of X-ray reflexions from zinc and cadmium.

The present paper will give an account of the experimental investigation of X-ray reflexions from zinc, and will compare the results with the theoretical work of Zener and with more empirical calculations by the writer which had been largely completed before the publication of Zener's paper. The measurements for cadmium have progressed sufficiently far to confirm the results for zinc, but certain points require further investigation before publication.

An examination of the apparent discrepancies which were found for the scattering factors of zinc and cadmium has shown that reflexions from planes of atoms which make specially small angles with the basal plane of the unit cell, the (0001) plane, give relatively low values for the scattering factors, while reflexions from planes making large angles with the basal plane give relatively large values for the scattering factors.

This connexion between the scattering factors and the reflecting planes suggests either that the atoms in zinc and cadmium have a marked asymmetry, and

so have different scattering factors in different directions, or that the lattice vibrations have a similar asymmetry which makes the atoms *effectively* more diffuse in some directions than in others.

These two possibilities are easily distinguished, because asymmetry of the atoms would be confined mainly to the outer electron shells and therefore would affect mainly the low-order reflexions, while asymmetry of the lattice vibrations would mainly affect the high-order reflexions, since the effect of thermal vibration increases greatly with the order of the reflexion. Actually it is the high-order reflexions which show these apparent discrepancies (see fig. 1), and so we are led to consider the effect of anisotropic lattice vibrations.

2. *Experimental Results.*

Since the experimental method has already been fully described in other papers [1],[4] we shall give directly the experimental results.

The previous measurements for zinc [1] were obtained by finding the relative intensities of X-ray reflexions from finely powdered zinc prepared by vaporizing zinc *in vacuo* and collecting the condensed vapour. The reflected intensities were standardized by comparing them with reflexions from finely powdered KCl.

Since the publication of these results additional reflexions have been measured and some of the previous measurements have been rechecked. With one exception the previous results have not been greatly modified. The exception is the (10$\bar{1}$1) reflexion, which occurs at a fairly small angle ($\theta = 21° 43'$ for CuKα radiation); the previous measurements were made with the plate of powder set at such an angle to the incident X-ray beam that this reflexion left the powder at a small glancing angle, and under these conditions the method is not very reliable; this has now been rectified.

Measurements have also been made of the intensities of reflexions from zinc powder produced by filing; within the limits of experimental error they agree with the measurements for the condensed powder, particularly for the high-order reflexions. This tends to confirm the measurements with the condensed powder, and also indicates incidentally that any lattice distortion produced

by filing is too small to be detected by X-ray measurements.

In the preceding paper [5] reasons have been given for preferring aluminium to KCl as a standardizing substance; the zinc reflexions have therefore been remeasured in terms of aluminium reflexions, for which the scattering factors have been given in the preceding paper (see Table II. column 5).

The scattering factors are calculated as follows:— The intensity of reflexion, I_r, for the block of powder is given by

$$I_r = (\text{constant})\, pF^2\phi(\theta)A. \quad . \quad . \quad . \quad . \quad (1)$$

These symbols have been previously defined [1], and it is only necessary here to note that F, the amplitude reflected by the unit cell of the structure, in the case of a hexagonal crystal like zinc is given by

$$F = Sf_T, \quad . \quad . \quad . \quad . \quad . \quad . \quad . \quad . \quad (2)$$

where f_T is the effective scattering factor at temperature T and S is the crystal structure factor which equals 2, $\sqrt{3}$, or 1 for different types of reflexion. Also f_T is related to the true scattering factor, f, for the stationary atom by the equation

$$f_T = fe^{-M}. \quad . \quad . \quad . \quad . \quad . \quad . \quad . \quad . \quad (3)$$

We therefore have

$$I_r/A = (\text{constant})\, pS^2\phi(\theta)\, .f_T{}^2. \quad . \quad . \quad . \quad (4)$$

A is a geometrical factor depending on the setting of the powder with respect to the incident beam, and since several settings are used for each reflexion it is most convenient to tabulate values of I_r/A. The expression $pS^2\phi(\theta)$ is constant for a reflexion, and so by means of equation (4) relative values of f_T are easily obtained.

The experimental results are tabulated in Table I.; the columns, in order, give the indices of the reflexions, $(\sin\theta)/\lambda$, an angle ψ (which will be defined later), values of $pS^2\phi(\theta)$, the experimental values of I_r/A relative to the $(11\bar{2}2)$ reflexion, the relative values of f_T, and, finally, the absolute values of f_T obtained by comparison with the aluminium reflexions.

When two reflexions occur so close together that they cannot be measured separately a mean value, $\overline{f}_T$, may

be calculated, defined as follows:—If suffixes "1" and "2" indicate the two reflexions, then the combined intensity is given by

$$I_r/A = (\text{constant})\,[p_1 S_1^2 \phi_1(\theta) f_{T1}^2 + p_2 S_2^2 \phi_2(\theta) f_{T2}^2] \quad . \quad (5)$$

$$= (\text{constant})\,[p_1 S_1^2 \phi_1(\theta) + p_2 S_2^2 \phi_2(\theta)](\bar{f}_T)^2. \quad . \quad (6)$$

TABLE I.

(*a*) Atomic Scattering Factors for Zinc for CuKα Radiation at 290° abs.

1. Reflexion.	2. $(\sin\theta)/\lambda$.	3. ψ.	4. $pS^2\phi(\theta)$.	5. I_r/A (expt.).	6. f_T (relative).	7. f_T (absolute).
0002	0·203	0·0°	71·1	269	1·94	20·1
$10\bar{1}0$	0·218	90·0	45·3	212	2·16	22·4
$10\bar{1}1$	0·240	65·0	216·2	760	1·87	19·4
$10\bar{1}2$	0·298	47·0	43·0	113·8	1·63	16·8
$10\bar{1}3$	0·374	35·6	73·9	212·5	1·32	$13·6_5$
$11\bar{2}0$	0·378	90·0	48·3			
$11\bar{2}2$	0·428	61·7	74·7	**100·0**	1·16	12·0
$20\bar{2}1$	0·448	76·9	52·5	71·7	1·17	12·1
$20\bar{2}3$	0·532	55·1	52·1	31·0	0·77	8·0
$10\bar{1}5$	0·552	23·3	56·6	59·1	0·67	6·9
$11\bar{2}4$	0·554	42·9	76·2			
$21\bar{3}1$	0·585	80·0	141·9	76·2	0·73	7·6
0006	0·609	0·0	20·4	30·8	0·61	6·3
$21\bar{3}2$	0·611	70·6	63·6			

(*b*) Standardization Data.

				f_T(abs.). f_T(rel.).
Zn $(10\bar{1}3)+(11\bar{2}0)$ compared with	Al (220)	gave	$f_T=13·7_7$	$13·7_2$ $10·4_0$
„ „ „ „	Al (311)	„	$f_T=13·6_8$	
Zn $(11\bar{2}2)$ „	Al (220)	„	$f_T=11·9_2$	$11·9_8$ $10·3_5$
„ „ „	Al (311)	„	$f_T=12·0_4$	
Zn $(20\bar{2}1)$ „	Al (220)	„	$f_T=11·9_8$	$12·0_4$ $10·3_1$
„ „ „	Al (311)	„	$f_T=12·1_0$	

Mean value of f_T (absolute)/f_T(relative)=**10·3₅**.

If the temperature factors are the same for the two reflexions then $f_{T1}=f_{T2}=f_T$, but when they are different the relation of f_T to f_{T1} and f_{T2} will depend on the relative magnitudes of $pS^2\phi(\theta)$ for the two reflexions.

Data relating to the standardization of the relative f_T values are given in the lower part of Table I., and require no further explanation. The zinc reflexions are standardized with respect to Al (220) and Al (311), and from the results a mean value of f_T(abs.)/f_T(rel.) equal to $10{\cdot}3_5$ is obtained.

Fig. 1.

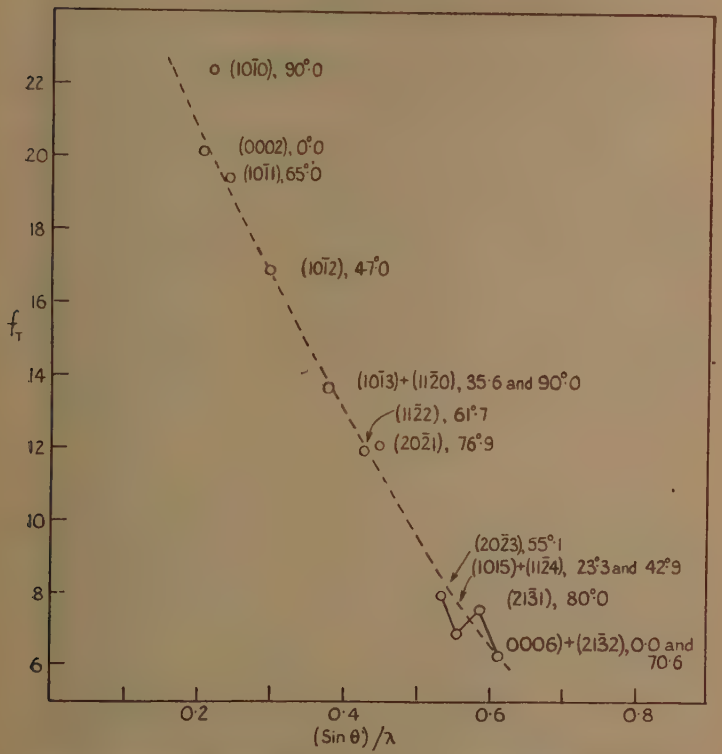

Atomic scattering factors for zinc at room-temperature, f_T. The numbers against each circle give the indices of the reflexion and the angle which the reflecting plane makes with the basal plane of the hexagonal cell.

3. *Discussion of the Experimental Results.*

The experimental results are shown graphically in fig. 1, where f_T is plotted against $(\sin\theta)/\lambda$. A mean curve is drawn through the experimental points.

In view of the general discussion in the introductory section it is of interest to calculate the angles between the various reflecting planes and the basal plane of the hexagonal cell; these are also the angles between the normals to the planes and the c-axis. It may easily be shown that, if ψ is the angle between the plane (h, k, $h+k$, l) and the basal plane (0001), then

$$\cos\psi=(l/\mathrm{R})\{4(h^2+hk+k^2)/3+(l/\mathrm{R})^2\}^{-\frac{1}{2}}, \quad . \quad . \quad (7)$$

where R denotes the axial ratio, c_0/a_0, which for zinc has the value 1·861 *. The values of ψ have been given in the third column of Table I.

At values of $(\sin\theta)/\lambda$ less than about 0·4 the experimental points in fig. 1 lie close to the mean curve with the exception of the second point, for the $(10\bar{1}0)$ reflexion, which lies extraordinarily high. At higher values of $(\sin\theta)/\lambda$ there is a pair of reflexions lying close together, (1122) and (2021), and a group of four reflexions. For the pair of reflexions $(11\bar{2}2)$ and (2021) the second has the larger f_v and the larger value of ψ, namely, 76°·9 as compared with 61°·7 for the first of these reflexions. In the group of four reflexions the (2131) lies furthest above the mean curve and has the largest ψ, 80°·0. The lowest point with respect to the mean curve is for the pair of reflexions $(10\bar{1}5)$ and (1124), both of which have small values of ψ, viz., 23°·3 and 42°·9. The other two points of this group have intermediate values of ψ and lie fairly near the mean curve. Returning now to the points at small values of $(\sin\theta)/\lambda$, we see that the first reflexion, (0002) with $\psi=0°·0$, is below the mean curve, while the third point for the (1011) reflexion with $\psi=65°·0$ lies above the mean curve. Apart, then, from the $(10\bar{1}0)$ reflexion, which appears to be exceptional, it may be said that the reflexions with large values of ψ tend to have large values of the scattering factor, and *vice versa*.

* Slightly different values of the axial ratio have been published since the calculations were carried out for R = 1·861. Owen and Iball have given 1·856; Owen, Pickup, and Roberts, 1·856; Jette and Foote, 1·858. The value R = 1·861 is based on the measurements of Freeman, Sillers, and Brandt. The change in the value of R indicated by these recent measurements is too small to affect appreciably the calculations given in the paper.

It follows from this discussion that the results may be explained qualitatively by supposing that the atoms have a larger amplitude of vibration normal to the basal plane than in it, and that the amplitude has intermediate values for intermediate directions.

The atomic scattering factor, f, for the stationary zinc atom, at all but the smallest values of $(\sin\theta)/\lambda$, will depend on the inner groups of electrons. The normal zinc atom has 28 electrons in completed groups, viz., 2 K, 8 L, and 18 M electrons, plus two valence, $4s$, electrons. The latter will contribute appreciably to f only at very small values of $(\sin\theta)/\lambda$. The inner electrons will be spherically symmetrical, or nearly so, and therefore will give a *smooth* variation of f with $(\sin\theta)/\lambda$. It would therefore be expected that when the observed scattering factors are corrected for lattice vibration, the points should lie on a smooth curve for all values of $(\sin\theta)/\lambda$ except, perhaps, for very small values of $(\sin\theta)/\lambda$, where the valence electrons may have an appreciable effect. In particular the prominent irregularities in f_T between $(\sin\theta)/\lambda$ equals 0·5 and 0·6 should be smoothed out when the correction is made for lattice vibration.

4. *Comparison with Zener's Theory.*

Since the completion of the experimental work described above a paper by Zener [3] has appeared in which he calculates the lattice vibrations in anisotropic crystals from their elastic constants; in the case of zinc and cadmium numerical results are given based on the experimental measurements of Grüneisen and Goens [6] for the elastic constants of these crystals.

The effect of lattice vibration is to reduce the scattering factor f for an atom according to the equation

$$f_T = fe^{-M}, \quad . \quad . \quad . \quad . \quad . \quad . \quad . \quad . \quad (8)$$

and for zinc at a temperature T near room-temperature Zener gives

$$M = 1{\cdot}1 \times 10^{-3}\{1{\cdot}80\cos^2\Theta + \sin^2\Theta\}T(\sin\theta/\lambda)^2, \quad . \quad (9)$$

where Θ is the angle between the normal to the crystal plane and the principal axis (the c-axis) of the crystal. Zener's angle Θ is therefore identical with ψ previously used; in order to eliminate possible confusion between

this Θ and the symbol Θ used later for the characteristic temperature in what follows we shall use ψ rather than the Θ used by Zener.

From equation (9) it is an easy matter to calculate the temperature factor e^{-M}, and hence to correct the observed values of f_r for lattice vibration.

Owing to the fact that certain pairs of reflexions occur together we cannot apply the temperature factor e^{-M} directly to the f_r values given in column 7 of Table I., because certain of these values are mean values defined according to equation (6).

TABLE II.

The Scattering Factor, f, for Zinc, using Zener's Data for the Temperature Factor, e^{M}.

1. Reflexions.	2. e^{M}.	3. $pS^2\phi(\theta) \cdot e^{-2M}$.		4. I_r/A (expt.).	5. f (relative).	6. f (absolute).
0002	1·022	68·1		269	1·99	20·6
$10\bar{1}0$	1·015	44·0		212	2·20	22·7
$10\bar{1}1$	1·020	208·0		760	1·91	19·8
$10\bar{1}2$	1·039	39·8		113·8	1·69	17·5
$10\bar{1}3$	1·071	64·4	108·4	212·5	1·40	14·5
$11\bar{2}0$	1·047	44·0				
$11\bar{2}2$	1·071	65·1		100·0	1·24	12·8
$20\bar{2}1$	1·069	45·9		71·7	1·25	12·9
$20\bar{2}3$	1·121	41·5		31·0	$0·86_5$	9·0
$10\bar{1}5$	1·177	40·9	98·5	59·1	$0·77_5$	8·0
$11\bar{2}4$	1·150	57·6				
$21\bar{3}1$	1·118	113·6		76·2	0·82	8·5
0006	1·238	13·3	62·3	30·8	$0·70_5$	7·3
$21\bar{3}2$	1·139	49·0				

We therefore proceed in the following way :—From equation (4) we have

$$I_r/A = (\text{constant}) pS^2\phi(\theta)e^{-2M}f^2, \quad . \quad . \quad (10)$$

and for a pair of reflexions which cannot be resolved we have, from equation (6),

$$I_r/A = (\text{constant}) [p_1S_1^2\phi_1(\theta)e^{-2M_1} + p_2S_2^2\phi_2(\theta)e^{-2M_2}]f^2. \quad . \quad . \quad . \quad (11)$$

We therefore take the measured values of I_r/A and remove the factor $pS^2\phi(\theta)e^{-2M}$, or the sum of two such factors, to obtain relative f values, and these are standardized as before, giving finally the absolute f values for the

stationary atom. The essential stages in the calculation are set out in Table II.

The values of f obtained by using Zener's expression for the temperature factor are shown by crosses in fig. 2.

Fig. 2.

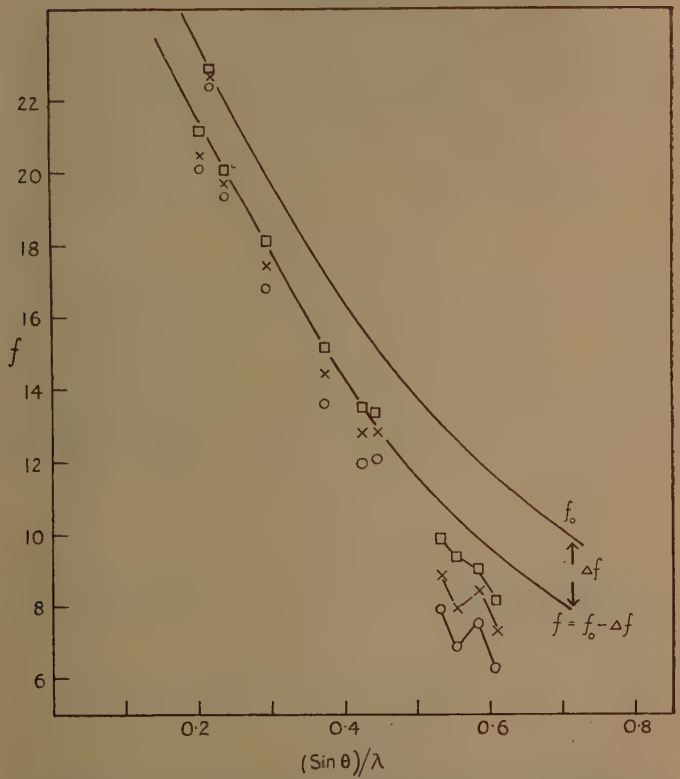

Comparison of experimental and theoretical results for zinc. The full curves show respectively f_0 the scattering factor for short waves and $f=(f_0-\Delta f)$, the scattering factor for CuKα radiation. The circles are the experimental results at room-temperature; the crosses show the result of correcting for lattice vibration by using Zener's data, and the squares show the result of correcting for lattice vibration by using the approximate calculations given in the paper.

The experimental values of f_T are shown by circles. The irregularities in the scattering factors are smoothed

out only very slightly as a result of applying this correction for lattice vibration. These results will be discussed further in a later section.

5. *An Approximate Calculation of the Lattice Vibrations in Zinc.*

The exponent M in the expression for the temperature factor is related in a simple way to the root-mean-square displacement of the atoms *normal* to the plane from which X-ray reflexion occurs. If u_ψ is the displacement of an atom in a direction ψ with respect to the c-axis, then for X-ray reflexions from the plane normal to ψ, M is given by the equation [7]

$$\mathrm{M} = 8\pi^2 u_\psi^2 (\sin\theta/\lambda)^2. \quad . \quad . \quad . \quad . \quad (12)$$

This equation involves no assumptions regarding the nature of the lattice vibrations. If we take the simple picture of an atom vibrating with simple harmonic motion, then $u_\psi^2 = k\mathrm{T}/\mathrm{F}$, where F is the force per unit displacement in the ψ-direction, and if ν is the frequency of vibration $\mathrm{F} = 4\pi^2\nu^2 m$, where m is the mass of the atom. Also, if the characteristic temperature Θ is defined in the usual way, $\Theta = h\nu/k$; then, combining these equations, we obtain

$$\overline{u_\psi^2} = h^2\mathrm{T}/4\pi^2 mk\Theta^2. \quad . \quad . \quad . \quad . \quad . \quad (13)$$

A similar result is obtained by taking expressions derived by Debye [8] and by Waller [9] for cubic crystals, based on the Born-Karman theory of specific heats. According to Debye and Waller

$$\mathrm{M} = \frac{6h^2}{mk\Theta}\left[\frac{\Phi(x)}{x} + \tfrac{1}{4}\right](\sin\theta/\lambda)^2, \quad . \quad . \quad . \quad (14)$$

where $x = \Theta/\mathrm{T}$. When $x < 2\pi$, $\Phi(x)$ may be expanded as follows [10] :—

$$\Phi(x) = 1 - x/4 + x^2/36. \quad . \quad . \quad . \quad . \quad (15)$$

Combining equations (12), (14), and (15), we obtain

$$\overline{u^2}_\psi = \frac{3h^2}{4\pi^2 mk\Theta}\left[\frac{1}{x} + \frac{x}{36}\cdots\right],$$

and neglecting $x/36$ compared with $1/x$ (which is legitimate

to a first approximation, since x is of the order of unity) we obtain

$$u^2_{\psi} = 3h^2T/4\pi^2mk\Theta^2. \quad . \quad . \quad . \quad . \quad (16)$$

This expression is identical in form with (13), and differs only in the numerical factor. This is really due to a difference in the Θ's, for in (13) Θ is defined with respect to a single frequency ν, as in the Einstein theory of specific heats, whereas in (16) Θ is defined with respect to the maximum frequency of the elastic spectrum, ν_m. As Debye [8] originally pointed out the simple theory gives the same result as the more complete theory if the single frequency ν is assumed to be $\nu_m/\sqrt{3}$*.

Now Grüneisen and Goens [11], from their work on the thermal expansion of zinc and cadmium crystals, obtained values for the characteristic temperatures in the direction of the c-axis, $\Theta_{\parallel}$, and normal to the c-axis, $\Theta_{\perp}$. For zinc they give $\Theta_{\parallel} = 200°$ abs. and $\Theta_{\perp} = 320°$ abs.

From specific heat data for zinc the mean characteristic temperature, Θ_s, is 235° abs. Since the theory of specific heats makes no allowance for anisotropy of the lattice vibrations, it is reasonable that Θ_s should lie between $\Theta_{\parallel}$ and $\Theta_{\perp}$.

The fact that $\Theta_{\parallel} < \Theta_s < \Theta_{\perp}$ implies that

$$\sqrt{\overline{u^2}_{\psi=0}} > \sqrt{\overline{u^2}_{\psi}} > \sqrt{\overline{u^2}_{\psi=90}},$$

i. e., that the root-mean-square displacements parallel to and normal to the c-axis are respectively greater than and less than the mean displacement in any direction, $\sqrt{\overline{u^2}_{\psi}}$.

Since the r.m.s. displacement is proportional to $1/\Theta$, as shown both by equations (13) and (16), we shall obtain approximately the r.m.s. displacements parallel to and normal to the c-axis by multiplying the mean displacement calculated from Θ_s by $\Theta_s/\Theta_{\parallel}$ and by $\Theta_s/\Theta_{\perp}$.

This leads to the following results :—

$\sqrt{\overline{u^2}_{\psi}}$ (from equation (16), taking $\Theta_s = 235°$) $= \underline{0{\cdot}1076 \text{ Å.}}$

$\sqrt{\overline{u^2}_{\psi=0}}$ ($\psi = 0°$, *i. e.*, parallel to the c-axis)

$$= 0{\cdot}1076 \times 235/200$$
$$= \underline{0{\cdot}1265 \text{ Å.}}$$

* Actually Debye gave $\sqrt{2}/3$, but the 2 has disappeared as a result of the modification of Debye's work due to Waller.

$\sqrt{\overline{u^2}}_{\psi=90}$ ($\psi=90°$, *i. e.*, normal to the *c*-axis)

$=0{\cdot}1076\times235/320$

$=\underline{0{\cdot}0791\text{ Å.}}$

We can also calculate $\sqrt{\overline{u^2}}_{\psi}$ from the expressions given by Zener, for by combining equations (9) and (12) we obtain

$$\overline{u^2}_{\psi}=\frac{1{\cdot}1\times10^{-3}}{8\pi^2}\{1{\cdot}80\cos^2\psi+\sin^2\psi\}\mathrm{T},\quad .\quad .\quad (17)$$

Fig. 3.

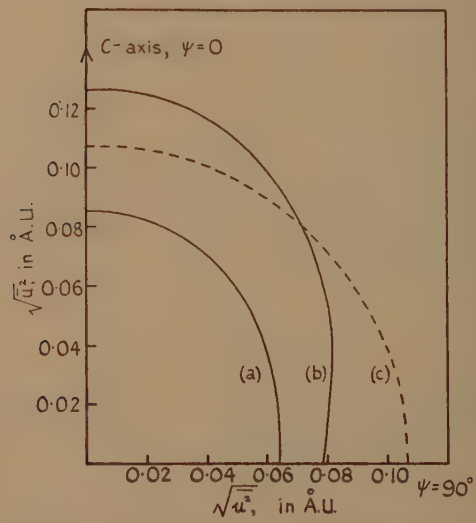

The r.m.s. amplitude of vibration of the atoms in zinc at room-temperature ; (*a*) according to Zener, (*b*) according to the approximate calculations given in the paper, and (*c*) using specific heat data.

where we have now written ψ in place of the Θ used by Zener. Taking T=290° abs., we have

$$\overline{u^2}_{\psi}=4{\cdot}04\times10^{-3}\{1{\cdot}80\cos^2\psi+\sin^2\psi\},\quad .\quad (17')$$

and for $\psi=0°$ $\qquad \sqrt{\overline{u^2}}_{0}=\underline{0{\cdot}0853\text{ Å.}}$

and for $\psi=90°$ $\qquad \sqrt{\overline{u^2}}_{90}=\underline{0{\cdot}0636\text{ Å.}}$

The r.m.s. displacements calculated from Zener's results are appreciably smaller than the approximate values based on the characteristic temperatures given by Grüneisen and Goens, but (what is more surprising) they are both considerably lower than the mean displacement calculated from the specific heat data.

The values of $\sqrt{u^2}$ given above, calculated from the data of Grüneisen and Goens, viz., 0·1265 Å. for $\psi=0°$ and 0·0791 Å. for $\psi=90°$, can be fitted to an expression

TABLE III.

The Scattering Factor, f, for Zinc, based on an Approximate Calculation of the Lattice Vibrations.

1. Reflexions.	2. e^M.	3. $pS^2\phi(\theta)\,.\,e^{-2M}$.		4. I_T/A (expt.).	5. f (relative).	6. f (absolute).
0002	1·054	64·0		269	2·05	21·2
$10\bar{1}0$	1·024	43·2		212	2·21	22·9
$10\bar{1}1$	1·037	201·0		760	1·94	20·1
$10\bar{1}2$	1·079	36·9		113·8	1·75	18·2
$10\bar{1}3$	1·151	55·8	97·8	212·5	1·47	15·2
$11\bar{2}0$	1·073	42·0				
$11\bar{2}2$	1·130	58·5		**100·0**	1·31	13·5
$20\bar{2}1$	1·113	42·4		71·7	1·30	13·4
$20\bar{2}3$	1·235	34·1		31·0	0·95	9·9
$10\bar{1}5$	1·417	28·2	71·9	59·1	0·91	9·4
$11\bar{2}4$	1·321	43·7				
$21\bar{3}1$	1·194	99·5		76·2	0·87	9·0
0006	1·598	8·0	49·2	30·8	0·79	8·2
$21\bar{3}2$	1·242	41·2				

of the type given by Zener for the angular variation of u^2_ψ, namely

$$\overline{u^2}_\psi = 6{\cdot}26\times10^{-3}\,\{2{\cdot}56\,\cos^2\psi+\sin^2\psi\}. \quad . \quad (18)$$

This equation should be compared with equation (17′) obtained from Zener's data; the equations are of the same form but have different numerical values.

The variation of $\sqrt{\overline{u^2}_\psi}$ with ψ is shown in fig. 3; curve (a) is calculated from Zener's results, equation (17′); curve (b) is the curve given by equation (18); and curve (c), a circle, shows the r.m.s. displacement calculated from the specific heat data.

6. *Application of the Approximate Calculation of Lattice Vibrations in Zinc to the Experimental Scattering Factors.*

The values of u^2_{ζ} calculated from equation (18) will now be used to correct the observed scattering factors for lattice vibration. The calculation is exactly the same as that described in section 4, except that equations (12) and (18) are to be used in place of equation (9).

The results are given in Table III., and are shown graphically in fig. 2 by small squares.

7. *Comparison of the Experimental Values of the Scattering Factor of Zinc with Theoretical Values.*

In the preceding paper on nickel and copper [5] it has been shown that the measured scattering factors for CuKα radiation agree well with the theoretical values valid for short waves when the latter are corrected for the effect of dispersion. We would therefore expect a similar agreement in the case of zinc, the next element to copper, if the temperature factor e^{M} has been obtained correctly. Within limits this constitutes a check on the calculated temperature factor. It is not an *exact* check, because the theoretically calculated scattering factors are not perfectly correct owing to approximations involved in the calculations of the electron distributions from which the scattering factors are derived, and the dispersion correction also may not be quite accurate. But in the light of the results obtained for nickel and copper a comparison between the observed and the theoretically calculated values should at least be a useful indication of whether the temperature correction and the experimental values are *approximately* correct.

Since the electron distribution for zinc has not yet been calculated by Hartree's method of self-consistent fields the scattering factor for zinc must be estimated in a manner similar to that used for nickel in the preceding paper [5].

Since zinc is the adjacent element to copper the estimation of the scattering factor for zinc in this way is not likely to introduce an error greater than about 0·2 in f for most values of $(\sin\theta)/\lambda$, and this will be good enough for the present purpose.

Figs. 4 *a* and 4 *b* illustrate the way in which the zinc scattering factor has been estimated; fig. 4 *a* relates to copper and fig. 4 *b* to zinc. The full curve marked H is the scattering factor for Cu^+ derived from Hartree's data. The curves T and P.S. are respectively the curves obtained by the methods of Thomas [12] and of Pauling and Sherman [13]. The full curve H′ is the estimated

Fig. 4.

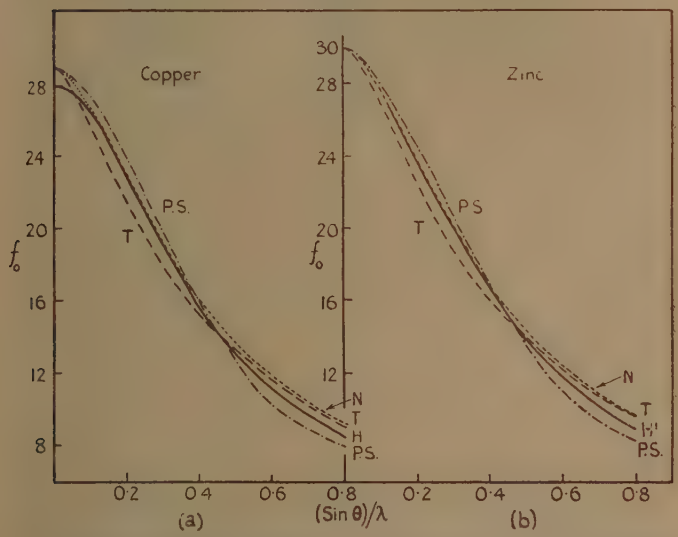

Theoretical scattering factors for copper and zinc; H is calculated from Hartree's data for Cu^+; H′ is the estimated curve for zinc; T,, P.S., and N are respectively Thomas, Pauling-Sherman, and Nagy curves for copper and zinc.

scattering factor for zinc. It has been drawn so that as far as possible it bears the same relation to the curves T and P.S. as the H curve does in the case of copper. A further check on the estimated curve for zinc is obtained from the scattering factors calculated by Nagy [14], using a modification of the Thomas method; for values of $(\sin\theta)/\lambda$ between 0·1 and 0·4 the curves of Nagy lie very close indeed to the H and H′ curves; the scattering factors given by Nagy are shown in fig 4 by dotted lines.

The estimated values of the scattering factor of zinc are given in Table IV., together with the values obtained by the various other methods.

When CuKα radiation is reflected from zinc dispersion has the effect of lowering the scattering factor by 2·14; this value has been obtained by Hönl's method [15]. To a first approximation Hönl shows that the effect is independent of $(\sin\theta)/\lambda$.

We may now compare the experimental results and the theoretical results. If f_0 denotes the theoretical scattering factor for short waves and Δf the dispersion correction, then the effective scattering factor for CuKα radiation is $f=(f_0-\Delta f)$. In fig. 2 the full lines show f_0 and f. The observed scattering factors at room-temperature are shown by circles. The scattering factors

Table IV.

Atomic Scattering Factors for Zinc.

$(\sin\theta)/\lambda$.	0·0	0·1	0·2	0·3	0·4	0·5	0·6	0·7	0·8	0·9	1·0
Estimated.	—	—	23·7	19·9	16·5	13·7	11·7	10·1	8·7	7·7	6·9
Thomas[12] .	30·0	26·9	22·4	18·6	15·8	14·0	12·2	10·6	9·5	8·5	7·7
Pauling-Sherman[13]	30·0	27·9	24·4	20·8	16·9	13·5	10·8	9·3	8·3	7·6	7·2
Nagy [14] .	30·0	27·7	23·6	19·8	16·7	14·3	12·4	10·9	9·5	8·5	7·7

corrected for lattice vibration according to Zener's data are shown by crosses, and the results obtained by correcting for lattice vibration by the more approximate method, utilizing the characteristic temperatures of Grüneisen and Goens, are shown by squares. The more prominent irregularities in the observed values of f_T are indicated in the figure by the lines joining the observed points.

It is seen that the approximate method of correcting for lattice vibration, based on the characteristic temperatures of Grüneisen and Goens, does smooth out very well the prominent irregularities in the f_T values at large $(\sin\theta)/\lambda$. The data given by Zener act in the right direction, but the correction is insufficient to smooth out the irregularities to any large extent.

Further, it is seen that the scattering factors corrected for lattice vibration by the approximate method show

a fairly satisfactory agreement with the theoretical f-curve. The agreement is particularly good up to $(\sin\theta)/\lambda = 0{\cdot}4$, but the higher-order reflexions give scattering factors which fall slightly below the calculated curve. A slightly larger correction for lattice vibration may be necessary.

The scattering factor for the (1010) reflexion is extraordinarily high. This result was repeatedly obtained both with filed zinc powder and with the condensed powder. If this high value is not due to some peculiar experimental error it may be due to an asymmetry of the valence electrons in the lattice; but the magnitude of the effect seems rather large to be explained in this way, and without additional evidence this could hardly be put forward as an explanation. A trace of impurity in the zinc powders giving a strong reflexion superimposed on this line might account for it, but in that case one would expect to find traces of other impurity lines, but none have ever been observed in the X-ray photographs. The question of why this reflexion gives an extraordinarily high scattering factor is therefore left open for the present.

8. *Experiments with Cadmium.*

As pointed out in the recent communication to 'Nature' [2] experiments have also been carried out with cadmium, and the results show almost precisely the same peculiarities as those described for zinc. There are, however, certain points of an experimental nature requiring further attention; these results will therefore be described in a later paper.

9. *Acknowledgments.*

Finally, it is with pleasure that I acknowledge Prof. Whiddington's interest in this work and a grant from the Government Grant Committee of the Royal Society, with which part of the essential apparatus was purchased.

10. *Summary.*

Measurements of the atomic scattering factor of zinc for CuKα radiation show that the scattering factor is

not a smooth function of $(\sin\theta)/\lambda$; reflecting planes making specially small angles with the basal plane of the structure give relatively low scattering factors, while planes making angles approximatng to 90° with the basal plane give relatively high scattering factors.

It is shown that these results are consistent with the amplitude of thermal vibration of the atoms being greater along the c-axis than normal to it, *i. e.*, in the basal plane.

The experimental results are considered in relation to calculations by Zener and to more approximate calculations by the writer for the magnitude of the lattice vibrations in zinc. When a correction is made for lattice vibration the resulting scattering factor for the stationary atom should be a smooth function of $(\sin\theta)/\lambda$. This is obtained with the calculations of the lattice vibrations given in the paper, but is not obtained so well with the calculations given by Zener.

A comparison is made between the experimental scattering factor corrected for lattice vibration and the scattering factor calculated theoretically. A reasonably close agreement is obtained when allowance is made for the effect of dispersion, which is important when CuKα radiation is reflected from zinc.

It is pointed out that cadmium gives very similar results to zinc; these will be discussed in a later paper.

References.

(1) G. W. Brindley and F. W. Spiers, Phil. Mag. xx. p. 865 (1935).
(2) G. W. Brindley, 'Nature,' cxxxvii. p. 315 (1936).
(3 C. Zener, Phys. Rev. xlix. p. 122 1936).
(4) G. W. Brindley and F. W. Spiers, Proc. Phys. Soc. xlvi. p. 841 (1934).
(5) G. W. Brindley, Phil. Mag. xxi. p. 798 (1936).
(6) E. Grüneisen and E. Goens, *Zeit. f. Phys.* xxvi. p. 235 (1924).
(7) I. Waller and R. W. James, Proc. Roy. Soc. A, cxvii. p. 214 (1927); see also C. Zener and G. E. M. Jauncey, Phys. Rev. xlix. p. 17 (1936).
(8) P. Debye, *Ann. der Physik*, xliii. p. 49 (1913).
(9) I. Waller, *Zeit f. Phys.* xvii p. 398 (1923); Uppsala Univ. Årsskrift (1925); *Ann. der Physik*, lxxxiii. p. 153 (1927).
(10) See P. Debye, ref. (8), p. 85.
(11) E. Grüneisen and E. Goens, *Zeit. f. Phys.* xxix. p. 141 (1924).
(12) See R. W. James and G. W. Brindley, *Zeit. f. Krist.* lxxviii. p. 470 (1931).
(13) L. Pauling and J. Sherman, *Zeit. f. Krist.* lxxxi. p. 1 (1932).
(14) B. v. Sz. Nagy, *Zeit. f. Phys.* xciv. p. 229 (1935).
(15) H. Hönl, *Ann. der Physik*, xviii. p. 625 (1932).

LXVI. *X-ray Measurement of the Thermal Expansion of Pure Nickel.* *By* Prof. E. A. Owen, *M.A., D.Sc., and* E. L. Yates, *M.Sc., Ph.D., University College of North Wales, Bangor* *.

THE thermal expansion of nickel near the temperature of magnetic transformation has been the subject of considerable investigation. Colby †, employing an optical method, found that the coefficient of expansion of electrolytic nickel of high purity showed an abnormal increase between 220° C. and 360° C. On further heating the coefficient decreased rapidly, returning to its normal value at about 370° C. With other specimens of nickel of lower purity the same effect was observed, the thermal coefficient increasing with temperature until the critical region in the neighbourhood of the magnetic transformation was reached, and then decreasing to a certain value before increasing again with further rise of temperature. Hidnert ‡, who measured the thermal expansion of a specimen of nickel, 99·4 per cent. pure, in the form of a rod 12 inches long, over the range of temperature 25° C. to 900° C., found an irregularity in the rate of expansion near 350° C. Recently Clarke Williams §, using a sensitive optical method and a single crystal of nickel, made a detailed investigation of the thermal expansion of the element near its transformation temperature. The curve showing the relation between coefficient of expansion and temperature obtained by him with the purest nickel available showed a maximum at about 355° C. and a sudden drop beyond this temperature.

In view of the interest attaching to the peculiar expansion of nickel near the critical temperature of magnetic transformation, it was decided to measure the thermal expansion of the crystal lattice of nickel over as wide a range of temperature as possible. The parameter measurements to be described were obtained with unstrained material, so that changes in the Curie point due to over-straining, which were recently reported by Quinney ‖, were avoided.

* Communicated by the Authors.
† Phys. Rev. xxx. p. 506 (1910).
‡ Bureau of Standards, Journ. Research, v. p. 1305 (1930).
§ Phys. Rev. xlvi. p. 1011 (1934).
‖ Journ. Inst. Metals, lv. p. 229 (1934).

Apparatus.

The high-temperature camera used in the investigation was of the same design as that already described *, except that the one now employed embodied a certain number of improvements. A detailed account of the improved camera and vacuum enclosure will be published elsewhere. The camera was mounted horizontally in its enclosure, the pressure in which during an exposure was not greater than 0·001 mm. of mercury. With the original high-temperature camera considerable trouble was experienced with the continued discoloration of the specimens under examination when heated above 400° C. The tarnishing which occurred had the effect of reducing the lattice parameter slightly, and the measurements were not considered to be reliable on this account. With the improved camera and its almost perfect air-tight enclosure the causes of the discoloration were removed, and it was possible to undertake a thorough investigation of the thermal expansion of nickel without risk of complications arising from contamination of the material.

Manganese radiation † was employed. This radiation, reflected in the (311) planes, gave lines on the film in positions favourable for accurate determinations of parameter.

The expansion of the lattice between 300° C. and 420° C. was studied in great detail. Exposures were made under varying conditions of heat treatment to find if thermal hysteresis could be detected. No effect was observed; exposures at a given temperature gave the same lattice parameter whether the specimen had been heated or cooled to the temperature at which the exposure was made.

The powders examined were prepared from four different samples of annealed filings. Specimens 1 and 2 had been annealed at 600° C. for 14 hours and slowly cooled over six days; specimen 3 annealed at 336° C. for one hour and quenched into iced water; specimen 4 annealed at 440° C. for one hour and then similarly quenched. These four specimens yielded identical values of the lattice parameter at the same temperature and were used in turn throughout the work.

* Owen and Yates, Phil. Mag. xvi. p. 606 (1933).

† The values of the wave-lengths adopted were as follows:—$K\alpha_1 = 2{\cdot}09751$ Å.; $K\alpha_2 = 2{\cdot}10149$ Å.

The thermocouple was calibrated frequently to ensure correct recording of temperature.

Crystal Structure of Nickel.

The crystal structure of nickel has been variously reported. Hull * mentions two forms, one possessing a face-centred cubic and the other a body-centred cubic structure. McKeehan † reports only a face-centred cubic structure for the nickel he investigated. Bredig ‡ has reported the existence of a hexagonal form of the element. Most workers have found nickel to possess a face-centred cubic structure, and Jesse § has recently shown that this structure persists for temperatures ranging from 450° C. to 1200° C. To determine the structure of the nickel used in the present investigation over the range of temperature in which anomalous expansion occurred, powder photographs ‖ were taken of specimen 1 at 18° C., 350° C., and 380 C°. *in vacuo* with a spectrum camera especially designed for high-temperature exposures. The lines in each photograph were those to be expected from a face-centred cubic lattice and no extra lines were observed. There can be, therefore, no doubt that the nickel under investigation possessed a face-centred cubic structure.

The purity of the nickel was 99·98 per cent.

Results.

The experimental values of the lattice parameters of nickel at different temperatures are recorded in Table I., each value recorded having been corrected for refractivity.

The parameter of pure nickel at 18° C. calculated from these figures is 3·5172 Å. and its density 8·897 gm. per c.c., assuming that the mass of an atom of unit atomic weight is $1{\cdot}649 \times 10^{-24}$ gm. and that the atomic weight of nickel is 58·69.

The number of the film in the first and fourth columns of Table I. gives an indication of the order in which the photographs were taken. The letter (*c*) in the second

* Phys. Rev. x. p. 661 (1917).
† Phys. Rev. xxi. p. 402 (1923).
‡ *Zeits. f. phys. Chem. Bandenstein-festband.* p. 172 (1931).
§ 'Physics,' v. p. 147 (1934).
‖ We are indebted to Dr. Pickup of this laboratory for taking these photographs.

and fifth columns indicates that the specimen was raised initially to a temperature slightly above the required temperature and was allowed to cool slowly to the final temperature before the exposure was commenced; the period of cooling was not less than half an hour in each case. The letter (*h*) in the same columns indicates that the specimen was raised initially to a temperature just below the required temperature and was then heated slowly to the final temperature for a period of at least half an hour before commencing the exposure. The

TABLE I.

Film no.	Temp. °C.	Lattice parameter, A.	Film no.	Temp. °C.	Lattice parameter, A.
601 & 617	12	$3{\cdot}5170_1$	586	349 (*h*)	$3{\cdot}5347_6$
563 & 608	13	$3{\cdot}5170_1$	612	352 (*h*)	$3{\cdot}5350_3$
569, 574	14	$3{\cdot}5170_0$	624	356 (*h*)	$3{\cdot}5355_3$
596, 597			592	359 (*c*)	$3{\cdot}5356_9$
560, 562	15	$3{\cdot}5170_7$	599	362 (*c*)	$3{\cdot}5359_7$
621, 625, 626			600	363 (*c*)	$3{\cdot}5360_2$
590	16	$3{\cdot}5171_8$	593	365 (*c*)	$3{\cdot}5361_9$
565	98 (*c*)	$3{\cdot}5212_1$	577 & 598	370 (*h*)	$3{\cdot}5367_8$
567	187 (*c*)	$3{\cdot}5259_2$	576	373 (*c*)	$3{\cdot}5367_2$
573	257 (*c*)	$3{\cdot}5295_0$	603	374 (*h*)	$3{\cdot}5367_9$
595	275 (*c*)	$3{\cdot}5302_2$	604	378 (*h*)	$3{\cdot}5371_0$
564	301	$3{\cdot}5319_2$	589	388 (*h*)	$3{\cdot}5379_3$
594	331 (*c*)	$3{\cdot}5335_8$	566	398 (*h*)	$3{\cdot}5383_4$
571	333 (*h*)	$3{\cdot}5337_8$	613	405 (*h*)	$3{\cdot}5386_5$
584	336 (*h*)	$3{\cdot}5337_6$	607	410 (*c*)	$3{\cdot}5388_0$
606	338	$3{\cdot}5338_8$	609	411 (*c*)	$3{\cdot}5388_5$
611	341 (*h*)	$3{\cdot}5343_0$	591	429 (*h*)	$3{\cdot}5402_6$
585	342 (*h*)	$3{\cdot}5343_5$	572	460 (*c*)	$3{\cdot}5422_2$
618	343 (*h*)	$3{\cdot}5342_4$	561	501 (*h*)	$3{\cdot}5448_3$
616 & 610	345 (*c*)	$3{\cdot}5345_4$	575	557 (*c*)	$3{\cdot}5481_8$
614	346 (*c*)	$3{\cdot}5347_2$	568	603 (*h*)	$3{\cdot}5508_0$
605	348 (*c*)	$3{\cdot}5346_8$	615	608	$3{\cdot}5516_7$

temperatures that are not marked indicate a steady heating at the temperature of exposure over at least half an hour before the exposure. Several determinations at room-temperature are included in the table. Some of these were obtained with fresh material, others with materials which had been used several times to obtain parameters at high temperatures.

The figures in Table I. are shown graphically in fig. 1. The thermal expansion curve shows that from 0° C. to 370° C. the lattice expands gradually at first but very

rapidly between 310° C. and 370° C., until at the latter temperature it has an abnormally high coefficient of expansion. Above 370° C. the coefficient of expansion rapidly decreases, falling to quite a low value before assuming at about 420° C. a value which gradually increases up to the highest temperatures at which lattice

Fig. 1.

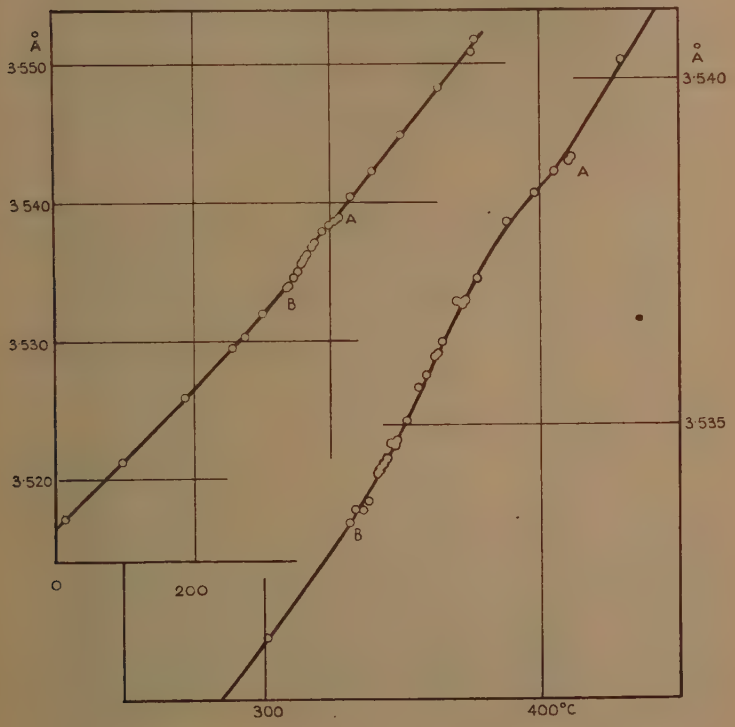

parameters were measured. A sufficient number of points was determined in the critical region to draw the temperature-parameter curve on a large scale and thereby determine its slope at different points. The variation of the true thermal coefficient of expansion of nickel with temperature, determined in this way, is shown in fig. 2, which is a graphical representation of the figures collected in Table II.

One of the difficulties experienced in the examination of crystal lattices at high temperatures has been the exact determination of the temperature of the irradiated powder. Although much care and time were spent in devising means of making accurate measurements of the temperature, it was considered desirable to have a separate check on the thermocouple method finally

Fig. 2.

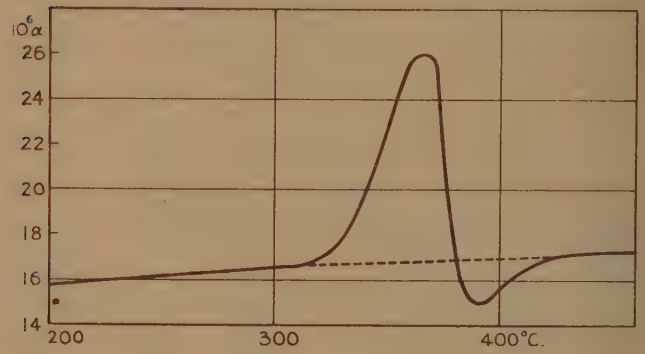

TABLE II.

Temp.	Lattice parameter, Å.	Thermal coef. of expansion $\times 10^6$.	Temp.	Lattice parameter, Å.	Thermal coef. of expansion $\times 10^6$.
0....	$3{\cdot}5164_5$	13·5	370....	$3{\cdot}5366_4$	26·0
100....	$3{\cdot}5212_5$	14·6	380....	$3{\cdot}5373_0$	17·5
200....	$3{\cdot}5263_7$	15·8	390....	$3{\cdot}5378_6$	15·0
300....	$3{\cdot}5317_7$	16·6	400....	$3{\cdot}5384_2$	15·6
350....	$3{\cdot}5347_7$	23·0	500....	$3{\cdot}5446_2$	17·6
360....	$3{\cdot}5357_5$	25·8	600....	$3{\cdot}5508_7$	17·8

adopted. The variation of the lattice parameter of silver with temperature had been studied previously, and the value of the lattice parameter at any temperature up to 600° C. was known to a high degree of accuracy. Measurements of the parameter of silver afforded a means of determining the temperature of the specimen and would serve as a check on the thermocouple. A direct comparison was therefore carried out between the

temperature recorded by the thermocouple and that deduced from the silver parameter.

Some annealed nickel powder (specimen 4) was mounted in the usual way on the thermo-sheet and the lattice parameter measured at 502° C., manganese radiation being used to obtain the photograph. The reflexions from the (311) planes yielded a value of 3·5449 Å. for the latter parameter at this temperature.

One half of the powder was now removed and replaced by annealed silver powder. Copper radiation was employed, giving reflexions from the (331) and (420) planes of nickel and the (511) or (333) planes of silver. It was known that at about 500° C. the reflexions from the higher order planes of nickel would coincide with

TABLE III.

Material	$\frac{\pi}{2}-\theta$.	Line.	Refl. plane.	Lattice parameter (Å.). Observed.	Corrected for refractivity.	Mean.
Ag ..	14° 7′ 44″	α_1	333	$4{\cdot}1188_7$	$4{\cdot}1190_1$	$4{\cdot}1188_7$
	13° 32′ 17″	α_2	511	$4{\cdot}1185_8$	$4{\cdot}1187_2$	
Ni ..	19° 3′ 45″	α_1	331	$3{\cdot}5448_2$	$3{\cdot}5449_4$	$3{\cdot}5448_9$
	18° 37′ 24″	α_2	331	$3{\cdot}5446_4$	$3{\cdot}5447_5$	
	14° 7′ 44″	α_1	420	$3{\cdot}5449_6$	$3{\cdot}5450_4$	
	13° 32′ 17″	α_2	420	$3{\cdot}5447_0$	$3{\cdot}5448_0$	

those from the silver lattice, and the temperature was adjusted accordingly. An exposure made at 504° C. as measured by the thermocouple resulted in two lines being exactly superimposed. The width of each line was less than 0·6 mm. at a glancing angle of 76°. This demonstrates the exactness of the coincidence. The measurement of the film gave the results shown in Table III.

On referring to the parameter-temperature curve for silver it was found that the lattice parameter 4·1189 Å. corresponded to a temperature of 505° C., which agrees very satisfactorily with the temperature 504° C. given by the thermocouple. The parameter of 3·5449 Å. at 502° C. referred to above and obtained with manganese radiation agrees almost exactly with the parameter value of nickel now calculated from spectra taken with copper radiation

when the temperature recorded by the thermocouple was 504° C.

The agreement also between the present lattice parameter measurements of the nickel powder, and those made about three months previously on another sample of the material, confirms the agreement in the temperature. The lattice parameter of nickel at 501° C. was previously found to be $3{\cdot}5448_3$ Å.

From measurements such as the above, it was concluded that the temperatures recorded were close to the true values and that the values of the nickel lattice parameter at the different temperatures could be relied upon to a high degree of accuracy.

Discussion of Results.

The results agree in general with those of previous workers in this field, but the thermal coefficient of expansion in the critical region now reaches a higher maximum value and the abnormal variation in the coefficient occurs over a shorter range of temperature. The present investigation differs from previous investigations on the coefficient of expansion of nickel in three respects: (i.) the material used was of a higher degree of purity (99·98 per cent.) than in any previous work on this metal; (ii.) a study of the thermal expansion of the crystal lattice was made with a very small quantity of material in powder form, whereas previous work, except that of Jesse, who investigated the expansion of the nickel lattice above 450° C., dealt with the expansion of comparatively large masses of the metal either in polycrystalline or in single-crystal form; and (iii.) the material being in powder form and thoroughly annealed is free from strain, and no change takes place in its elastic constants during measurement. The X-ray method therefore measures changes in length due to thermal expansion and eliminates those due to elastic effects.

Clarke Williams * found that the expansion in the critical region decreased and the maximum moved to a lower temperature with increasing degree of impurity of the specimen. It would be expected, therefore, that with pure material the maximum would become more pronounced and would occur at a higher temperature.

* *Loc. cit.*

This is in agreement with the results now recorded. The maximum value of the coefficient occurs at about 370° C. and its value is 26×10^{-6}.

Measuring the area under the curve in the region of the maximum it is found that the ferromagnetic change in length per unit length for nickel containing 99·98 per cent. nickel is about $2{\cdot}4 \times 10^{-4}$. This is about double

Fig. 3.

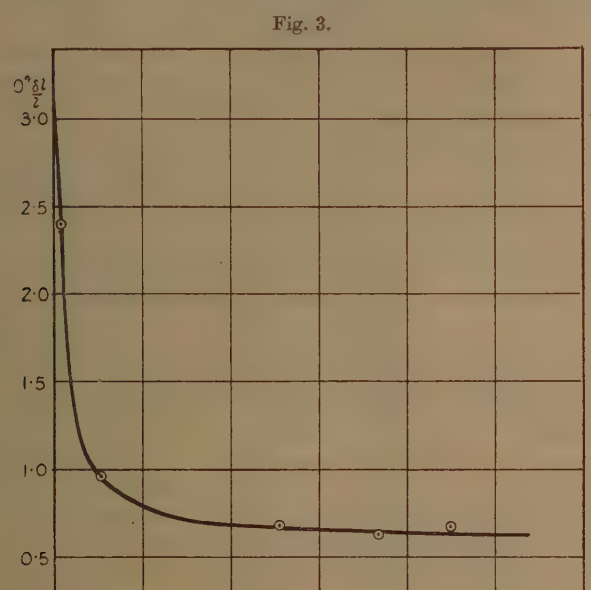

the value for pure nickel given by Clarke Williams as deduced by the extrapolation of the curve obtained by using nickel of different degrees of purity. It would appear from this that the ferromagnetic change in length diminishes rapidly with the introduction of impurity into the metal. When the present results are combined with those of Clarke Williams, the curve connecting the total percentage impurity with the ferromagnetic change in length per unit length takes the form shown in fig. 3, the value of the ferromagnetic change in length per unit

length for pure nickel being in the neighbourhood of 3×10^{-4}. The precise shape of the curve will doubtless depend upon the nature of the impurities.

The crystal structure of nickel does not change as the material passes through the temperature of magnetic transformation. It remains face-centred cubic above as well as below this temperature, but when the material changes from the magnetic to the non-magnetic condition a sudden increase in parameter occurs; after passing through the critical region the lattice returns to its normal rate of expansion, the expansion curve above about 420° C. being approximately a continuation of that below 300° C.

We have previously investigated the β-transformation in the copper-zinc series *, when an increase in the thermal expansion of the lattice was observed after passing through the transformation temperature at about 470° C. But in contrast to nickel the lattice of the β-alloy continued to increase at the greater rate at all temperatures above the transformation temperature, and the alloy contained two different atoms in equal proportions. The conclusion arrived at was that the transformation was probably concerned with the change from an "ordered" to a "disordered" arrangement of atoms in the lattice structure, as suggested by Bragg and others. That is, the zinc atoms would take up definite symmetrical positions in relation to the copper atoms below the temperature of transformation, but would take up any positions in the lattice above that temperature.

With nickel there is only one kind of atom present, and to account for the sudden expansion that occurs near the transformation temperature it must be assumed that a local disturbance may occur at each lattice point without the transference of atoms from one point to another. The atoms at temperatures below the magnetic transformation may lie at definite "orientations" relative to one another, but at the transformation temperature the thermal energy of the atoms is sufficient to overcome the binding forces in the crystal which keep the atoms in their relative "orientations." On such a view it would be necessary to consider at transformation temperatures not only the possibility of change from

* Owen and Pickup, Proc. Roy. Soc. A, clxv. p. 258 (1934).

" order " to " disorder " of the atoms amongst points in the lattice, but also the possibility of changes occurring at lattice points without the transference of atoms from one point to another.

We have pleasure in thanking the Department of Scientific and Industrial Research for a grant to help us carry out the work and also the Mond Nickel Company, Birmingham, for supplying us with nickel of high purity.

Summary.

The thermal expansion of the crystal lattice of nickel, the purity of which was 99·98 per cent., was measured over the range of temperature from 12° C. to 600° C.

The structure of nickel remained face-centred cubic over the whole range of temperature investigated.

The parameter of nickel at 18° C. was found to be $3{\cdot}5172_4$ Å. and its density 8·897 gm. per c.c.

The variation in the thermal coefficient of expansion with temperature was investigated in detail. An abnormally high rate of expansion followed by a rapid decrease was observed in the region of the temperature of magnetic transformation. No evidence was obtained that the phenomenon was accompanied by thermal hysteresis. The maximum value of the thermal coefficient of expansion occurred at 370° C.

In the region of the magnetic transformation the thermal coefficient of expansion had the following values: 17×10^{-6} at 320° C., 26×10^{-6} at 370° C., and 15×10^{-6} at 390° C. On either side of this region the expansion was normal.

The ferromagnetic change in length per unit length for nickel of 99·98 per cent. purity is found to be about $2{\cdot}4\times10^{-4}$, which is much higher than the values previously recorded for nickel of lower purity.

It is suggested that in order to explain generally the occurrence of transformations at certain temperatures in alloy systems it may be necessary to consider, in addition to migration of atoms from point to point in the lattice, changes occurring at lattice points when no migration of atoms takes place.

Bangor.
25th November, 1935.

LXVII. *The Surface Structure of Polished Cleavage Faces of Calcite.* *By* H. G. Hopkins, *A.R.C.S., B.Sc.**

[Plates XIII. & XIV.]

THE author has already published an account of his investigations into the nature of the surface structure of a polished gold surface [1].

The present contribution describes a series of experiments carried out using electron optical technique to supplement Beilby's [2] original work with the microscope.

The investigation may be conveniently divided into two parts: the first deals with the precise nature of the polish layer on calcite and its mode of formation; the second deals with the effect of etching the polished surface.

Previous Work.

Raether [3], using electron diffraction methods, has found that when a cleavage face of calcite is ground and polished the surface layer is crystalline, but that severe distortion of the crystal occurs at the surface.

As his conclusions were at variance with those of Beilby it was decided to investigate in rather greater detail the nature of this distortion, using methods of polishing as near as possible identical with those used by Beilby.

Experimental Procedure.

1. *Choice of Specimen.*

Freshly cloven crystals were used in these experiments. Each specimen, before polishing, was examined under the microscope, using dark background illumination. By this method any faults in the surface showed up as very bright spots. No crystal showing more than a few specks was used in the subsequent experiments. The actual experimental arrangement employed was to allow the condensed beam from a baby arc to fall obliquely on the surface of the specimen.

* Communicated by Prof. G. P. Thomson, M.A., F.R.S.

2. *Method of Polishing.*

A cleavage face selected in the above way was then treated by one of two distinct methods :

(*a*) Rubbing on chamois-leather.

(*b*) Grinding and subsequent cloth polishing.

(a) *Rubbing Method.*—The selected cleavage face was rubbed very lightly on clean dry chamois-leather stretched on a polishing board. Cleavage faces were polished in various directions with respect to their crystallographic axes.

(b) *Grinding and Cloth Polishing Method.*—A good cleavage face was ground to a uniform matt appearance on a rotating steel lap, using wet flour emery as abrasive. The ground surface was then polished on a rotating cloth, using wet rouge as the polishing medium. The surface in general after polishing was " lemon-peeled "—that is, it had a wavy appearance. Before examination by electron diffraction the surface was washed free from rouge and then rinsed in alcohol.

Diffraction Patterns obtained.

The specimen was examined at various stages in the polishing process, using 30 kv. electrons at glancing incidence.

A. *From Specimens Polished by Method* (a).

The patterns obtained as the polishing process proceeded were not consistent from specimen to specimen, but fall into two main groups :

(1) Some specimens gave no change in pattern except a general rise in background scattering, accompanied by broadening of Kikuchi lines.

(2) Other specimens gave an extended pattern of blurred spots, showing extension of the spots perpendicular to the shadow edge.

An example of this type of pattern is shown in Pl. XIII. (fig. 1).

B. *From Specimens Polished by Method* (b).

Consistent results were given by this method.

(1) *From the ground surface* no pattern could be obtained owing to excessive charging up of the specimen.

(2) *From the ground surface roughly polished* charging up became less marked as the polishing process on the cloth lap continued. A picture was taken when the surface had begun to take on a shiny appearance. No pattern was given; the angle of incidence used was about 3°, smaller angles causing charging up.

(3) *From the well polished surface* the patterns consisted of an extended array of blurred spots. While the patterns showed little, if any, extension of the spots perpendicular to the shadow edge, each spot was deflected from its normal position towards the shadow edge. Photographs were taken in the various principal azimuths (Pl. XIII. fig. 2; Pl. XIV. fig. 3).

Discussion.

It will be convenient to consider together the results obtained from specimens polished by the two methods.

The patterns of the second type obtained from a gently rubbed surface and those obtained from a well polished surface (previously ground) have this common feature—an extended array of spots.

Let us consider the types of structure that can give rise to such a pattern.

It is well established that an extended pattern can be produced by transmission of the electron beam through extremely thin projecting crystalline lumps on a surface [4].

An extended pattern of spots can also be formed if the crystal surface is distorted so that it is broken up into small blocks making small angles with each other.

Now for the formation of a row of central orders θ must take on a series of values determined by the equation $2d \sin\theta = n\lambda$, where θ is the glancing angle in the crystal between the beam and the cleavage planes and λ is the wave-length of the electron inside the crystal, n is the order number of the spot concerned, d is the cleavage plane spacing.

Since θ is governed by the angle of incidence at the crystal surface this equation implies that the angle of incidence at the surface must be different at different parts of the surface.

The distortion suggested will produce an effect of this nature, and the angle between any two blocks in the area covered by the beam need not exceed 4° to give

rise to patterns as extended as those observed. The pattern given by such a distorted surface because of the small angles of incidence at the surface will show a shift of the spots towards the shadow edge due to the refraction of the electrons on entering and leaving the surface. A true cross-grating pattern, on the other hand, will show no effects of refraction.

Further, the distorted crystal surface cannot give rise to sharp Kikuchi lines, and the background on a pattern obtained from such a surface will be high, due to the effective traversing of these lines across the plate.

Bearing these points in mind it seems certain that the extended spot patterns given by the polished surface result from distortion of the surface.

The extended patterns obtained by rubbing show elongation perpendicular to the shadow edge, while the well-polished specimens show almost complete absence of this effect.

The elongation results from diffracted electrons of any one order leaving surfaces not parallel with the corresponding entrance surfaces, the angular deviation between entrance and exit surfaces varying from electron to electron.

An electron of 30 kv. energy cannot penetrate more than about 500 Å. of crystal before an inelastic collision occurs. The presence of tailing indicates that the average length of the blocks does not greatly exceed this value. In such circumstances a diffracted electron will probably not leave the specimen by the same surface through which it entered.

In the case of a ground and well polished surface, however, the absence of tailing shows that the coherent areas extend on the average over lengths considerably larger than 500 Å.

It should be emphasized that tailing of the spots depends on surface variations over distances comparable with the mean free path for ionization of a 30 kv. electron (5×10^{-6} cm.), but that surface imperfections over distances comparable with the length of specimen covered by the beam (3×10^{-1} cm.) are effective in producing the extended spot pattern.

It seems probable that the first type of pattern obtained from certain lightly rubbed specimens results from the

first stages in the distortion process already described. Transition from the perfect cleavage face to the distorted crystal surface necessitates a blurring of the Kikuchi lines and a general rise in background intensity due to the increase in inelastic scattering. This view is supported by the fact that in some cases a rubbed surface initially showing the first type of pattern by subsequent polishing developed a pattern of elongated spots.

It was also noticed that if the rubbing process was carried out on chamois which was slightly soiled the extended pattern of spots always resulted. This, again, points to the conclusion that the extended pattern produced by rubbing is caused by rather more vigorous treatment than that necessary to produce the first type.

Conclusions.

1. The surface of a polished cleavage face of calcite is crystalline. This confirms the work of Raether.

2. The polishing process breaks up the surface into small blocks making small angles with each other.

3. The ratio of the area of distorted crystal to that of the undistorted increases as the polishing process is pushed further.

Etching Experiments with Polished Cleavage Faces.

Preliminary Experiments.

It was found impossible to obtain a cross-grating pattern from unpolished specimens of calcite on etching in dilute hydrochloric acid. Cleavage faces, however, which had previously been rubbed for a few minutes on chamois readily gave rise to a cross-grating pattern on etching in dilute acid (0·08 per cent. HCl).

In cases when the polished surface initially showed an extended pattern of spots the etched pattern was always of similar geometrical form—for a given azimuth—to that given by the polished surface. The distinction between the two types was that the etched pattern was much sharper and the spots were not shifted by any refraction effects.

From experiments of this nature it was shown that the polishing action had caused no very large rotation of the crystal blocks about an axis normal to the surface.

Step-by-Step Etching of the Polished Surface.

In this series of experiments the procedure was analogous to that employed by Beilby.

Specimens ground and cloth polished as already described were used.

Uniform etching conditions were achieved by supporting the specimen, polished surface downwards, immediately above and parallel to a clean glazed porcelain slip. The latter was carried on a small table, which could be raised by a rack-and-pinion device. A drop of acid, about 0·1 c.c., was allowed to fall on the slip. By carefully raising the table on which the slip was supported the acid was brought into contact with the whole of the polished surface of the specimen. The specimen was left in this position until all the acid in the drop had reacted with the calcite. The time necessary for acids of various concentrations was found by a preliminary series of experiments, using methyl red as indicator.

The weakest acid used 0·00015 per cent., and acids of progressively increasing concentration were used until about 12,000 Å. had been removed.

The surface structure was examined at each stage by means of the electron diffraction camera. Photographs were generally taken in the symmetrical azimuth only, but the pattern on the fluorescent screen was carefully studied at various azimuths in order to observe any abnormalities.

Electron Diffraction Results.

Results may be summarized as follows :—

As the etching process proceeded the pattern of spots sharpened, background intensity became less, the spots moved out gradually to their unrefracted Bragg positions, and Kikuchi lines became first apparent at 200 Å.

No abnormal features were noted in this gradual process except that in one series of plates at 6000 Å. below the polished surface extra spots were noticed in asymmetrical azimuths. Fig. 4 (Pl. XIV.) shows this effect.

No extra spots were shown in the pattern taken from the same specimen after further etching to 12,000 Å.

Discussion of Results.

The most significant feature of the series of patterns obtained by the step-by-step exploration is the gradual shift of the spots outwards from the shadow edge as the etching process continued.

An estimate of the apparent inner potential was obtained at each stage by a graphical method used by Tillman [5].

Nominal depth, Å.	ϕ' volts.	d, Å.
0	9·0	3·00
6	8·8	3·01
12	6·0	3·02
17	5·5	2·98
25	2·1	3·09
30	5·0	3·05
35	3·5	3·05
40	1·5	3·08
50	2·1	3·02
75	1·0	3·02
90	1·5	3·06
130	2·5	3·02
180	0	3·01
220	1·0	3·03
630	0	3·01
1250	0	3·04
5850	0	3·01

The table shows the values for ϕ' and d calculated from plates taken after various depths of calcite had been removed. $\phi' = \frac{p_r}{p}\phi$, where ϕ is the mean inner potential, p is the voltage of the electron beam, and p_r is the voltage of the beam with the relativity correction applied. The depths have been calculated on the assumption that the acid removes the calcite atoms without pitting the surface. This is known not to be true, but the calculated depths serve as useful reference

figures and indicate the order of the mean etching effect over the whole surface.

Calculated mean cleavage plane spacing d from above results :—3·03 Å.

Value calculated from X-ray data :—3·03 Å.

It will be noticed that, taking into account the experimental error of about ± 1 volt, there appears to be a steady falling off in the magnitude of the inner potential as more and more of the surface is eroded.

It seems unlikely that such a decrease in the inner potential does, or indeed can, occur, for the mean inner potential of a crystal is determined by the relative positions of the various atomic groups. No indication has been obtained to indicate any structural change.

Before considering the suggested explanation of the effect it will be helpful to consider the mechanism of etching. Electron diffraction results show that, in general, chemical etching of the cleavage face of a crystal exposes crystallographic planes with simple indices. Erosion does not proceed evenly, but leaves projections through the thin parts of which the major portion of the beam passes and gives rise to a cross-grating pattern at appropriate azimuths of the crystal.

Bearing this picture of the etching process in mind, let us examine the results of the present series of experiments.

It is suggested that the apparent decrease in inner potential results from the local pitting set up by the etching action.

In these experiments the etching action has been allowed to proceed in very slow stages. Initially sufficient acid to dissolve a layer of calcite only 6 Å. thick over the whole surface reacts with the polished crystal surface. Since the etching action does not produce uniform removal this mean figure of a few Ångströms implies that the number of pits in a given area of the etched surface must be very small. The majority of electrons will therefore still impinge at glancing incidence on the broad unbroken crystal blocks, and leave by the same surface at which they enter.

Very few will enter or leave at the sides of the pits.

The first group of electrons will give rise to a diffraction pattern of the type obtained from the unetched polished surface, and will suffer the full deviation due to the

refraction effect at the surface. The second group will form an extended pattern showing no elongation perpendicular to the surface.

The position of the maximum blackening on the plate will be determined by the relation between the numbers of electrons in the two groups. Since, however, there are only a few electrons of the second group the blackening on the plate actually observed will result to a very large extent from electrons of the first type.

As more of the surface is removed by etching the unattacked surface area becomes smaller while the pits become more numerous and deeper. The proportion of the electrons which enter or leave the pit surfaces will increase. The areas of maximum blackening will move out from the shadow edge.

We should expect some elongation of the spots to occur at a stage when the areas giving rise to the two types of pattern are about equal. This stage appears to have been reached at a nominal depth of less than 50 Å. The extension effect, however, owing to the very diffuse nature of the spots resulting from the small resolving power normal to the surface is not marked.

The fact that the unetched polished surface shows an apparent inner potential of only 9 volts compared with the normal value of 12·9 volts for calcite suggests that a few pits exist even on the well polished surface.

Kikuchi lines also become apparent at a depth of 200 Å. At this depth the exposed surface must consist mainly of undistorted crystal.

The extra spots found at 6000 Å., fig. 4 (Pl. XIV.) are attributable, with the exception of that on the central axis, to the presence of a certain amount of twinned crystal at this depth.

That this explanation is reasonable will be seen from the following argument.

In an asymmetrical azimuth if the crystal is turned through 180° the mirror image of the original pattern about the normal passing through the undiffracted spot is obtained. In Pl. XIV. we have these two patterns present at the same time. This indicates that the surface is not homogeneous, but crystals are present so orientated to give both types of pattern. Since the spots are quite sharp, and Kikuchi lines are shown on the same plate, it can be assumed that the orientation of the two sets

of crystals with respect to each other is sensibly perfect. It seems that such "mirror image" type of orientation of two sets of crystal on the same surface over an area of a few square millimetres can only be due to twinning on the cleavage plane.

Conclusions.

1. No evidence of the existence of an amorphous layer at the polished crystal surface was obtained.

2. The results show that even with very dilute acids the action of etching is essentially one of pitting.

3. Although Kikuchi lines occurred at only 200 Å. below the polished surface it seems that the polishing action must extend to a depth of at least 6000 Å., as at this depth a twinned layer was observed, due presumably to working the surface.

Acknowledgments.

The author is deeply indebted to Professor G. P. Thomson for the great interest he has taken in the research, and to the Department of Scientific and Industrial Research for a maintenance grant, during the tenure of which the work was carried out.

References.

(1) Hopkins, Trans. Far. Soc. p. 1095 (1935).
(2) Beilby, 'Aggregation and Flow of Solids.' London, 1921.
(3) Raether, *Z. Physik*, lxxxvi. p. 82 (1933).
(4) Thomson, Phil. Mag. xviii. p. 640 (1934).
(5) Tillman, Phil. Mag. xviii. p. 656 (1934).

LXVIII. *Correction to my Paper, "On the Theoretical Determination of Earth Resistance from Surface Potential Measurements."* *By* A. F. Stevenson, *M.A., Ph.D., Department of Applied Mathematics, University of Toronto* *

In a recent paper with the above† title, I attempted to give a solution of the problem (in the case where the conductivity is a function of depth only) in terms of Fourier series. Professor R. E. Langer has, however,

* Communicated by the Author.
† Phil. Mag. xix. p. 297 (1935).

communicated to me a criticism of the paper which unfortunately invalidates much of the work.

The reason is briefly as follows :—Equations (9) of the paper are an infinite set of linear equations for determining the Fourier coefficients of the potential from those of the conductivity. Groups of these equations were then summed in a certain way in order to obtain a direct relation between the Fourier coefficients of the *surface* potential and of the conductivity. But by a closer consideration of the structure of the original differential equation, Langer has shown that this process of summation leads merely to a series of identities $0=0$ *, and that, consequently, the subsequent work can have no real significance. The equations (9) still hold for the determination of the potential when the conductivity is an assigned Fourier series (and might be of a certain use in this connexion), but this does not, of course, solve the converse problem of determining conductivity from surface potential, and this was the main object of the paper.

I wish, therefore, to withdraw the conclusions of the paper in question and to express my regrets that the error was not detected earlier.

LXIX. *Notices respecting New Books.*

Early Science in Oxford.—Vol. X. *The Life and Work of Robert Hooke* (Part IV.). Edited by Dr. R. T. Gunther. (Oxford, printed for the Author, 1935. Published price, 21*s*.)

THIS volume begins with a reprint of an essay written in 1661, *i. e.*, in Hooke's Oxford period, entitled "An attempt for the explication of the phænomena published by the Honourable Robert Boyle, Esq., in confirmation of a former conjecture made by R. Hooke." This essay was certainly written in Oxford, but it is the only connexion of Oxford with this volume. In regard to the title 'Early Science' this essay may certainly be classed as such, and it contains many scientific observations concerning the ascent of liquids

* This is, presumably, because we are dealing with an infinite, rather than a finite, set of equations.

in tubes. The explanation given of this ascent is, however, an absolutely impossible one: the rise is attributed to the pressure of air being less in the tube than it is outside! The most important fact in regard to the essay is that it attracted the attention of the early Royal Society, and in the following year Hooke was appointed its curator of experiments. From that time he dwelt in London until his death in 1703.

It is difficult to judge how the volume has been put together; it appears to be a haphazard medley of fragments. It includes the correspondence of Newton and Hooke on the gravitation problem in facsimile, together with other fragments.

The main contribution is the concluding part of his Diary, MS. Sloane 4024, which has not previously been copied or printed. It is doubtful whether it was ever intended to meet any eyes but his own. It appears to be a rough note-book in a very abbreviated style, and even Dr. Gunther's examination fails to disentangle their meaning, though he admits that "their solution is not less exhilarating than that of cross-word puzzles, and is quite as useful." It covers much of the period of Hooke's surveying work It is rather surprising that there are so few scientific remarks in it. Some of his discourses read at the Royal Society were of a very different character from those read to-day, *e. g.*, that delivered on Wednesday, April 12, 1693.

The Diary has been annotated by the editor throughout, but the general impression left after reading this compilation is that he might have done it much better.

The most surprising thing, if the book was ever intended for publication, is that there is so little of Hooke's own scientific cogitations in it. Was it ever intended to be anything but a rough day-book or remembrancer in connexion with his numerous daily appointments as surveyor etc. ?

Physical Principles and Applications of Magnetochemistry. By Prof. S. S. Bhatnagar, M.Sc., D.Sc., F.Inst.P., and K. N. Mathur, M.Sc., D.Sc., A.Inst.P., A.R.P.S. (Macmillan and Co. Price 21*s*.)

The work before us constitutes the first attempt to present a complete account in English of a relatively new branch of physical chemistry, for which the name "magneto-chemistry" was suggested by Wedekind. Magnetochemistry, which deals with the interrelation of magnetism and chemistry, may now take its place alongside its elder brethren, electro-, photo-, and thermochemistry. The book follows historical, experimental, and theoretical lines. Of some 350 pages, about 210 are devoted to the more purely physical back-ground, the remainder dealing with the chemical applications.

The book commences with an historical review and description of the experimental methods available in the selected field. A chapter on the pan-magnetism of matter follows, which contains a valuable account of the periodic classification in relation to magnetic properties, and also a fuller record than has appeared elsewhere of the work of Pascal on diamagnetism and structure, often insufficiently appreciated up to the present time. An outline of spectroscopy and atomic structure then prepares the way for a detailed account of dia-, para-, and ferromagnetism, which follows more or less usual lines.

The reader's appetite is now whetted for chemical applications, and the authors lead us into chemical fields in the following chapter on magnetism and valency. This seems particularly well done, and especially so in relation to the subject of complex compounds. In connexion with the theory of Welo and Baudisch, the reader will perhaps be surprised to find no reference to the experiments of Rosenbohm, and we miss an account of the chemically interesting work of Sadron on the magneton numbers of non-ferromagnetic atoms.

The remainder of the book deals with sundry topics, and contains, *inter alia*, a detailed account of the work of Perkin on the Faraday Effect, the influence of magnetic fields on chemical reactions, and the uses of magnetic properties in physico-chemical investigations. A valuable discussion on outstanding problems, together with full tables of susceptibility data, bring the work to a close. Excellent indexes are provided.

A slip appears in the atomic susceptibility of tin (2·37) in the folded page facing p. 62, since the number does not agree either with the value in Table I. (grey tin, −41·55) or that in Table II. (white tin, 2·96, misprinted 296·0).

Professor Bhatnagar and Dr. Mathur are to be congratulated on the selection and treatment of their material, and the production may be recommended to all workers in the borderlands of physics and chemistry, as well as to the scientific public in general. For the non-mathematical reader, the book is not disturbingly algebraical.

[*The Editors do not hold themselves responsible for the views expressed by their correspondents.*]

Fig. 1.

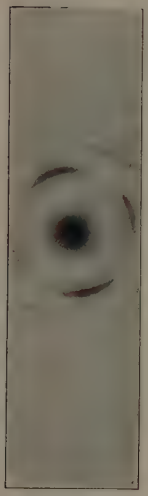

Fig. 2.

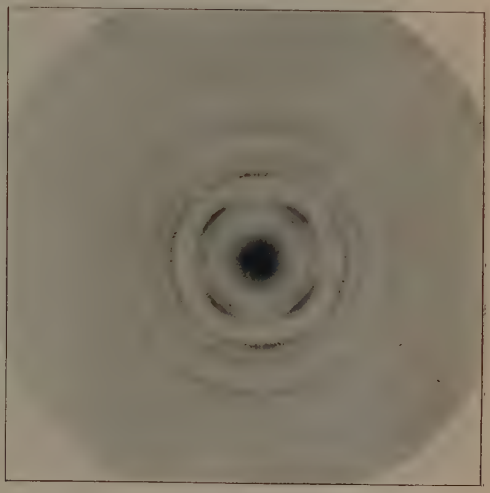

Fig. 3.

Fig. 4.

FIG. 1.

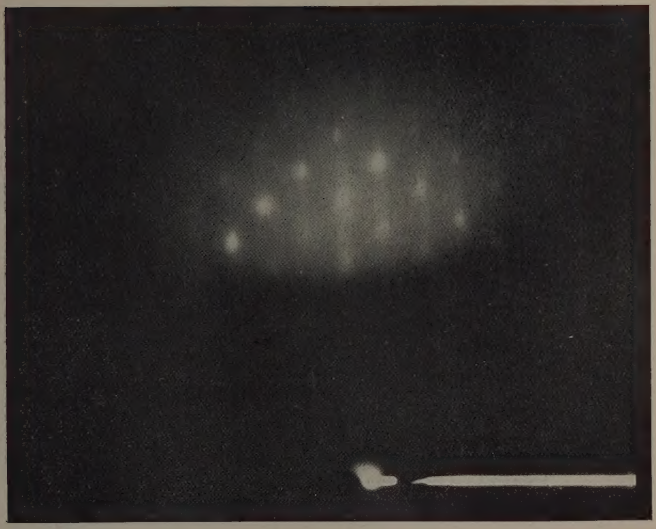

Surface rubbed on chamois leather.

FIG. 2.

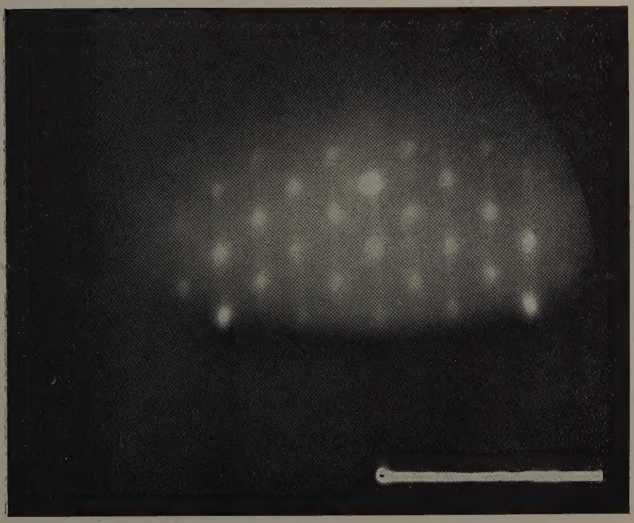

Ground and cloth polished surface.

FIG. 3.

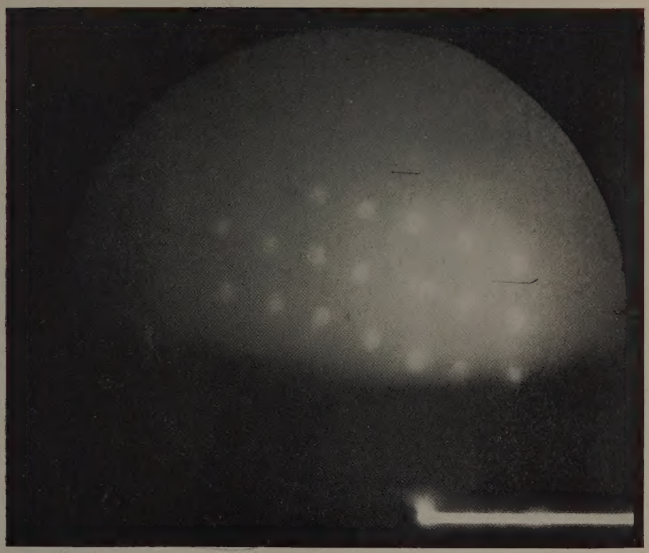

Ground and cloth polished surface.

FIG. 4.

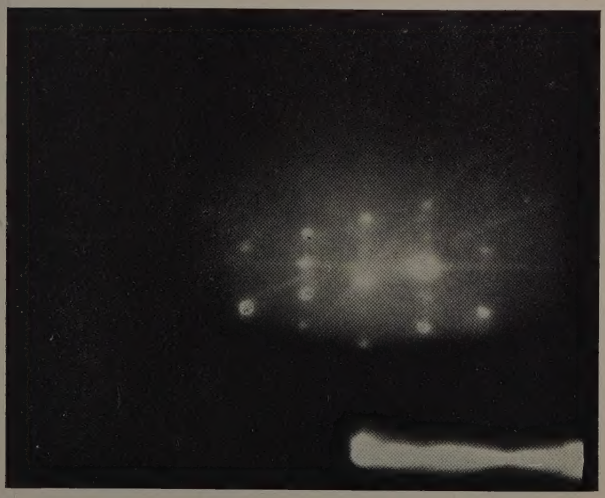

Etched surface. Nominal depth 6000 Å.